NATIONAL ACADEMY OF SCIENCES OF UKRAINE INSTITUTE OF MOLECULAR BIOLOGY AND GENETICS

Qualification scientific work
as a manuscript

Lavrynenko Kyrylo Dmytrovych

UDC 577.22

DISSERTATION

THE INTERACTION BETWEEN CAPRIN1 AND G3BP1 PROMOTES G3BP1-MEDIATED mRNA RECRUITMENT TO STRESS GRANULES

09 - Biology
091 - Biology and Biochemistry

Submitted for the degree of Doctor of Philosophy in Biology

The dissertation contains the results of the author's own research. The use of ideas, results, and texts of other authors is accompanied by references to the corresponding sources.

_____ (Lavrynenko K.D.)

Scientific supervisor: **Kropyvko Serhii Viktorovych**, Candidate of Biological Sciences, Senior Researcher, Department of Functional Genomics, Institute of Molecular Biology and Genetics of the National Academy of Sciences of Ukraine

Kyiv – 2026

ABSTRACT

Lavrynenko K. D. **The interaction between Caprin1 and G3BP1 promotes G3BP1-mediated mRNA recruitment to stress granules – Qualifying scientific work as a manuscript.**

Dissertation for the degree of Doctor of Philosophy in the specialty 091 Biology and Biochemistry. – Institute of Molecular Biology and Genetics of the National Academy of Sciences of Ukraine, Kyiv, 2026.

RNA-binding proteins play a key role in the regulation of all stages of the RNA life cycle, including RNA maturation, transport, localization, translation, stabilization, and degradation. These processes become particularly important under cellular stress conditions, when cells need to rapidly reorganize their translational program, suppress the synthesis of most housekeeping proteins, and preserve mRNAs required for recovery after stress termination. One of the key mechanisms of such adaptation is the formation of stress granules, which are cytoplasmic non-membrane ribonucleoprotein condensates composed of mRNAs stalled at the stage of translation initiation, RNA-binding proteins, translation initiation factors, and other regulatory components.

Stress granule formation is closely associated with liquid-liquid phase separation, which is mediated by weak multivalent interactions between proteins and RNA molecules. Such interactions are enabled by the modular organization of many RNA-binding proteins, which contain structured domains, RNA-binding motifs, and intrinsically disordered regions. The combination of RNA-binding activity, protein-protein interaction capacity, and participation in phase separation determines the role of individual proteins in stress granule nucleation, growth, maturation, and disassembly.

One of the central proteins of stress granules is G3BP1. It is considered a key node within the interaction network that supports stress granule formation. G3BP1 contains an NTF2-L domain, intrinsically disordered regions, an RRM domain, and an RGG-rich region, which together determine its ability to dimerize, interact with protein partners, bind RNA, and participate in liquid-liquid phase separation. G3BP1 is able to induce stress granule formation, whereas cells lacking both G3BP1 and G3BP2 show severe defects in stress granule assembly under oxidative stress conditions. However, the precise mechanisms by which G3BP1 mediates mRNA recruitment to stress granules remain incompletely understood.

The function of G3BP1 in stress granules is closely connected with Caprin1. Caprin1 is an RNA-binding protein involved in translational regulation, neuronal RNA granule function, cellular stress responses and stress granule assembly. Caprin1 interacts with G3BP1 through the NTF2-L domain of G3BP1 and competes with USP10 for binding to G3BP1. The G3BP1–Caprin1 interaction is known to promote stress granule assembly, whereas the interaction between G3BP1 and USP10 is associated with suppression or disassembly of these structures. Nevertheless, although the protein-protein aspect of G3BP1–Caprin1 interaction has been relatively well characterized, the role of this complex in mRNA binding and mRNA recruitment to stress granules has remained insufficiently investigated.

The aim of this dissertation was to investigate the interaction between G3BP1 and Caprin1 *in vivo* and *in vitro*, to characterize the mRNA-binding capacity of both proteins and the G3BP1-Caprin1 complex, and to clarify the role of the G3BP1–Caprin1 complex in mRNA recruitment to stress granules.

To achieve this aim, the interaction between G3BP1 and Caprin1 was analyzed in a cellular system and compared with the interactions of G3BP1 with other stress granule-associated RNA-binding proteins. The dependence of Caprin1, G3BP2, YBX1, and mRNA recruitment to stress granules on G3BP1

levels was investigated. Special attention was given to the characterization of the RNA-binding properties of the G3BP1-Caprin1 complex both in cells and in vitro. The role of individual functional domains of G3BP1 in Caprin1 interaction, mRNA binding and stress granule formation was determined, and the influence of Caprin1 on the efficiency of mRNA recruitment by G3BP1 was evaluated.

The study used a combination of molecular and cellular biology methods, including HeLa cell culture, transfection, siRNA-mediated knockdown of G3BP1, immunofluorescence staining, fluorescent in situ hybridization of mRNA, high-content microscopy, microtubule bench assays for protein and mRNA recruitment analysis, add-back experiments, plasmid cloning, expression and purification of recombinant proteins, co-immunoprecipitation, western blot analysis, electrophoretic mobility shift assay, atomic force microscopy and statistical analysis of experimental data.

The obtained results demonstrated that G3BP1 forms a pronounced interaction with Caprin1 in the cellular environment. Comparison of the interaction between G3BP1 and several cytoplasmic RNA-binding proteins associated with stress granules showed that Caprin1 is one of the most prominent functional partners of G3BP1. It was established that recruitment of Caprin1 to stress granules strongly depends on the presence of functional G3BP1, confirming the key role of G3BP1 in organizing the protein composition of stress granules.
The RNA-binding properties of the G3BP1-Caprin1 complex were characterized. In cells, Caprin1 overexpression increased mRNA recruitment to G3BP1-containing condensates. This indicates that Caprin1 not only interacts with G3BP1 as a protein partner but also functionally affects the ability of G3BP1 to recruit mRNA. In vitro experiments using electrophoretic mobility shift assay showed that the combination of G3BP1 and Caprin1 forms larger protein-RNA complexes compared with either protein alone. Atomic force microscopy data also confirmed the formation of larger RNA-enriched complexes in the presence of both proteins.

Thus, the obtained results indicate a cooperative mode of G3BP1 and Caprin1 interaction during RNA binding.

Functional analysis of G3BP1 domains demonstrated that both the N-terminal and C-terminal regions of the protein are necessary for the full realization of its functions in stress granules. Deletion of the N-terminal region disrupted interaction with Caprin1, whereas deletion of the C-terminal region, which contains the major RNA-binding elements, caused a strong decrease in mRNA recruitment. It was shown that Caprin1 enhances mRNA recruitment only in the presence of full-length G3BP1, which retains the ability to interact simultaneously with both Caprin1 and mRNA. These findings indicate that Caprin1 cannot fully compensate for the loss of G3BP1 RNA-binding activity and instead acts as a regulatory cofactor that enhances the intrinsic mRNA recruitment capacity of G3BP1.

Particular attention was given to the G3BP1-ΔIDR2 construct. Despite retaining the RRM domain and RGG-rich region, this construct showed a strongly reduced ability to recruit mRNA both in cells and in vitro. At the same time, G3BP1-ΔIDR2 partially retained the ability to interact with Caprin1 and localize to stress granules. The obtained data indicate that IDR2 is important not only as a linear protein region but also as an element required for maintaining the proper spatial and conformational organization of G3BP1. Deletion of IDR2 likely disrupts conformational transitions of G3BP1 that are necessary for efficient exposure or function of RNA-binding regions, resulting in impaired mRNA binding.

The scientific novelty of the work consists in demonstrating that Caprin1 enhances mRNA recruitment by G3BP1, but this effect requires intact RNA-binding capacity and domain organization of G3BP1. For the first time, it was shown that Caprin1 enhances the ability of G3BP1 to recruit mRNA and promotes the formation of larger RNA-enriched protein complexes. It was established that efficient enhancement of mRNA recruitment depends on the integrity of G3BP1

functional domains and preservation of its own RNA-binding activity. Caprin1 was shown to function primarily as a regulatory partner of G3BP1 that enhances G3BP1-mediated mRNA binding but does not replace the requirement for direct interaction between G3BP1 and mRNA. In addition, the important role of IDR2 in maintaining the RNA-binding functionality of G3BP1 was demonstrated, expanding current understanding of the mechanisms of G3BP1 conformational regulation during stress granule formation.

The practical significance of the obtained results lies in expanding current understanding of the molecular mechanisms of stress granule formation and regulation of RNA-protein condensates. The characterized functional interaction between G3BP1 and Caprin1 may serve as a basis for further studies of mechanisms controlling recruitment of specific mRNAs to stress granules, as well as for investigations of pathological conditions associated with disrupted stress granule dynamics and aggregation of RNA-binding proteins. These results are relevant for further studies of pathological RNP granule remodeling, particularly in neurodegenerative diseases and viral infection, where altered stress granule dynamics and RNA-binding protein aggregation are frequently observed. In addition, the optimized approaches for quantitative analysis of mRNA and protein recruitment to cellular condensates may be applied to the study of other RNA-binding proteins and biomolecular condensates.

Thus, the dissertation established that the G3BP1-Caprin1 complex is a functionally important element in the regulation of mRNA recruitment to stress granules. Caprin1 enhances the RNA-binding activity of G3BP1 and promotes the formation of larger RNA-enriched nucleoprotein complexes; however, this effect depends on the preservation of G3BP1 structural integrity and its ability to directly bind mRNA. The obtained results complement the current model of stress granule formation, according to which RNA concentration, the conformational state of G3BP1, and multivalent protein-protein interactions jointly determine the

efficiency of liquid-liquid phase separation and formation of functionally active ribonucleoprotein condensates.

Keywords: RNA-binding proteins, G3BP1, Caprin1, mRNA, stress granules, ribonucleoprotein condensates, liquid-liquid phase separation, protein-protein interactions, protein-RNA interactions, mRNA recruitment.

AUTHOR'S PUBLICATIONS RELATED TO THE DISSERTATION TOPIC

Articles in specialized scientific journals:

1. Lavrynenko K., Rengifo-Gonzalez J. C., Joshi V., Pankivskyi S., Pastré D., Kropyvko S., Hamon L. mRNA recruitment by G3BP1 condensates is regulated by Caprin1 but requires G3BP1 binding to mRNA. Scientific Reports. 2025. 15:21066. doi: 10.1038/s41598-025-21066-7. Personal contribution of the applicant: performance of the main part of experimental work, acquisition, processing and analysis of experimental data, interpretation of the obtained results, preparation of illustrative material and participation in manuscript writing.

2. Lavrynenko K., Hamon L., Kropyvko S. Intrinsically disordered region 2 of G3BP1 is required for RNA recruitment by G3BP1–Caprin1 complex. Biopolymers and Cell. 2026. Vol. 42, No. 1. P. 44–53. doi: 10.7124/bc.000B34. Personal contribution of the applicant: performance of the main part of experimental work, analysis and interpretation of the obtained results, preparation of figures, and writing of the manuscript.

Conference abstracts

1. Lavrynenko K., Kropyvko S., Pastré D., Hamon L. Defining the interactions of G3BP1 with cytoplasmic RNA-binding proteins on cellular and

biochemical levels. Biopolymers and Cell. 2023. Vol. 39, No. 1. P. 60–73. doi: 10.7124/bc.000A89.

АНОТАЦІЯ

Лавриненко К. Д. **Взаємодія Caprin1 і G3BP1 сприяє G3BP1-опосередкованому рекрутуванню мРНК до стресових гранул. – Кваліфікаційна наукова праця на правах рукопису.**

Дисертація на здобуття наукового ступеня доктора філософії за спеціальністю 091 Біологія і біохімія. – Інститут молекулярної біології і генетики НАН України, Київ, 2026.

РНК-зв’язувальні білки відіграють ключову роль у регуляції всіх етапів життєвого циклу РНК, зокрема її дозрівання, транспорту, локалізації, трансляції, стабілізації та деградації. Особливе значення ці процеси мають за умов клітинного стресу, коли клітина повинна швидко перебудувати трансляційний профіль, призупинити синтез більшості білків і водночас забезпечити збереження мРНК, необхідних для відновлення нормального функціонування після припинення дії стресового чинника. Одним із ключових механізмів такої адаптації є утворення стресових гранул – цитоплазматичних немембранних рибонуклеопротеїнових конденсатів, що складаються з мРНК, зупинених на етапі ініціації трансляції, РНК-зв’язувальних білків, факторів ініціації трансляції та інших регуляторних компонентів.

Формування стресових гранул тісно пов’язане з явищем рідинно-рідинного фазового розділення, яке забезпечується слабкими мультивалентними взаємодіями між білками та РНК. Такі взаємодії можливі завдяки модульній будові багатьох РНК-зв’язувальних білків, які містять

структуровані домени, РНК-зв’язувальні мотиви та внутрішньо невпорядковані ділянки. Саме поєднання РНК-зв’язувальної активності, здатності до білок-білкових взаємодій та участі у фазовому розділенні визначає роль окремих білків у нуклеації, рості, дозріванні та розбиранні стресових гранул.

Одним із центральних білків стресових гранул є G3BP1. Він розглядається як ключовий вузол у мережі взаємодій, що забезпечують формування цих конденсатів. G3BP1 містить NTF2-L домен, внутрішньо невпорядковані ділянки, RRM-домен та RGG-збагачену ділянку, що разом визначають його здатність до димеризації, взаємодії з білковими партнерами, зв’язування РНК та участі у рідинно-рідинному фазовому розділенні. G3BP1 здатний індукувати формування стресових гранул, а клітини з одночасною втратою G3BP1 та G3BP2 мають суттєві порушення здатності до утворення стресових гранул за умов окисного стресу. Водночас точні механізми, за допомогою яких G3BP1 забезпечує рекрутинг мРНК до стресових гранул, залишаються недостатньо з’ясованими.

Функція G3BP1 у стресових гранулах тісно пов’язана з білком Caprin1. Caprin1 є РНК-зв’язувальним білком, який бере участь у регуляції трансляції, функціонуванні нейрональних РНК-гранул, клітинній відповіді на стрес та формуванні стресових гранул. Caprin1 взаємодіє з G3BP1 через NTF2-L домен останнього та конкурує з USP10 за зв’язування з G3BP1. Відомо, що взаємодія G3BP1 з Caprin1 сприяє формуванню стресових гранул, тоді як взаємодія G3BP1 з USP10, навпаки, пов’язана з пригніченням або розбиранням цих структур. Проте, незважаючи на відносно добре охарактеризований білок-білковий аспект взаємодії G3BP1–Caprin1, роль цього комплексу у зв’язуванні мРНК та її рекрутингу до стресових гранул залишалася недостатньо вивченою.

Метою дисертаційної роботи було дослідити взаємодію G3BP1 з Caprin1 *in vivo* та *in vitro*, охарактеризувати здатність цих білків і комплексу

G3BP1-Caprin1 до зв’язування мРНК, а також з’ясувати роль комплексу G3BP1-Caprin1 у рекрутингу мРНК до стресових гранул.

Для досягнення поставленої мети було проаналізовано взаємодію між G3BP1 та Caprin1 у клітинній системі та порівняно її з взаємодіями G3BP1 з іншими РНК-зв’язувальними білками стресових гранул. Було досліджено залежність рекрутингу Caprin1, G3BP2, YBX1 та мРНК до стресових гранул від рівня G3BP1. Окрему увагу приділено характеристиці РНК-зв’язувальних властивостей комплексу G3BP1-Caprin1 у клітинних умовах та in vitro. Було визначено роль окремих функціональних доменів G3BP1 у взаємодії з Caprin1, зв’язуванні мРНК та формуванні стресових гранул, а також оцінено вплив Caprin1 на ефективність рекрутингу мРНК білком G3BP1.

У роботі використано комплекс методів молекулярної та клітинної біології, зокрема культивування клітин HeLa, трансфекцію, siRNA-опосередковане зниження експресії G3BP1, імунофлуоресцентне фарбування, флуоресцентну in situ гібридизацію мРНК, високопродуктивну мікроскопію, microtubule bench assay для аналізу рекрутингу білків і мРНК, add-back експерименти, клонування плазмідних конструкцій, експресію та очищення рекомбінантних білків, ко-імунопреципітацію, вестерн-блот аналіз, електрофоретичний аналіз рухливості нуклеопротеїнових комплексів, атомно-силову мікроскопію та статистичну обробку експериментальних даних.

У результаті проведених досліджень було показано, що G3BP1 утворює виражену взаємодію з Caprin1 у клітинній системі. Порівняння взаємодії G3BP1 з низкою цитоплазматичних РНК-зв’язувальних білків, асоційованих зі стресовими гранулами, продемонструвало, що Caprin1 є одним із найбільш помітних функціональних партнерів G3BP1. Було встановлено, що рекрутинг Caprin1 до стресових гранул суттєво залежить

від наявності функціонального G3BP1, що підтверджує ключову роль G3BP1 у формуванні білкового складу стресових гранул.

Було охарактеризовано РНК-зв'язувальні властивості комплексу G3BP1-Caprin1. У клітинних умовах надекспресія Caprin1 підвищувала рекрутинг мРНК до G3BP1-вмісних конденсатів. Це свідчить про те, що Caprin1 не лише взаємодіє з G3BP1 як білковий партнер, але й функціонально впливає на здатність G3BP1 залучати мРНК. In vitro експерименти із застосуванням електрофоретичного аналізу рухливості нуклеопротеїнових комплексів показали, що суміш G3BP1 та Caprin1 утворює більші білок-РНК комплекси порівняно з кожним білком окремо. Дані атомно-силової мікроскопії також підтвердили формування більших РНК-збагачених комплексів у присутності обох білків. Таким чином, отримані результати вказують на кооперативний характер взаємодії G3BP1 та Caprin1 під час зв'язування РНК.

Функціональний аналіз доменів G3BP1 показав, що як N-кінцева, так і C-кінцева частини білка є необхідними для повноцінної реалізації його функцій у стресових гранулах. Делеція N-кінцевої частини порушувала взаємодію з Caprin1, тоді як делеція C-кінцевої частини, що містить основні РНК-зв'язувальні елементи, призводила до різкого зниження рекрутингу мРНК. Було показано, що Caprin1 здатний підвищувати рекрутинг мРНК лише у присутності повнорозмірного G3BP1, який зберігає здатність одночасно взаємодіяти з Caprin1 та мРНК. Це свідчить про те, що Caprin1 не може повністю компенсувати втрату РНК-зв'язувальної активності G3BP1, а виконує роль регуляторного кофактора, який підсилює власну здатність G3BP1 до рекрутингу мРНК.

Особливий інтерес становили результати, отримані для конструкта G3BP1-ΔIDR2. Попри збереження RRM-домену та RGG-збагаченої ділянки, цей конструкт демонстрував різко знижену здатність до рекрутингу мРНК як у клітинних умовах, так і in vitro. Водночас G3BP1-ΔIDR2 частково

зберігав здатність взаємодіяти з Caprin1 і локалізуватися у стресових гранулах. Отримані дані свідчать, що IDR2 є важливою не лише як лінійна ділянка білка, але і як елемент, необхідний для підтримання правильної просторової та конформаційної організації G3BP1. Імовірно, видалення IDR2 порушує конформаційні переходи G3BP1, необхідні для ефективного відкриття або функціонування РНК-зв'язувальних ділянок, що призводить до втрати здатності до ефективного зв'язування мРНК.

Наукова новизна отриманих результатів полягає у комплексній характеристиці функціональної взаємодії G3BP1 та Caprin1 у контексті рекрутингу мРНК та формування стресових гранул. Уперше показано, що Caprin1 підвищує здатність G3BP1 до рекрутингу мРНК і сприяє формуванню більших РНК-збагачених білкових комплексів. Встановлено, що ефективне посилення мРНК-рекрутингу залежить від цілісності функціональних доменів G3BP1 та збереження його власної РНК-зв'язувальної активності. Показано, що Caprin1 функціонує переважно як регуляторний партнер G3BP1, який підсилює G3BP1-опосередковане зв'язування мРНК, але не замінює необхідність прямої взаємодії G3BP1 з мРНК. Окремо встановлено важливу роль IDR2 у підтриманні РНК-зв'язувальної функціональності G3BP1, що розширює уявлення про механізми конформаційної регуляції G3BP1 під час формування стресових гранул.

Практичне значення отриманих результатів полягає у розширенні сучасних уявлень про молекулярні механізми утворення стресових гранул та регуляції РНК-білкових конденсатів. Охарактеризована функціональна взаємодія G3BP1-Caprin1 може бути використана як основа для подальших досліджень механізмів рекрутингу специфічних мРНК до стресових гранул, а також для вивчення патологічних станів, пов'язаних із порушенням динаміки стресових гранул і агрегацією РНК-зв'язувальних білків. Отримані результати можуть бути корисними для майбутніх досліджень

нейродегенеративних захворювань, вірусних інфекцій та онкологічних процесів, у яких стресові гранули та РНК-зв'язувальні білки відіграють важливу роль. Крім того, оптимізовані підходи до кількісного аналізу рекрутингу мРНК і білків у клітинних конденсатах можуть бути застосовані для вивчення інших РНК-зв'язувальних білків та біомолекулярних конденсатів.

Таким чином, у дисертаційній роботі встановлено, що комплекс G3BP1-Caprin1 є функціонально важливим елементом регуляції рекрутингу мРНК до стресових гранул. Caprin1 підсилює РНК-зв'язувальну активність G3BP1 і сприяє формуванню більших РНК-збагачених нуклеопротеїнових комплексів, однак цей ефект залежить від збереження структурної цілісності G3BP1 та його здатності безпосередньо зв'язувати мРНК. Отримані результати доповнюють сучасну модель формування стресових гранул, згідно з якою концентрація РНК, конформаційний стан G3BP1 та мультивалентні білок-білкові взаємодії разом визначають ефективність рідинно-рідинного фазового розділення та формування функціонально активних рибонуклеопротеїнових конденсатів.

Ключові слова: РНК-зв'язувальні білки, G3BP1, Caprin1, мРНК, стресові гранули, рибонуклеопротеїнові конденсати, рідинно-рідинне фазове розділення, білок-білкові взаємодії, білок-РНК взаємодії, рекрутинг мРНК.

ПУБЛІКАЦІЇ АВТОРА ЗА ТЕМОЮ ДИСЕРТАЦІЇ

Статті у наукових фахових виданнях:

1. **Lavrynenko K.**, Rengifo-Gonzalez J. C., Joshi V., Pankivskyi S., Pastré D., Kropyvko S., Hamon L. mRNA recruitment by G3BP1 condensates is regulated by Caprin1 but requires G3BP1 binding to mRNA. Scientific Reports.

2025. 15:21066. doi: 10.1038/s41598-025-21066-7. Особистий внесок здобувача: виконання основної частини експериментальних досліджень, збір, обробка та аналіз експериментальних даних, інтерпретація отриманих результатів, підготовка ілюстративного матеріалу та участь у написанні рукопису.

2. **Lavrynenko K.**, Hamon L., Kropyvko S. Intrinsically disordered region 2 of G3BP1 is required for RNA recruitment by G3BP1–Caprin1 complex. Biopolymers and Cell. 2026. Vol. 42, No. 1. P. 44–53. doi: 10.7124/bc.000B34. Особистий внесок здобувача: виконання основної частини експериментальних досліджень, аналіз та інтерпретація отриманих результатів, підготовка ілюстрацій, написання і підготовка статті до друку.

Тези наукових доповідей

1. **Lavrynenko K.**, Kropyvko S., Pastré D., Hamon L. Defining the interactions of G3BP1 with cytoplasmic RNA-binding proteins on cellular and biochemical levels. Biopolymers and Cell. 2023. Vol. 39, No. 1. P. 60–73. doi: 10.7124/bc.000A89.

CONTENTS

LIST OF ABBREVIATIONS 18

INTRODUCTION 21

CHAPTER 1 LITERATURE REVIEW 28

1.1. RNA-binding proteins and Ribonucleoproteins 28

1.1.1. Organization of RBPs 28

1.1.2. Principles of RNA-protein granules 29

1.1.3. Stress granules overview 30

1.1.4. Stress granule dynamics 31

1.1.5. SG composition 33

1.1.6. Roles of stress granules in health and disease 33

1.2. The ins and outs of G3BP1 34

1.2.2. G3BP1 structure and domains 35

1.2.3. Regulation and post-translational modification of G3BP1 36

1.2.4. G3BP1 enzymatic activity 37

1.2.5. G3BP1 in stress granules 37

1.2.6. G3BP1 functions outside of stress granules 40

1.2.7 G3BP1 in pathology 40

1.3. Caprin1 and G3BP1 interaction in and out of stress granules 41

1.3.1. Overview of Caprin1 structural features 41

1.3.2. Caprin1 interaction with G3BP1 and role in stress granule assembly 43

1.3.3. Caprin1 in neuron function and neurodegenerative disease 45

1.3.4. Caprin1 in cancer 47

CHAPTER 2 MATERIALS AND METHODS 48

2.1 *In vivo* methods 48
2.1.1 Plasmid preparation 48
2.1.2. Cell Culture 53
2.1.3 Microtubule Bench assay: Recruitment and mixing experiments 53
2.1.4. Immunofluorescence staining for endogenous proteins visualization 56
2.1.5. RNA *in situ* hybridization 58
2.1.6. Overexpression and siRNA treatment for High-content imaging assays 58
2.1.7. Addback experiments 59
2.1.8. Data acquisition for MT bench assays, overexpression, silencing and add-back experiments 60
2.1.9. HCS experiments data processing 62
2.1.10. Statistical analysis 63
2.2 *In vitro* methods 63
2.2.1. Protein production and purification 63
2.2.2. Immunoprecipitation assay and western blot 64
2.2.3. Electrophoretic mobility shift assay 65
2.2.4. Atomic Force Microscopy (AFM) imaging 66
CHAPTER 3 RESULTS AND DISCUSSION 67
3.1. G3BP1 binds Caprin1 *in vivo*, and the recruitment of Caprin1 to stress granules is affected by G3BP1 67
3.2. G3BP1-Caprin1 complex RNA-binding properties 76
3.3 Roles of G3BP1 domains in SG assembly and mRNA recruitment to SG 100

CHAPTER 4 ANALYSIS AND SUMMARY OF THE OBTAINED RESULTS..... 108

CONCLUSIONS..... 114

BIBLIOGRAPHY 117

SUPPLEMENTARY A……..136

LIST OF ABBREVIATIONS

ALS - Amyotrophic Lateral Sclerosis

ATP - Adenosine TriPhosphate

CAPRIN1 - Cell cycle Associated PRoteIN 1

CSD - Cold Shock Domain

cGAS - Cyclic GMP-AMP synthase

DEP - Disassembly Engaged Proteins

DENV - dengue virus

eIF2α - eukaryotic initiation factor 2 subunit alpha

eIF2B - eukaryotic translation initiation factor 2B

EIF2AK1 - Eukaryotic Translation Initiation Factor 2-alpha Kinase 1

ESWR1 - EWS RNA Binding Protein 1

FMDV - foot-and-mouth disease virus

FMRP - Fragile X mental Retardation Protein

FTD - frontotemporal dementia

FUS - Fused in sarcoma

GCN2 - general control nonderepressible 2

GAP - GTPase-activating protein

GAPDH - glyceraldehyde-3-phosphate dehydrogenase

G3BP1 - Ras-GTPase-activating protein (GAP)-Binding Protein 1

GR - Glucocorticoid Receptor

IDR - intrinsically disordered region

IGF2 - insulin-like growth factor 2

ISR - integrated stress response

JEV - Japanese encephalitis virus

JMJD6 - Jumonji C domain containing protein 6

KH domain - K Homology domain

LCs - low complexity sequence

LLPS - Liquid-Liquid Phase Separation

miR - microRNA

mRNA - messenger RiboNucleic Acid

mRNP - messenger RiboNucleoProtein

mTOR - mammalian target of rapamycin

NLS - Nuclear Localization Signal

NTF2-L - Nuclear Transport Factor 2-Like

OB - Oligosaccharide/oligonucleotide-Binding fold

PAAG - Polyacrylamide gel

PABP - Poly(A)-binding protein

PB - Processing bodies

PERK - Protein Kinase RNA-Like ER Kinase

PKR - Protein kinase R

PRMT - protein arginine methyltransferases

RBD - RNA-Binding Domain

RBP - RNA-Binding Protein

RNG105 - RNA granule protein 105

RNP - Ribonucleoprotein

RRM - RNA recognition motif

SAM68 - Src Associated in Mitosis of 68 kDa

SG - Stress Granule

SELEX - Systematic Evolution of Ligands by EXponential enrichment

SEV - Sendai virus

SDS-PAGE - Sodium Dodecyl Sulfate PolyAcrylamide Gel Electrophoresis

SLiM - short linear motif

SUMO - Small ubiquitin-like modifier

TDP-43 - TAR DNA-binding protein 43

TIA-1 - T-cell-restricted intracellular antigen-1

TIAR - TIA-1 Related protein

T-STAR - Testis-Specific Alternative Splicing Regulator

TNF - Tumor Necrosis Factor

TMEV - Theiler's murine encephalomyelitis virus

TTP - Tristetraprolin

USP10 - Ubiquitin specific peptidase 10

UTR - UnTranslated Region

YBX1 - Y-Box binding protein 1

INTRODUCTION

Relevance of the topic. RNA is a nucleic acid whose existence underlines the entirety of cells' functionality. Both protein-coding and non-coding RNAs are essential for every aspect of cellular life, from growth and protein production to regulating cellular metabolism in response to current needs. RNA-binding proteins (RBP) are responsible for RNA maintenance at all stages of its lifecycle. RBPs perform various roles, from transcription to degradation, decay, and everything in between. When facing adverse conditions, cells need to protect fragile RNA from damage and reroute their translation processes to the production of the proteins that partake in the defense of the cells from stressors. To accomplish that, a special type of transient non-membrane organelles - Stress Granules (SGs)- are assembled in the cytoplasm from mRNA stalled in translation and a special subclass of RBPs. The formation of stress granules is possible due to the phenomenon of liquid-liquid phase separation (LLPS). In cells, LLPS is a concentration-dependent process of proteins and nucleic acids demixing into separate phases. Since biopolymers are complex and can interact with multiple partners in different ways, both intra- and intermolecular interactions contribute to RNA-protein complexes formed due to phase separation. Such a mechanism allows sequestering of mRNAs, whose products are not involved in adverse conditions response, to SGs, to preserve them from potential damage and ultimately facilitate their return to the translation pool whenever the cell returns to a non-stressed state. The process of stress granule assembly, function, and disassembly is orchestrated by a particular class of RBPs, which are called stress granule RBPs. These proteins broadly conform to similar domain organization, with self-oligomerization domains, RNA-binding domains, and intrinsically disordered regions (1). Stress granule RBPs and RNAs maintain a complex network of connections, which allows rapid assembly and disassembly of SGs in a controlled and regulated fashion. SGs are activated in response to not only

transient stresses but also in case of chronic changes in the cell microenvironment, such as inflammation, viral infections, or cancer. This makes SG proteins potent targets for research as diagnostic markers or treatment targets. Some proteins are more important for SG functionality than others, and no single protein plays a more important role in SGs than G3BP1 – stress granule assembly factor 1. The centrality of G3BP1 in SG function is well researched, as it is one of the first proteins that is recruited by the stalled pre-initiation complex in the eIF2α-P-dependent SG assembly route (2) and continues to be a central node in the SG network (3). Apart from its role in SGs, G3BP1 participates in the regulation of mRNA stability (4), and structure-mediated RNA decay (5).

G3BP1's role in SGs is closely interlinked with another SG protein – Caprin1. Caprin1 competes with USP10 for binding with G3BP1 in a pH-dependent manner, in which G3BP1-Caprin1 interaction drives SG assembly, while USP10 outcompetes Caprin1 in binding to G3BP1, facilitating SG disassembly (6). While the protein-protein aspect of G3BP1-Caprin1 binding is relatively understood (7), there are still important questions about the dynamics of RNA-binding of this complex and the roles of individual proteins in bringing particular mRNAs to stress granules.

Apart from their role in SGs both G3BP1 and Caprin1 are components of neuronal transport granules, which are ribonucleoprotein (RNP) granules that act as a way for mRNAs to reach distant areas of axons and dendrites to partake in the local translation process. Here G3BP1 is a component of axonal transport RNPs (8), while both Caprin1 (9) and G3BP1 (10) have prominent roles as dendrite local translation regulators. While G3BP1-Caprin1 complex functions in stress granules are well-described, the relationship between these proteins in neuronal transport granules is relatively unknown.

RNA-binding proteins are heavily involved in neuronal diseases that manifest in abnormal aggregations of proteins in cytoplasm. For instance, pathological mutations in several SG proteins, namely FUS, TDP-43 (11), TIA-

1/TIAR (12–13) are known hallmarks of protein aggregation in such diseases as amyotrophic lateral sclerosis (ALS) and frontotemporal dementia (FTD), while relatively recently, Caprin1 missense mutation was linked to early-onset ataxia (14). RBPs with pathologic mutations are recruited to SGs, which leads to major dysfunction in SG composition and consequently alters the fate of mRNAs that are partitioned to SGs. There is an undeniable link between pathological aggregation of RBPs and their RNA-binding ability. Normally, cytoplasmic RNAs promote LLPS and the formation of granules to a certain threshold, but past that point high local concentration of RNAs prevents excessive aggregation of RBPs (15). RBPs that cannot bind RNA due to pathological mutations or truncations are still recruited to SGs but are unable to dissociate from them, causing hyperaggregation, which turns normally soluble RBPs into solid-like inclusions that cannot disassemble and release trapped mRNAs, which decreases the pool of mRNAs ready for translation (16). Since the G3BP1-Caprin1 complex is a central node in SGs, the role of this protein in such diseases is an intriguing avenue of research.

Connection of the work with scientific programs, plans, and research topics. The dissertation corresponds to the main research plan of the Department of Functional Genomics of the Institute of Molecular Biology and Genetics of the National Academy of Sciences of Ukraine and was carried out within the framework of the state-funded research topic No. 2.2.4.2 “The role of scaffold protein complexes of the TKS and ITSN families in the regulation of normal and pathological cellular processes.”

Aim and Objectives of the study

The aim of this work is to investigate the interplay of G3BP1 with Caprin1 *in vivo* and *in vitro,* assess the mRNA binding capabilities of both proteins and the G3BP1-Caprin1 complex, and shed light on the role of the G3BP1-Caprin1 complex in the recruitment of mRNA to stress granules.

To achieve this aim, we defined the following objectives:

1. Evaluate the interaction between G3BP1 and Caprin1 in the cellular system and compare it to G3BP1 interactions with stress granule RBPs hosting diverse RNA-binding domains
2. . Analyze the dependency between the level of G3BP1 in stress granules and the recruitment of partner proteins such as Caprin1, YBX1 and G3BP2, as well as mRNA, to SGs.
3. Characterize the RNA-binding properties of the G3BP1-Caprin1 complex in the cellular environment as well as in vitro.
4. Determine the roles of G3BP1 functional domains and their interplay with Caprin1 in G3BP1-mediated mRNA binding and analyze the influence of Caprin1 on the efficiency of mRNA binding by G3BP1.
5. Evaluate the role of the G3BP1-Caprin1 complex in the mRNA recruitment to stress granules.

Object of the study

Stress granule assembly and RNA-binding protein interactions with mRNA in cells under stress conditions.

Subject of the study

The molecular mechanisms of G3BP1 and Caprin1 interaction, the role of G3BP1 domains in mRNA binding, and the involvement of the G3BP1–Caprin1 complex in stress granule assembly.

Research methods. Molecular and cellular biology methods, plasmid construct cloning, HeLa cell culture, cell transfection and siRNA-mediated knockdown, immunofluorescence staining and RNA *in situ* hybridization, high-content imaging analysis, addback experiments, microtubule bench recruitment and mixing assays, recombinant protein expression and purification, immunoprecipitation assay and western blot analysis, electrophoretic mobility shift assay (EMSA), atomic force microscopy (AFM), analysis of mRNA

recruitment to stress granules, confocal and fluorescence microscopy, statistical data analysis methods, and others.

Scientific novelty of the obtained results lies in the comprehensive characterization of the functional interplay between the stress granule proteins G3BP1 and Caprin1 in the context of messenger RNA recruitment and stress granule assembly.

For the first time, it was demonstrated that Caprin1 enhances the mRNA-binding capacity of G3BP1 and promotes the recruitment of mRNA into stress granules through cooperation with G3BP1. The study established that the RNA-binding domain and intrinsically disordered regions of G3BP1 are required for efficient mRNA recruitment and stress granule assembly.

The functional contribution of individual G3BP1 domains to Caprin1 interaction, RNA binding, and condensate formation was dissected using a combination of cellular and structural biology approaches. It was shown that deletion of either the N-terminal or C-terminal regions of G3BP1 impairs stress granule formation and reduces Caprin1 recruitment to stress granules. In contrast, the enhancement of mRNA recruitment by Caprin1 was observed only in the presence of full-length G3BP1, demonstrating the importance of intact G3BP1 domain organization for the cooperative function of the complex.

In addition, the work demonstrated that the G3BP1–Caprin1 complex forms larger RNA-enriched assemblies than either protein alone, supporting the concept that Caprin1 acts as a functional cofactor of G3BP1 during RNA-dependent phase separation. The obtained results complement the current model of stress granule assembly by showing that Caprin1-mediated enhancement of mRNA recruitment contributes to the central role of G3BP1 in stress granule nucleation and dynamics.

The study further expands the understanding of molecular mechanisms governing RNA–protein condensate formation under cellular stress conditions and provides new insights into the regulation of stress granule assembly, which

may be relevant for stress-associated pathologies, including neurodegenerative diseases and cancer.

The practical significance of the obtained results lies in the expansion of the current understanding of the molecular mechanisms governing stress granule assembly and RNA recruitment under cellular stress conditions. The obtained results clarify the functional role of the G3BP1-Caprin1 interaction in the regulation of messenger RNA dynamics and RNA-protein condensate formation.

The study identifies specific domains of G3BP1 required for efficient mRNA recruitment, which may serve as potential molecular targets for modulation of stress granule dynamics. The presented findings contribute to the broader understanding of RNA-binding protein cooperation during liquid-liquid phase separation and may be useful for further studies focused on stress-associated cellular responses.

The results may be applied in future biomedical research related to pathological stress granule formation observed in neurodegenerative disorders, viral infections, and cancer. In particular, the characterization of the G3BP1-Caprin1 complex provides a basis for the development of therapeutic approaches aimed at regulating aberrant RNA-protein aggregation and stress granule persistence in disease conditions.

In addition, the methodological approaches developed and optimized in this work, including microtubule bench assays and quantitative analysis of mRNA recruitment to stress granules, may be used in future investigations of RNA-binding proteins and biomolecular condensates.

Personal contribution. All presented experiments were performed personally by the doctoral candidate or with his direct participation. The majority of the experiments, as well as the processing and analysis of the obtained results, were carried out personally by the doctoral candidate. The Atomic Force Microscopy was performed in collaboration with Prof. Loic Hamon from the «Structure and Activity of Normal and Pathological Biomolecules»(SABNP)

laboratory, Paris-Saclay University, Inserm, University of Évry (France). Recombinant protein production and purification were performed in collaboration with Dr. Juan Carlos Rengifo-Gonzalez from the SABNP laboratory, Paris-Saclay University, Inserm, University of Évry (France).

The author expresses sincere gratitude to the Head of the Department, Prof. A. V. Rynditch, the scientific supervisors, PhD S. V. Kropyvko and Prof. Loic Hamon, as well as Prof. David Pastre (SABNP laboratory, Paris-Saclay University, Inserm, University of Évry, France) for their assistance in the planning and execution of experimental research, discussion of the obtained results, and preparation of the results for publication. The author also expresses sincere gratitude to Vandana Joshi and Dr. Serhii Pankivskyi (SABNP laboratory, Paris-Saclay University, Inserm, University of Évry, France) for assistance with the use of the necessary equipment and research methods.

Scientific Publications. The results of the dissertation research have been published in 2 articles indexed in the international scientometric database Scopus, including 1 article published in a Q1 journal (*Nature Scientific Reports*), and were also presented in 1 report at an international scientific conference.

Structure and size of the dissertation

Structure and size of the dissertation. The dissertation consists of an introduction, a literature review, materials and methods, results and discussion, a general discussion, conclusions, and a bibliography comprising 127 references. The dissertation is presented on 136 pages of standard manuscript text and contains 38 figures and 5 tables. This dissertation is an adapted version of the PhD thesis previously defended by the author on 16.12.24 at Paris-Saclay University, INSERM, University of Évry, France.

CHAPTER 1

LITERATURE REVIEW

1.1. RNA-binding proteins and Ribonucleoproteins

In order to present a comprehensive overview of G3BP1 and Caprin1 interaction in view of their RNA-binding function, the literature review will be divided into three chapters. In the first part, we will address the general principles of RNA-binding protein organization and function, as well as RNP granules and the details of RBP function within them, specifically stress granules. The second part will focus on an in-depth assessment of the G3BP1 structure, the diverse functions inside and outside of stress granules, the various factors of G3BP1 regulation, and its involvement in disease. The third chapter will highlight Caprin1 structure, functions, and involvement in disease, as well as a closer look at the specifics of G3BP1 and Caprin1 interaction.

1.1.1. Organization of RBPs. The life cycle of RNA is closely connected with RNA-binding proteins (RBPs), which regulate RNA maturation, transport, localization, translation, stability, and degradation. More than 2000 RBPs have been identified, and their functional diversity is largely determined by modular organization. Most RBPs contain one or several RNA-binding domains (RBDs), which usually recognize short RNA motifs with moderate affinity. The combination of several RBDs within one protein increases RNA-binding specificity and allows RBPs to recognize longer or structurally complex RNA targets (17-19).

In addition to structured RBDs, many RBPs contain intrinsically disordered regions (IDRs). These regions are characterized by flexible structure, low hydrophobicity, and biased amino acid composition, allowing them to participate

in weak and dynamic protein-protein and protein-RNA interactions. In RBPs, IDRs may contribute directly to RNA binding, mediate interactions with partner proteins, or regulate the accessibility of structured RNA-binding domains (20, 21). IDRs are especially abundant in proteins involved in stress granule formation, where they promote multivalent interactions required for liquid-liquid phase separation (LLPS). Stress granule proteins are often enriched in low-complexity regions, RGG motifs and other disordered sequences that support interactions with RNA and other RBPs (1, 24, 25).

The modular organization of RBPs also allows them to form homo- and heteromeric complexes with altered RNA-binding properties. Such interactions may enhance or inhibit RNA binding, promote assembly of higher-order ribonucleoprotein complexes, or change the localization and function of associated RNAs (27-29). Therefore, the ability of RBPs to bind RNA, interact with protein partners, and form multivalent assemblies is central to the formation of RNA-protein condensates.

1.1.2. Principles of RNA-protein granules. In the cytoplasm, many RBPs function as components of dynamic membraneless ribonucleoprotein (RNP) granules. These structures consist of RNAs and RNA-binding proteins and are formed without a surrounding lipid membrane. Their composition and function depend on the cellular context and stress conditions. Stress granules (SGs) are one of the most studied types of cytoplasmic RNP granules. They form under adverse conditions and contain mRNAs stalled at translation initiation together with translation initiation factors, RBPs, and other regulatory proteins.

The formation of RNP granules is supported by liquid-liquid phase separation (Figure 1.1.). In a biological context, LLPS is a concentration-dependent process in which proteins and/or nucleic acids demix into a dense phase and a surrounding dilute phase (30). This process is driven by weak multivalent interactions, including interactions between structured protein domains,

disordered regions, RNA-binding motifs and RNA molecules. In stress granules, both RNA-protein and protein-protein interactions contribute to condensate assembly, while ATP-dependent remodeling helps maintain their dynamic organization (31).

IDRs are particularly important for LLPS because they provide flexible interaction platforms that can engage in electrostatic, cation-π, hydrophobic, and other weak interactions. These regions may also bind RNA directly and serve as targets for post-translational modifications, such as phosphorylation, methylation and PARylation, thereby regulating condensate assembly and disassembly (32-34). Thus, RNP granules arise from the combined effects of RNA binding, multivalent protein interactions, and dynamic regulation of disordered protein regions.

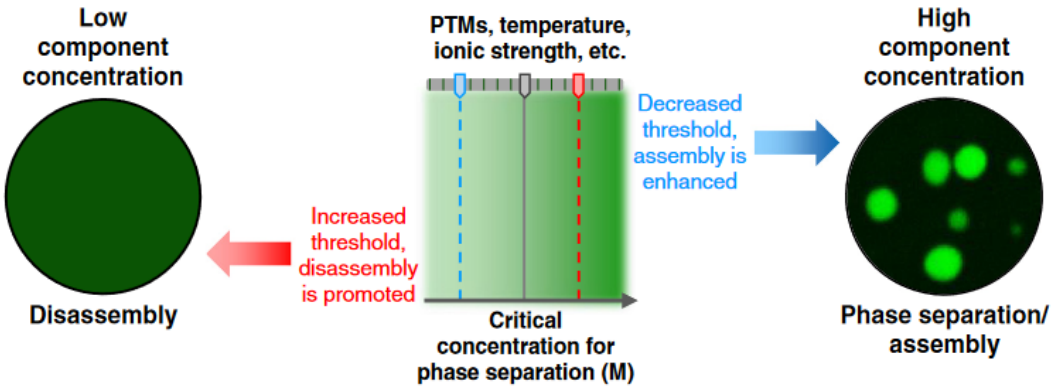

Figure 1.1. Liquid-liquid phase mechanism. LLPS is concentration-dependent and can be tuned by physicochemical alterations to the system, such as changes in temperature or ionic strength, and post-translational modifications in the case of proteins (adapted from Mitrea and Kriwacki, 2016 (1))

1.1.3. Stress granules overview. Stress granules are cytosolic ribonucleoprotein condensates that form rapidly in response to cellular stress and disassemble after stress termination. They contain translationally stalled mRNAs, RNA-binding proteins, translation initiation factors, and additional regulatory

proteins. Due to their dynamic nature, complex composition, and dependence on weak multivalent interactions, SGs are widely used as a model system for studying RNA-protein condensates, liquid-liquid phase separation, and RNA-dependent regulation of cellular stress responses (35, 36).

Stress granules are transient structures that may reach microscopically visible sizes, although smaller submicroscopic assemblies and pre-existing interaction networks between SG components have also been reported (37). Their assembly and disassembly are ATP-dependent processes (38). Functionally, SGs participate in the protection and storage of untranslated mRNAs, redistribution of translation toward stress-response transcripts, regulation of signaling pathways, antiviral responses and suppression of cell death-associated signaling (39). Because SGs are connected with viral infection, cancer, inflammation and neurodegenerative disease, they represent an important model for understanding stress-dependent RNA-protein regulation.

1.1.4. Stress granule dynamics. Stress-induced translation arrest can occur through eIF2α phosphorylation-dependent or eIF2α-independent mechanisms (Figure 1.2). Oxidative stress, amino acid deprivation, and viral infection commonly activate the eIF2α-dependent pathway, whereas stresses such as H_2O_2 treatment, hippuristanol exposure, or starvation may induce SGs through eIF2α-independent mechanisms (41). Despite mechanistic differences, both pathways inhibit translation initiation while allowing elongation to continue, resulting in ribosome runoff and accumulation of untranslated mRNAs that can nucleate SG formation.

In the eIF2α-dependent pathway, stress activates the integrated stress response through one of four eIF2α kinases: PKR, PERK, GCN2, or EIF2AK1. Phosphorylated eIF2α inhibits eIF2B-dependent nucleotide exchange, blocks formation of the ternary initiation complex, and suppresses global translation

initiation. The resulting pool of untranslated mRNAs recruits SG nucleators, including G3BP1/2 and TIA-1/TIAR, which increase local mRNA and protein concentration and promote LLPS-driven SG assembly (2).

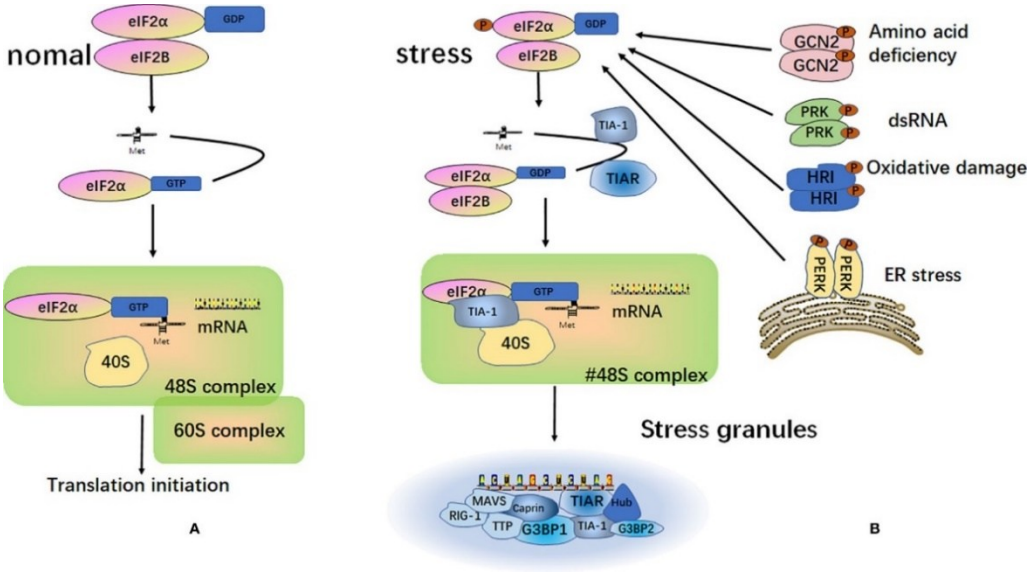

Figure 1.2. The phosphorylation of eIF2α alters the fate of the pre-initiation complex and leads to the formation of stress granules (adapted from Kang et al., 2021(2))

Although global translation is reduced during stress, translation of selected stress-response mRNAs can continue or even increase (42-44). This selective translation allows cells to maintain the synthesis of proteins required for adaptation and recovery. Meanwhile, untranslated mRNAs and associated RBPs form SGs organized into denser cores and more dynamic shells (38). SG nucleators such as G3BP1/2, TIA-1/TIAR, FMRP, and Caprin1 recruit additional RBPs, translation factors, helicases, kinases, and other regulatory proteins, thereby supporting SG maturation and remodeling (40).

Two general models have been proposed to describe SG assembly. In the “cores first” model, small RNP cores form initially and later fuse into larger microscopically visible granules. In the “LLPS first” model, weak interactions between RNAs and proteins first generate phase-separated droplets, followed by

recruitment and organization of denser core structures (38). SG disassembly is less well understood, but it is associated with translation recovery, removal of mRNAs from SGs, and destabilization of protein-protein interaction networks within the granule (47, 48).

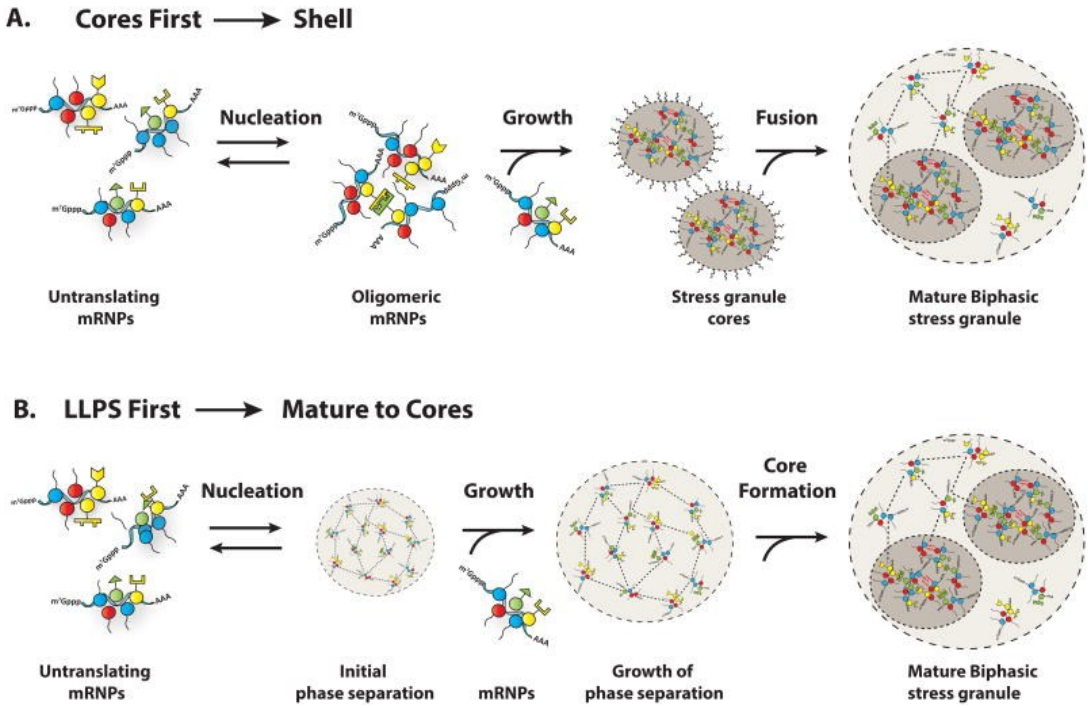

Figure 1.3. Two models of SG assembly (adapted from Protter and Parker, 2016 (49))

1.1.5. SG composition. Stress granules contain stalled 48S pre-initiation complexes, small ribosomal subunits, translation initiation factors, and numerous RNA-binding proteins. Classical SG markers and nucleators include TIA-1/TIAR, G3BP1/2, TTP, FMRP, and Caprin1 (23, 49, 50). Proteomic studies have identified more than 200 confirmed SG proteins and many additional candidate SG-associated proteins, including proteins involved in translation control, mRNA stability, splicing, RNA metabolism, and cellular signaling (40, 51).

1.1.6. Roles of stress granules in health and disease. The major function of SGs is to regulate translation during stress by sequestering mRNAs encoding

housekeeping proteins while allowing translation of selected stress-response transcripts, such as HSP70 mRNA (52, 53). SGs can also serve as signaling hubs, for example, in mTOR, MAPK, and TNF-associated pathways (54, 55).

Stress granules are closely linked to pathological processes. During viral infection, they contribute to innate immune defense and can be induced through PKR-dependent eIF2α phosphorylation. At the same time, many viruses have evolved mechanisms to suppress SG formation, sequester SG proteins, or exploit SG components for viral replication (56-60). In cancer, SGs may support tumor cell survival under hypoxia, endoplasmic reticulum stress, osmotic stress, and chemotherapy, although some forms of SG induction may also promote apoptosis and translational inhibition in cancer cells (39, 61). In neurodegenerative diseases, altered SG dynamics and aggregation-prone RNA-binding proteins, including TDP-43, FUS, TIA-1/TIAR and FMRP, have been linked to ALS, FTD, fragile X syndrome, and related disorders (11-16, 62-67). Disease-associated mutations may increase cytoplasmic accumulation or aggregation of SG-associated RBPs, impair SG clearance, and disrupt the mRNA pool maintained by SG machinery. Thus, SGs are important not only for adaptive stress responses but also for understanding pathological RNA-protein aggregation.

1.2. The ins and outs of G3BP1

1.2.1 Multifunctional stress granule assembly factor G3BP1. G3BP1 was first described as a 68 kDa cytosolic RNA-binding protein associated with Ras-GTPase-activating protein (GAP), although this initial functional assignment was later reconsidered (68, 69). Subsequent studies identified G3BP1 as a multifunctional RNA-binding protein involved in stress granule assembly, mRNA stability and decay, antiviral responses, neuronal RNA regulation and several pathological processes. Among these functions, its role as a central stress granule assembly factor is the most relevant for this dissertation.

G3BP1 belongs to the G3BP protein family, which includes G3BP1 and two G3BP2 isoforms, G3BP2a and G3BP2b. G3BP1 is encoded by the G3BP1 gene and produces a 466-amino-acid protein. G3BP1 and G3BP2 are broadly expressed, although their expression levels vary between tissues (5, 70).

1.2.2. G3BP1 structure and domains. G3BP1 has a modular domain organization typical of RNA-binding proteins involved in stress granule biology. It contains an N-terminal NTF2-like domain, acidic intrinsically disordered region IDR1, proline-rich IDR2, RNA recognition motif (RRM), and C-terminal RGG-rich IDR3 (Figure 1.4). Together, these regions support G3BP1 dimerization, interaction with protein partners, RNA binding and participation in liquid-liquid phase separation.

The NTF2-like domain is required for G3BP1 dimerization and mediates interactions with several partner proteins, including Caprin1 and USP10 (74, 78). These interactions are important for the regulation of stress granule assembly and disassembly. The same domain also contributes to viral protein interactions through recognition of FxDF-like motifs (73). IDR1 is an acidic region that functions as an autoinhibitory element during RNA-dependent phase separation, while IDR2 is a positively charged proline-rich region that counteracts this inhibition and contributes to stress granule assembly (3). IDR2 also participates in PKR recruitment to stress granules, linking G3BP1 to innate immune signaling during viral infection (56).

The C-terminal part of G3BP1 contains the main RNA-binding elements: the RRM and RGG-rich IDR3. The RRM provides canonical RNA recognition, whereas IDR3 contributes additional RNA-binding capacity through positively charged RGG motifs (3, 80). The interplay between IDR1, IDR2 and IDR3 regulates the accessibility of RNA-binding regions and determines the ability of G3BP1 to undergo RNA-dependent phase separation. Thus, G3BP1 combines

protein-interaction, RNA-binding and regulatory disordered regions within one modular scaffold.

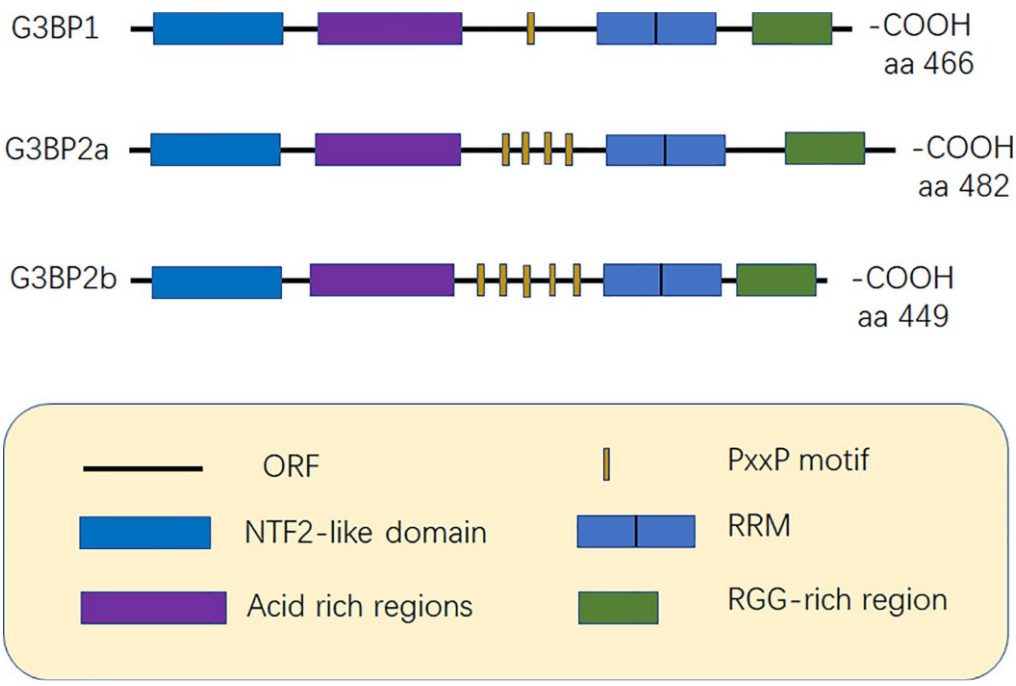

Figure 1.4. Structural features of G3BP protein family (adapted from Kang et al., 2021(2))

Overall, G3BP1 RBP, with RRM and IDR3 responsible for RNA binding, and NTF2-L, IDR1, and 2, play crucial roles in dimerization, interactions with other proteins, subcellular localization, and the enzymatic activity of G3BP.

1.2.3. Regulation and post-translational modification of G3BP1. G3BP1 function in stress granules is regulated through mechanisms that affect its expression, localization, conformational state, RNA-binding activity and interaction with partner proteins. At the level of expression, YBX1 promotes G3BP1 translation under oxidative stress by binding the 5′UTR of G3BP1 mRNA, whereas TDP-43 can stabilize G3BP1 mRNA through interaction with its 3′UTR (5, 61, 81).

Post-translational modifications are central regulators of G3BP1 activity. Phosphorylation affects G3BP1 conformation, dimerization and RNA-binding capacity. In particular, phosphorylation of S149 and S232 modulates the open/closed conformational switch of G3BP1, in which the balance between intramolecular IDR interactions and RNA binding controls phase separation (3, 82). Phosphorylation of Y40 in the NTF2-like domain is also important for dimerization and antiviral stress granule formation (77).

Other modifications further tune G3BP1 function. Arginine methylation within the RGG-rich region affects stress granule formation and may influence RNA binding, whereas JMJD6-dependent demethylation promotes G3BP1 dimerization and SG assembly (83). Acetylation of K376 disrupts interaction with Poly(A)-binding protein and mRNA, thereby promoting SG disassembly, while deacetylation supports SG formation (84). PARylation promotes SG assembly, whereas ubiquitination is mainly associated with SG clearance and disassembly (85–87). Together, these modifications regulate G3BP1-dependent stress granule assembly, maturation, and disassembly by controlling RNA binding, protein interactions, and phase separation.

1.2.4. G3BP1 enzymatic activity. G3BP1 was initially reported to possess phosphorylation-dependent endoribonuclease activity directed toward the 3′UTR of specific mRNA targets, including c-myc mRNA (75, 88). Subsequent work suggested that G3BP1 recognizes defined RNA sequence elements and may contribute to the regulation of mRNA stability. Although this enzymatic activity is less central to the present dissertation than the role of G3BP1 in stress granule assembly and mRNA recruitment, it supports the broader view of G3BP1 as an RNA-binding protein involved in post-transcriptional regulation.

1.2.5. G3BP1 in stress granules. G3BP1 is widely regarded as a central protein in stress granule assembly and function. The first mention of G3BP1 being

a part of cytoplasmic protein-RNA condensates dates back to 2003, where it was shown that G3BP1 co-localizes with HuR and TIA-1 in cytoplasmic foci also containing polyadenylated mRNA (89). While not interacting with eIF2α directly, as opposed to TIA-1, over the years of research, G3BP1 was shown to be the key protein in stress response and subsequent formation of SGs.

The structure of G3BP1 and its ability to bind both RNA and proteins at the same time defines its role in stress granule function. G3BP1 is recruited to SGs from cytoplasm in times of cellular stress but also can generate SGs on its own (89). Moreover, double knockdown of G3BP1 and G3BP2 reduces the formation of SGs (90), while the knockout of both proteins abolishes SG assembly under sodium arsenite-induced stress (3), thus demonstrating the key role of G3BP proteins in SG formation.

There are two main intrinsic properties of G3BP1 that contribute to SG assembly: dimerization via NTF2-L domain and RNA binding. LLPS of G3BP1 is triggered by RNA, mRNA in particular. Furthermore, G3BP1 was shown to prefer long, single-stranded RNA and the availability of RNA-RNA interactions. Both RRM and IDR3 contribute to RNA binding of G3BP1, with deletion mutants ΔRRM and ΔIDR3 having either severely reduced or completely absent ability to bind RNA. Consequently, both ΔIDR3 and ΔRRM variants of G3BP1 were shown to have reduced ability to participate in SG assembly. The interplay between three IDRs of G3BP1 modulated by phosphorylation of S149 and S232 of IDR1 lies in the core of LLPS of this protein. Dephosphorylation of G3BP1 in those sites causes a conformational change, exposing RRM and IDR3 to RNA and thus driving LLPS and subsequent SG formation. Mechanistically, in cases of low RNA availability the intramolecular interaction between IDR1 and IDR3 is favored, thus protein adopts a closed conformation. As the concentration of RNA rises, the intermolecular interaction in the form of RNA replaces IDR1 in interaction with IDR3, and G3BP1 dimer adopts open conformation. The

phosphorylation strengthens IDR1-IDR3 interaction, and IDR2 contributes to this tuning by spacing acidic IDR1 and basic IDR3 (Figure 1.5).

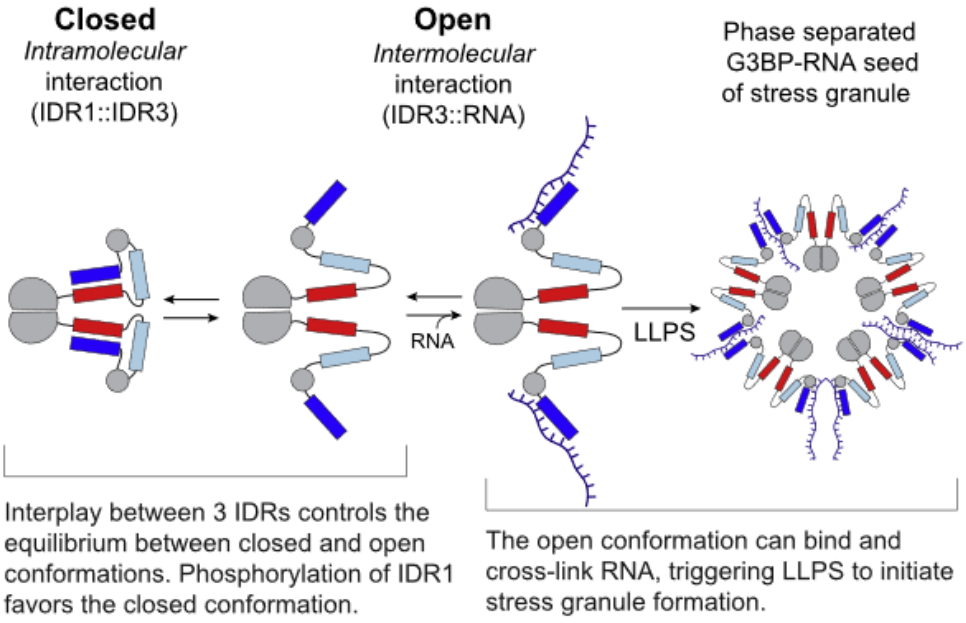

Figure 1.5. Competition between intramolecular IDR1-IDR3 and intermolecular IDR3-RNA interactions facilitate molecular switch in G3BP1 (adapted from Yang et al., 2020(3))

In a model developed on patchy colloids theory, in order to phase separate into a dynamic network, each particle (protein, RNA, or complex) of a system (condensate in this case) has to have a sufficient "valency" – a number of sites to engage other components of the system. The valency of G3BP1, as well as other stress granule proteins, is crucial to their ability to enhance or inhibit stress granule formation. The centrality of G3BP1 in the SG network is a product of its high valency, meaning that G3BP1 has the capacity to mediate multiple interactions; the same is the case with, for instance, UBAP2L, which also has a large valency, and its complex with G3BP1 is essential for SG condensation. Such high-valency proteins are called nodes. The proteins with lower valencies act as bridges from node to node, for example, both TIA-1 and Caprin1 decrease the

concentration of RNA needed to trigger LLPS of G3BP1. In opposition, USP10 has low valency and competes with Caprin1 to limit RNA binding of G3BP1 and thus reduce the SG formation (35).

It is unclear if G3BP1 affects the precise protein composition of SGs, but it was shown that knockdown of G3BP1 results in smaller SGs, which still contain SG markers such as HuR, eIF3G, and eIF4A (91). In light of valency theory, it may be the case that the reduced overall valency of SG is a result of a central node - G3BP1 being limited by knockdown.

1.2.6. G3BP1 functions outside of stress granules. Although G3BP1 is best known as a central stress granule assembly factor, it also participates in RNA-related processes outside canonical SGs. G3BP1 can associate with specific groups of mRNAs and influence transcript partitioning during stress. G3BP1-bound transcripts include mRNAs involved in mitochondrial transport, cytoprotection, and stress-response pathways, indicating that G3BP1 contributes to the regulation of mRNA fate beyond SG nucleation (4). G3BP1 has also been implicated in ribosome-associated quality control, where it cooperates with USP10 in recycling of the 40S ribosomal subunit after aberrant translation events (92).

In addition, G3BP1 participates in structure-mediated RNA decay through RNA-dependent interaction with the RNA helicase UPF1 and may contribute to regulation of mRNAs containing structured 3′UTRs (93). G3BP1 also performs neuron-specific functions, including participation in axonal SG-like granules involved in local mRNA transport and translation during axon growth and regeneration. In dendrites, G3BP1 contributes to local translation and dendritic maturation (8, 10, 94). Thus, G3BP1 functions outside canonical stress granules are mainly connected with RNA transport, transcript regulation and localized translation.

1.2.7 G3BP1 in pathology. G3BP1 has been implicated in multiple pathological processes, including cancer progression, antiviral defense, cardiovascular disorders and neurodegeneration (95). In cancer, altered G3BP1 expression has been associated with proliferation, invasion, metastasis and poor prognosis in several tumor types. For example, elevated G3BP1 levels were linked to reduced survival in oral squamous cell carcinoma, while in gastric, breast, prostate and lung cancers G3BP1 has been connected with signaling pathways involved in tumor growth, stress adaptation and mRNA regulation (96–103). These findings indicate that G3BP1 may act as both a marker of tumor progression and a potential molecular target in cancer-associated stress response pathways.

G3BP1 is also an important component of antiviral defense. During viral infection, it contributes to antiviral stress granule formation and participates in innate immune signaling pathways. In particular, G3BP1, Caprin1, and PKR can form a complex that promotes PKR activation, eIF2α phosphorylation, and SG assembly (56). G3BP1 has also been linked to cGAS/STING and RIG-I/MAVS signaling, which mediate type I interferon responses to viral nucleic acids (95). Several viruses counteract this antiviral function by cleaving G3BP1, sequestering it or exploiting it for viral replication, as shown for enteroviruses, foot-and-mouth disease virus and Chikungunya virus (104–108). Thus, the pathological relevance of G3BP1 is closely connected to its roles in RNA metabolism, stress granule assembly, and cellular stress responses.

1.3. Caprin1 and G3BP1 interaction in and out of stress granules

1.3.1. Overview of Caprin1 structural features. The story of Caprin1 research starts with it being characterized under the name of p137, a 136kDa GPI-anchored membrane protein (109). This proved to be incorrect, as in 2004, Grill et al. reintroduced the same cDNA product under a new name in research

dedicated to finding novel proteins involved in the proliferation of immune system cells. The search resulted in the identification of a pair of highly conserved intracellular proteins, which subsequently were assigned names Cell cycle-associated protein 1 (Caprin1) and Cell cycle-associated protein 2 (Caprin2), respectively, and designated into a separate Caprin family of proteins.

Newly named Caprin1 was shown to have higher levels of expression in dividing cells, specifically T or B lymphocytes, and decreased levels in the absence of proliferation. This is reflected in the analysis of Caprin1 expression in tissue, with the highest expression observed in the thymus, and lowest in tissues with a low percentage of dividing cells, such as muscle and kidney. Additionally, Caprin1 was highly expressed in brain tissue, drawing a resemblance to proteins of MAP and Ras signaling pathways, which have brain-specific functions separated from their role in non-brain cells. Under the name of RNA granule protein 105 (RNG105) was shown to be a component of neuronal RNA granules (110) with RNA-binding ability.

Figure 1.6. Structural features of Caprin family proteins (adapted from Wu et al., 2016 (83))

Caprin1 is a 78 kDa RNA-binding phosphoprotein (116 kDa on PAAG)) encoded by gene membrane component, chromosome 11, surface marker (M11S1) at 11p13 on chromosome 11.

Caprin1 contains two highly conserved Homology Region (HR) domains, HR1 and HR2, with an E-rich region in between and RGG-boxes and RG-rich sequences at the C-terminus. HR1 domain of Caprin1 contains residues

responsible for dimerization (111), and HR2 hosts G3BP1 interaction sequence 369-378 AA called G3BP1 interaction motif (GIM) (Figure 1.6) (7).

Caprin1 is involved in several processes in cells, namely stress granule assembly, cell cycle progression in health and cancer, RNA mediation in neurodegenerative disease, and viral infection resistance, making it a potent research and therapeutic target.

1.3.2. Caprin1 interaction with G3BP1 and role in stress granule assembly. Caprin1 presence in stress granules is closely interwoven with its best-studied partner – G3BP1. Solomon et al. (23) first showed Caprin1 localization into cytoplasmic granules. This study highlighted several important features of Caprin1 regarding its novel, at the time, role in cytoplasmic stress-induced RNPs. Firstly, it was shown that Caprin1 could enter pre-existing SGs in arsenite-induced stress, as well as induce SGs in non-stressed cells. Secondly, the C-terminal region of Caprin1 is required and sufficient for SG entry, since it contains an RGG-box that facilitates RNA binding. Thirdly, the NTF2-L domain of G3BP1 interacts with the C-terminal region of Caprin1. Moreover, RNA-binding domains of G3BP1 and Caprin1 were both shown to bind several mRNAs associated with cell cycle progression, the mRNA of c-Myc and cyclin D2 in particular (23). Lastly, Caprin1 appears to be non-essential for SG formation, as overexpressed G3BP1 induced SG assembly in cells with Caprin1 absent.

The same study described the increase of eIF2α phosphorylation levels when Caprin1 is overexpressed, and the mechanism in play is dependent on Caprin1 ability to bind RNA, as overexpression of Caprin1 with C-terminal region and RGG removed abolished the phosphorylation of eIF2α (23). Authors speculated on the potential role of PKR in this process, as well as the importance of RNA presence generated by Caprin1 when it is overexpressed, stating that

Caprin1 possibly induces conformational changes in RNA in a manner that drives activation of PKR.

Later studies confirmed this hypothesis, as G3BP1 and Caprin1 co-precipitate with inactive PKR. In the model presented by Reineke et al., (2015), G3BP1 and Caprin1 recruit PKR to SGs in a dynamic fashion, so that PKR may be activated and act on eIF2α, which in turn promotes SG assembly as a part of the innate immune response to viruses.

Kedersha et al. (78) expanded upon the role of Caprin1 as a non-essential mediator of SG function. Here, G3BP-null cells (cells with both G3BP1 and G3BP2 knocked out via CRISPR/Cas9) were unable to generate SGs in both the presence and absence of arsenite while Caprin1 was overexpressed. The same article established a competition model between Caprin1 and USP10 in binding with G3BP1 (Figure 1.7). In this model, Ubiquitin specific peptidase (USP10), a deubiquitinase with FDGF sequence that specifically binds G3BP1 is mutually exclusive in its binding to G3BP1 with Caprin1. G3BP1 rapidly shuttles between two states, soluble and insoluble. The binding of G3BP1 by Caprin1 drives SG assembly by lowering the LLPS threshold, while USP10 forces the soluble state of G3BP1 and facilitates SG disassembly.

Several modern studies (6) highlighted the precise picture of this competition. The YNFI(Q) segment of Caprin1 within 356-386 aa of G3BP1 interaction motif (GIM) binds exactly the same hydrophobic groove of G3BP1 NTF2-L domain as the FGDF motif of USP10, with central phenylalanine being the main aromatic anchor residue, adopting the exact conformation for both ligands. G3BP1 possesses 2 pH-sensitive histidine residues on its NTF2-L. The affinity for Caprin1 binding is slightly lower than that of the FGDF motif of USP10 at acidic pH.

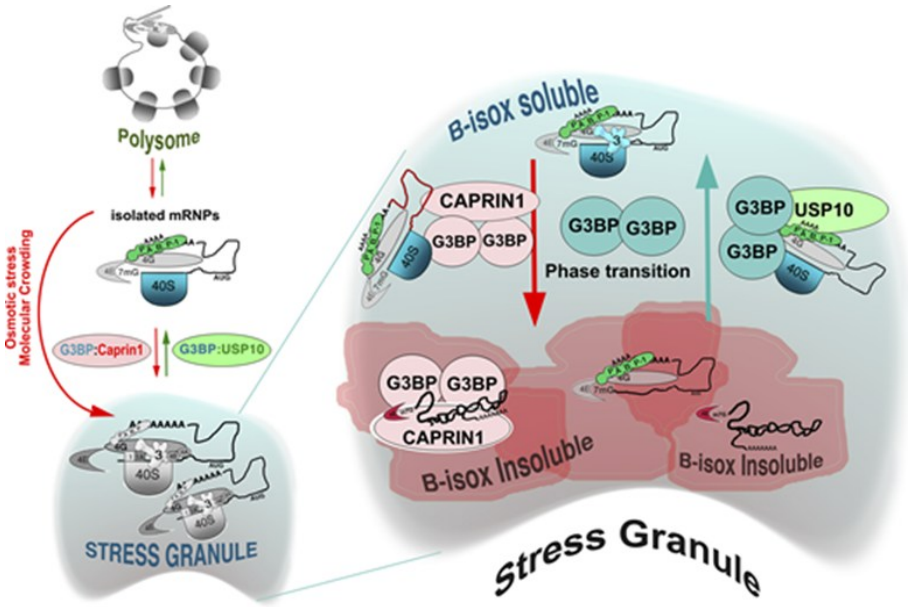

Figure 1.7. G3BP1-USP10-Caprin1 competition acts on SG assembly in an antagonistic manner. Cellular stress leads to an influx of mRNA free from polysomes to cytoplasm. G3BP1 shuttles between two states, in where G3BP1 – Caprin1 interaction leads to the formation of SGs and G3BP1-USP10 interaction leads to the disassembly of SGs (adapted from Kedersha et al., 2016 (58))

Under normal conditions, the G3BP1-Caprin1 complex competes with other NTF2-L binding proteins like USP10 or UBAP2L, but upon stress, Caprin1/G3BP1 condenses into SGs that are mediated by multivalent interactions between IDRs and RNA. This results in pH being lower in SG compared to the surrounding cytoplasm due to a local increase of RNA concentration, upon which Caprin1-G3BP1 complex is destabilized, and USP10 outcompetes Caprin1, shuttling G3BP1 out of SGs, thus facilitating disassembly (6).

1.3.3. Caprin1 in neuron function and neurodegenerative disease. Caprin1 plays an important role in neuronal RNA granules, where it participates in dendritic mRNA transport and local translation regulation. Caprin1 was shown to localize to neuronal dendrites as a component of mRNA-containing neuronal

granules and to bind specific mRNA targets whose products are involved in synaptic plasticity (110). In this context, Caprin1 appears to function primarily as a translational repressor: Caprin1-enriched neuronal RNA granules remain translationally stalled until stimulation, for example by brain-derived neurotrophic factor, promotes Caprin1 release and subsequent translation of associated mRNAs. Caprin1-deficient neurons display reduced dendritic localization of mRNAs encoding Na+/K+ ATPase subunits and regulators of AMPAR retention, Ras, Rho, PI3K, and Rac pathways, resulting in impaired synapse formation, dendritic spine plasticity, and synaptic responses (9, 112).

The role of Caprin1 in neuronal RNA granules also links it to neurodegenerative disease mechanisms. In ALS and FTD, pathological accumulation of FUS and TDP-43 in neuronal RNA granules disrupts local translation by interfering with RNA scaffold proteins such as Caprin1 (113–114). Although Caprin1 contains a prion-like domain, it does not appear to drive these pathological aggregates directly. Instead, FUS- and TDP-43-dependent disruption of neuronal RNA granules promotes Caprin1 dissociation, leading to reduced translation of Caprin1-associated mRNAs required for synapse formation. Caprin1 also interacts with FMRP independently of RNA and co-localizes with it in neuronal cell bodies and RNA granules, supporting a role for Caprin1 in multi-protein ribonucleoprotein complexes involved in translational repression and neuronal mRNA transport (115).

Structurally, Caprin1 can act as a scaffold for interactions with several RNA-binding proteins. The HR1 domain of Caprin1 contains a dimerization region, while distinct interaction sites allow binding of FMRP and G3BP1 without directly overlapping the RNA-binding regions of these proteins (7, 111, 115).

This organization suggests that Caprin1 may simultaneously participate in protein-protein interactions and RNA binding within neuronal or stress-related ribonucleoprotein assemblies. In addition, Caprin1-containing granules have been implicated in antiviral responses in the nervous system, including Japanese

encephalitis virus infection, where viral proteins can interact with Caprin1 and other stress granule-associated factors to interfere with granule formation (111, 116). Thus, Caprin1 represents a multifunctional RNA-binding protein involved in neuronal mRNA transport, local translation, stress granule biology, and disease-associated disruption of ribonucleoprotein granules.

1.3.4. Caprin1 in cancer. Due to its ability to bind mRNAs encoding cell cycle regulators, such as c-Myc and cyclin D2, and its involvement in stress granule biology, Caprin1 has attracted attention in cancer research. Abnormal Caprin1 expression and regulation by non-coding RNAs have been reported in tumor tissues, and Caprin1 has been implicated in pathways controlling proliferation, ubiquitination, glycolysis, and therapy resistance (117). In particular, disruption of Caprin1 degradation through mutations in the SPOP–CUL3 ubiquitin ligase pathway may promote prostate cancer cell proliferation, while Caprin1-dependent regulation of SUMO1 ubiquitination and glycolysis-associated gene expression has been linked to the progression of several cancers. These findings indicate that Caprin1 may contribute to tumor development and stress adaptation, although in the context of this dissertation, its role as a G3BP1-interacting RNA-binding protein involved in stress granule assembly is of primary relevance.

CHAPTER 2

Materials and Methods

2.1 *In vivo* methods

2.1.1 Plasmid preparation. Plasmids encoding Caprin1, G3BP2, FXR1, FXR2, KIF5C, PABPC1L, and EIF4B fused to GFP-tag on C-terminus were constructed by PCR amplification of cDNAs of genes of interest with primers containing appropriate restriction sites and insertion into pEGFP-N1 vector (Clontech).

Plasmids containing cDNA of the G3BP1-DC (aa 1-230), G3BP1-DN (aa 230-466) were obtained from SABNP Lab and full length G3BP1 and YBX1 fused with RFP/GFP-MBD (microtubule binding domain of Tau) were obtained previously (118). The constructs harboring cDNA for, G3BP1-ΔIDR2 fused with C-terminal RFP-MBD, Caprin1 and PABPC1L fused with C-terminal GFP-MBD were obtained using gateway strategy as described in (119). Briefly, cDNA was amplified with primers containing PacI ad AscI sites, cleaved with corresponding restriction enzymes and inserted into backbone entry plasmid RFP/GFP-pCR8/GW/TOPO cut with PacI and AscI enzymes. Next, LR recombination reactions (Invitrogen™) were performed to clone cDNA of genes of interest fused with RFP/GFP-MBD into Gateway® pEF-DEST51 plasmid (Invitrogen™) in accordance with the manufacturer's protocol. In case of G3BP1-ΔIDR2-RFP-MBD, two fragments of cDNA encoding G3BP1 amino acids 1-221 and 340-466 respectively were amplified using pairs of primers with PacI-BamHI and BamHI-AscI restriction sites following digestion using corresponding digestion enzymes. Following ligation of the two fragments using T4 DNA ligase (ThermoFisher), the product was gel-purified and used as a template for a follow up PCR with primers containing PacI and AscI restriction sites. Gateway cloning strategy

described above was used to obtain - G3BP1-ΔIDR2-RFP-MBD in pEF-DEST51 vector.

Plasmids encoding G3BP1, G3BP1-ΔC, G3BP1-ΔN, G3BP1-ΔIDR2 fused with RFP-tag on N-terminus were constructed by amplification of corresponding cDNAs with primers containing appropriate digestion sites and inserted into mRFP-C1 vector (Addgene).

Site-directed mutagenesis of the residues F15W, F33W, and Y40A of human G3BP1 and residue L378P of human Caprin1 was carried out directly on the G3BP1-RFP-MBD-pEF-DEST51 and Caprin1-GFP-MBD-pEF-DEST51 expression plasmids, respectively, by using the ”Quikchange II XL site-directed mutagenesis kit” (Stratagene) and appropriate oligonucleotides (Eurofins Genomics).

Sequences of all obtained plasmids and introduced point mutations were verified with DNA sequencing (Eurofins Genomics)

Table 1.1.

List of the primers used for PCR amplification of cDNAs

PCR primers	Sequence 5`- 3`
Caprin1-Xho1-For	CGCCTCGAGATGAAGCAGATTCTCGGGGTGATC
Caprin1-BamHI-Rev	CGCGGATCCAGATTCACTTGCTGAGTGTTCATTTG
G3BP2-XhoI-For	GCGCTCGAGATGGTTATGGAGAAGCCCAGTCCG
G3BP2-KpnI-rev	CGCGGTACCACGCGACGCTGTCCTGTGAAGCGGCC
FXR1-XhoI-for	GCGCTCGAGATGGCGGAGCTGACGGTGGAGGTTC
FXR1-KpnI-rev	CGCGGTACCTCTGAAACACCATTCAGGACTGCTGC
FXR2-SalI-for	CGCGTCGACATGGGCGGCCTGGCCTCTGGGGGGG
FXR2-KpnI-rev	GCGGGTACCGCTGAAACCCCATTCACCATACTACCC
KIF5C-SacI-for	CGCGAGCTCATGGCGGATCCAGCCGAATGCAGC
KIF5C-KpnI-rev	CGCGGTACCGCCAATTTCTGGTAGTGAGTGGAATTG

Cont. Table 2.1.

PABPC1L-XhoI-for	CGCCTCGAGATGAACGCCAGCGGTTCTGGCTATC
PABPC1L-XhoI-for	CGCCTCGAGATGAACGCCAGCGGTTCTGGCTATC
PABPC1L-KpnI-rev	CGCGGTACCAGGTGCATGTAAGCCTTCGGCTGTTCC
EIF4B-HindIII-for	GCGAAGCTTATGGCGGCCTCAGCAAAAAAGAAG
EIF4B PstI Rev	GCGCTGCAGTTCGGCATAATCTTCTCCCTCATTTTC
G3BP1 PacI For	CGCTTAATTAAATGGTGATGGAGAAGCCTAGTCCCCTG
G3BP1ΔIDR2 BamHI Rev	GCGGGATCCTTCTTCTAATACTGGCTCAGGCTTTTC
G3BP1ΔIDR2 BamHI For	GCGGGATCCCAACTCTTCATTGGCAACCTGCCTCATG
G3BP1 AscI Rev	CGCGGCGCGCCAGGTACTGCCGTGGCGCAAGCCCCCTTCCC
G3BP1 F15W For	GCTGGTCGGGCGGGAATGGGTGAGACAGTATTAC
G3BP1 F15W Rev	GTAATACTGTCTCACCCATTCCCGCCCGACCAGC
G3BP1 F33W For	GACATGCTGCATAGATGGTATGGAAAGAACTCT
G3BP1 F33W Rev	AGAGTTCTTTCCATACCATCTATGCAGCATGTC
G3BP1 Y40A For	GGAAAGAACTCTTCTGCTGTCCATGGGGGATTG
G3BP1 Y40A Rev	CAATCCCCCATGGACAGCAGAAGAGTTCTTTCC
Caprin1 PacI For	GCGTTAATTAAATGAAGCAGATTCTCGGGGTGATCG
Caprin1 AscI Rev	GCGGGCGCGCCCGATTCACTTGCTGAGTGTTCATTTGCG
Caprin1 L378P For	CATACAGGATTCAAAATCCGGCATTGAAAATCAG
Caprin1 L378P Rev	CTGATTTTCAAAATCCGGCATTGAATCCTGTATG
PABPC1L PacI For	GCGTTAATTAAATGAACGCCAGCGGTTCTGGCTATCCG

Cont. Table 3.1.

PABPC1L AscI Rev	GCGGGCGCGCCGCGTGCATGTAAGCCTTCG GCTGTTCC
G3BP1 1-230 HindIII For	CGCAAGCTTGCATGGTGATGGAGAAGCCTAGT CCCC
G3BP1 1-230 RFP EcorI Rev	GCGGAATTCCTAACTCTTCTGAGCATCCTCAG GGGCA
G3BP1 230-466 RFP HindIII For	CGCAAGCTTGCAGTTCTTCTCCAGCACCTGCA GACA
G3BP1 230-466 RFP Ecor1 Rev	GCGGAATTCCTTACTGCCGTGGCGCAAGCC CCCTT
G3BP1-ΔIDR2 RFP HindIII For	CGCAAGCTTGCATGGTGATGGAGAAGCCTA GTCCCC
G3BP1-ΔIDR2 RFP EcoRI Rev	GCGGAATTCCTAGTACTGCCGTGGCGCAAG CCCCCTTC
Caprin1-NdeI For	GCGCATATGAAGCAGATTCTCGGGGTGATCG
Caprin1-XhoI Rev	GCGCTCGAGATTCACTTGCTGAGTGTTCATTTGCG
G3BP1 Nde1 For	CGCCATATGGTGATGGAGAAGCCTAG
G3BP1 HindIII Rev	GCGAAGCTTGTACTGCCGTGGCGCAAGCC

Table 4.2.

Recombinant DNAs

Name of the plasmid	Source	Identifier
pDONR221-Caprin1	DNASU	HsCD00076190
pLX304-G3BP2	DNASU	HsCD00445433
pLX304-FXR2	DNASU	HsCD00435983
pLenti6.3/V5-DEST-KIF5C	DNASU	HsCD00860737
pDONR221-FXR1	DNASU	HsCD00744973

Cont. Table 5.2.

pLenti6.3/V5-DEST-PABPC1L	DNASU	HsCD00870816
pLX304-EIF4B	DNASU	HsCD00446265

Table 6.3.

Mammalian expression vectors

Name of the plasmid	Expression vector	Accession numbers
Caprin1-GFP	pEGFP-N1	NP_005889.3
G3BP2-GFP	pEGFP-N1	NP_001386948.1
FXR1-GFP	pEGFP-N1	NP_005078.2
FXR2-GFP	pEGFP-N1	NP_004851.2
KIF5C-GFP	pEGFP-N1	NP_004513.1
PABPC1L-GFP	pEGFP-N1	NP_001359108.1
EIF4B-GFP	pEGFP-N1	NP_001408.2
G3BP1-RFP-MBD	PEF-DEST51	NP_005745.1
G3BP1-GFP- MBD	PEF-DEST51	NP_005745.1
Caprin1-GFP- MBD	PEF-DEST51	NP_005889.3
Caprin1(L378P)-GFP-MBD	PEF-DEST51	
PABPC1L-GFP- MBD	PEF-DEST51	NP_001359108.1
YBX1-GFP-MBD	PEF-DEST51	
G3BP1(F15W)-RFP-MBD	PEF-DEST51	
G3BP1(F33W)-RFP-MBD	PEF-DEST51	
G3BP1(Y40A)-RFP-MBD	PEF-DEST51	

Cont. Table 7.3.

Caprin1-His	pET-22b	NP_005889.3
G3BP1-His	pET-22b	NP_005745.1
G3BP1-ΔIDR2-His	pET-22b	
RFP-G3BP1	mRFP1-C1	
RFP-G3BP1-ΔC	mRFP1-C1	NP_005745.1
RFP-G3BP1-ΔN	mRFP1-C1	
RFP-G3BP1-ΔIDR2	mRFP1-C1	
G3BP1-ΔC-RFP-MBD	PEF-DEST51	
G3BP1-ΔN-RFP-MBD	PEF-DEST51	
G3BP1-ΔIDR2-RFP-MBD	PEF-DEST51	

2.1.2. Cell Culture. HEK293 (Human Embryonic Kidney 293) cell line was used for cell extract preparation in immunoprecipitation experiments, and HeLa cells (American Type Collection, USA) were used in immunofluorescence experiments due to their size, shape and well-defined microtubule network. Cells were maintained at 37^{O}C 5% CO_2 in high glucose DMEM (Dulbecco`s Modified Eagle Medium, Life Technologies) with the addition of 10% FBS (Fetal Bovine Serum, Thermofisher) and a combination of antibiotics, penicillin at 100 U/ml and streptomycin at 100 μg/ml.

2.1.3 Microtubule Bench assay: Recruitment and mixing experiments. HeLa cells were seeded in 96-well plates with 15000 cells/well density (PhenoPlate^{tm} -96, Perkin Elmer) and co-transfected the following day with indicated plasmids using Lipofectamine 2000 according to manufacturer's instructions for 22-24 hours. For recruitment experiments, GFP/RFP-MBD plasmids were used at starting quantities of 0.7 μg/well and GFP/RFP plasmids

were used at starting quantities of 0.2 µg/well and then adjusted to normalize expression levels to be similar for different plasmids. For mixing experiments GFP/RFP-MBD plasmids were used at starting quantities 0.6 µg/well and the also normalized. After 22-24 hours of transfection, before fixing procedure, cells were rinsed once with PBS. Fixing procedure was conducted in 2 steps; firstly, cells were incubated in ice-cold methanol for 10 minutes at -20°C, washed with PBS and after that, 4% PFA (paraformaldehyde) in PBS was used to fix the cells during 25 min at 37°C. After rinsing with PBS 3 times, cells were stained with 250 mM 4',6-diamidino-2-phenylindole (DAPI) to visualize the nuclei. Cell images were obtained with the Opera Phoenix Plus High-Content Screening System (PerkinElmer) at 40x magnification using a water-immersion objective (Figures 2.1, *b*, 2.2, *b*).

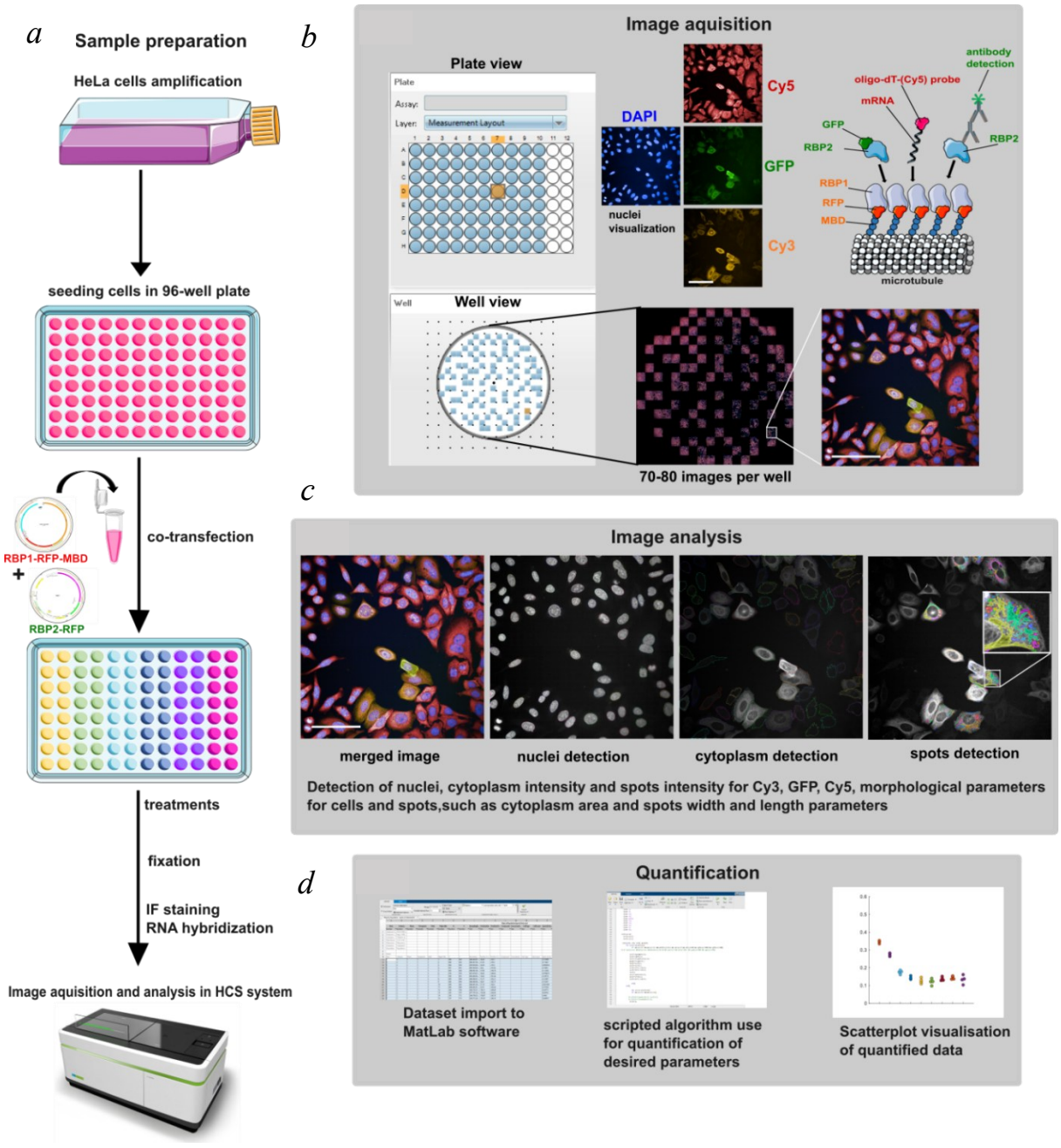

Figure 2.1. Microtubule bench recruitment assay experimental procedure: *a* - HeLa cells cultivation, transfection, and fixing procedures. *b* - Image acquisition *c* - Image analysis within the parameters of the automated pipeline *d* - Quantification of obtained data per cell and per well using Matlab 2021b software

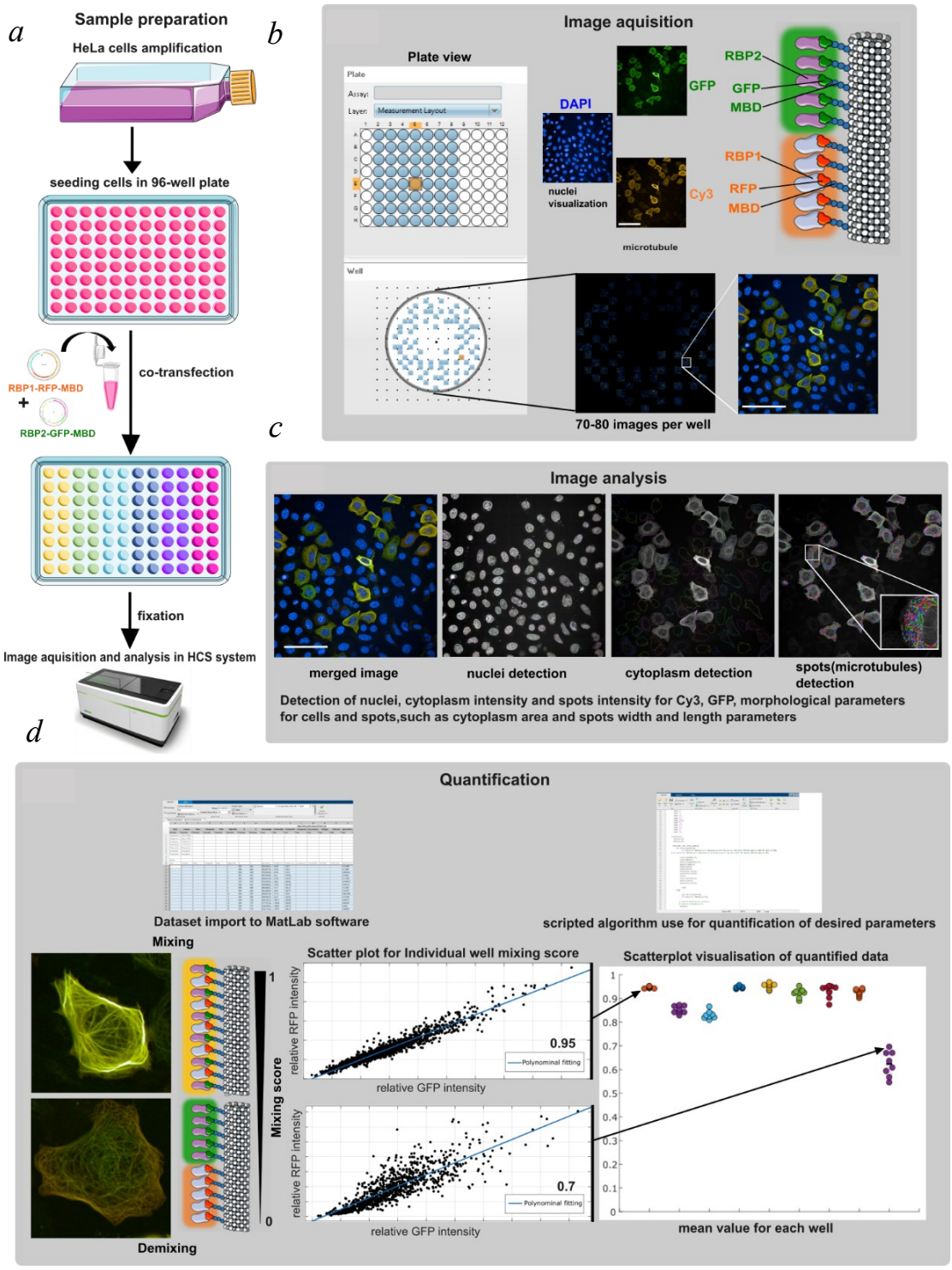

Figure 2.2. Microtubule bench mixing assay experimental procedure *a* - HeLa cells cultivation, transfection, and fixing procedures. *b* - Image acquisition *c* - Image analysis within the parameters of the automated pipeline *d* - Quantification of obtained data per cell and per well using Matlab 2021b software

2.1.4. Immunofluorescence staining for endogenous proteins visualization. Fixed cells were incubated in blocking buffer (NaCl 1M, Tris-HCl 1M pH 7.4, Triton x100 1%, BSA 2%, sodium azide 0.1%, filtered with 22 µm filter) for 30 minutes at 37°C. Next, primary antibodies (rabbit Anti-G3BP1 polyclonal antibody, Sigma, rabbit anti-Caprin1 polyclonal antibody, Proteintech) diluted 1:2000 in blocking buffer were added overnight on shaker at 4°C. Next day, cells were washed twice with PBS and corresponding fluorophore-tagged secondary antibodies (goat anti-rabbit, Alexa 488, Alexa 594, Invitrogen) diluted 1:2000 in blocking buffer, were added to it, left on shaker for 1 hour at RT. Cells were washed 3 times with PBS afterwards.

Table 8.4.

List of antibodies

Antibody	Source	Identifier
rabbit Anti-G3BP1 polyclonal antibody	Sigma	HPA004052
Caprin1 rabbit polyclonal antibody	Proteintech	Cat. 15112-1-AP
rabbit TagRFP Polyclonal Antibody	ThermoFisher	Cat. R10367
Mouse Anti-GFP monoclonal antibody	Sigma	Cat. 11814460001
goat anti-rabbit, Alexa 488	Invitrogen	Cat. A11008
goat anti-rabbit, Alexa 594	Invitrogen	Cat. A11012
IRDye® 680RD Goat anti-Mouse IgG Secondary Antibody	LI-COR	P/N: 926-68070

Cont. Table 9.4.

IRDye® 800CW Goat anti-Rabbit IgG Secondary Antibody	LI-COR	P/N: 926-32211

2.1.5. RNA *in situ* hybridization. mRNA hybridization *in situ* was performed to visualize poly(A) mRNA. Firstly, fixed cells were incubated with 70% ethanol for 10 minutes at RT and then in Tris-HCl 1M pH 8 for 5 minutes at RT. Then the cells were incubated with oligo-dT-(Cy5) fluorescent probe (Molecular Probes Life Tech.) for 2 hours at 37°C in Hybridization buffer (yeast tRNA 0.1%, 0.001% BSA, 10% dextran sulfate, 25% formamide and 10% of 20xSSC buffer) Washings were carried out using 4×SSC buffer twice and then twice with 2×SSC buffer.

2.1.6. Overexpression and siRNA treatment for High-content imaging assays. For overexpression and silencing experiments, HeLa cells were seeded on 96-well plate with $1.3x10^4$ cells/well density and transfected with plasmids expressing the protein of interest at a final concentration up to 0.3 µg/well using Lipofectamine 2000 transfection reagent (Thermofisher) for about 22-24 hours according to manufacturer's instruction. For silencing of G3BP1 experiments, cells were transfected with corresponding small interfering RNA (siRNA) (GeneSolution G3BP1 siRNA, Qiagen) at final concentration of 0.25 µg/well using Lipofectamine 2000 for 24 hours. To detect non-specific effects, a negative control siRNA (AllStars Negative Control siRNA) was used. The efficiency of silencing was measured on a single cell level by comparing cytoplasm fluorescence intensity of endogenous G3BP1 for cells that were treated with siRNA targeting endogenous G3BP1 versus cells that were treated with negative control siRNA.

Table 10.5.

siRNA oligonucleotides

Reagent	Source	Identifier	Sequence
AllStar Negative Control siRNA	QIAGEN	Cat#1027281	
GeneSolution G3BP1 siRNA	QIAGEN	Cat#1027416	
siRNA-G3BP1 3`UTR			Sense (5'->3') (AACUUAAGCAGUUUAUAAC)(dAdG) Antisense (5'->3') (GUUAUAAACUGCUUAAGUU)(dUdA)

2.1.7. Addback experiments. For add-back experiments. HeLa cells were seeded on 96-well plate with $1.1x10^4$ cells per well and transfected with siRNA targeting 3`UTR region of G3BP1 mRNA at final concentration of 0.25 µg/well using Lipofectamine 2000 for 24 hours. Then cells were co-transfected with the plasmids encoding full-length G3BP1 or G3BP1 mutants fused to RFP tag and Caprin1-GFP or plasmid encoding GFP tag. The efficiency of silencing was measured on a single cell level by comparing cytoplasm fluorescence intensity of endogenous G3BP1 for cells that were treated with siRNA targeting 3`UTR of G3BP1 mRNA versus cells that were treated with negative control siRNA (Figure 2.3).

For overexpression, silencing and add-back experiments, HeLa cells were treated with 300 µM sodium arsenite for 1 hour at 37°C with 5% CO_2 to induce oxidative stress and generate stress granules.

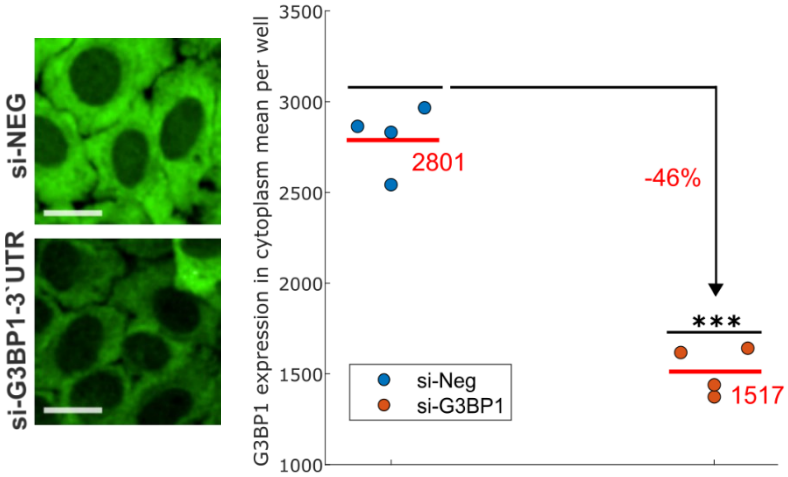

Figure 2.3. Quantification of endogenous G3BP1 silencing in HeLa cells A. Representative images of HeLa cells treated with control siRNA (siNEG) and siRNA targeting 3`UTR of G3BP1. Anti-G3BP1 antibodies were used to quantify the expression of endogenous G3BP1. Scale bar: 20 µm B. Decrease in G3BP1 expression was calculated for four independent samples and amounted to 46%

2.1.8. Data acquisition for MT bench assays, overexpression, silencing and add-back experiments. For both MT bench recruitment and mixing experiments, cell images were obtained using Opera Phoenix Plus High-Content Screening System (Perkin Elmer) on 40x magnification in confocal mode with water immersion (Figures 2.1, *b*, 2.2, *b*). For overexpression, silencing, and add-back experiments, cell images were obtained at 20x magnification in confocal mode, yielding data from 20000 cells per well, with all overexpression experiments performed in 4 repeats.

Up to four channels were used to capture the images with the following values for excitation and emission:

a) DAPI (excitation 405 nm; emission 435-480 nm)

b) Cy2 (excitation 488 nm; emission 500-550 nm)

c) Cy3 (excitation 561 nm; emission 570-630 nm)

d) Cy5 (excitation 640 nm; emission 650-760 nm)

Images were analyzed using Harmony 5.2 software. DAPI signal was used for nuclei detection, Cy2 (for GFP-tagged proteins) and Cy3 (for RFP-tagged proteins) channels were used to detect proteins (fluorescent-tag fused recombinant proteins or indirectly, using secondary fluorochrome-tagged antibodies in case of endogenous proteins) and Cy5 channel was used to detect mRNA through oligo-dT-(Cy5) fluorescent probe (for MT-bench recruitment experiments). HCS system automatically detects fluorescence intensity of nuclei, cytoplasm and objects of interest – spots (microtubules with RFP/GFP-MBD protein attached). Fluorescence analysis included processing the signal by selecting only co-transfected cells, filtering out cells with low co-transfection level (RFP/GFP fluorescence intensity in the cytoplasm >300) and spots with a low width-to-length ratio (<0.2). The channel corresponding to the fluorescence signal of the RFP/GFP-MBD protein was selected to detect microtubules, and a list of readings was acquired. These readings include, number of cells analyzed, the cytoplasm fluorescence of GFP, RFP and mRNA (for MT bench recruitment experiments, Figure 2.1, c) in corresponding channels for each cell, morphology of each cell (roundness, cytoplasm area), number of spots detected and, on the spot level, spots fluorescence of GFP, RFP and mRNA (for MT bench recruitment experiments, Figure 2.1, *c*) in corresponding channels in each spot and width and length parameters for each spot (Figures 2.1, *c*, 2.2, *c*).

For overexpression, silencing, and add-back experiments, similarly, the HCS system automatically detects fluorescence intensity of nuclei, cytoplasm, and objects of interest – spots (stress granules). In silencing and addback experiments, the threshold values of fluorescence intensity in the cytoplasm for the silenced protein were set to cut off the background signal and obtain the data from all the cells in the well. The channel corresponding to the fluorescence signal

of oligo-dT-(Cy5) fluorescent probe was selected to detect stress granules, and a list of readings was acquired. These readings include: number of cells analyzed, the cytoplasm fluorescence of GFP, RFP, and mRNA in corresponding channels for each cell, morphology of each cell (roundness, cytoplasm area), number of spots detected, area of spots detected, and on the spot level, spot fluorescence of GFP, RFP, and mRNA in corresponding channels in each spot.

2.1.9. HCS experiments data processing. The datasets acquired from Harmony 5.2 software analysis were presented in the form of scatterplots and violin plots using MATLAB R2021b software. For microtubule bench recruitment and mixing experiments, The RFP/GFP/Cy5 fluorescence intensity values of each spot were normalized to the values of RFP/GFP/Cy5 intensity in the cytoplasm (Figures 2.1, *d*, 2.2, *d*). The mixing scores were calculated as the squared value of the correlation coefficient (corr function in MATLAB R2021b software) between mean values of fluorescence intensity in spots to mean values of fluorescence intensity in the cytoplasm of RFP-MBD-fused protein to the same parameter of GFP-MBD-fused protein, showing how well the observed data fit the regression model. For MT-bench recruitment experiments, the recruitment scores were calculated as the correlation coefficient (corr function in MATLAB R2021b) between mean values of fluorescence intensity in spots and mean values of fluorescence intensity in cytoplasm on bait protein, to the same parameter of prey, be that mRNA or protein (Figure 2.1, *d*).

In silencing and addback experiments, all data are presented in the form of a violin plot (violin function in MATLAB R2021b) for mean per cell quantification, and mean values per cell-per well were presented in the form of a univariate scatterplot (UnivarScatter function in MATLAB R2021b software). The enrichment values for proteins and mRNA are quantified as the mean per-cell (well) ratio between the fluorescence level in spots (SGs) and the mean per-cell

(well) fluorescence level in the cytoplasm. For the total SG area per cell, the mean value of all spots (SGs) per cell was selected. For the total mRNA enrichment parameter, the mean values of the single spot area of SGs per cell were multiplied by the mean value of the number of spots per cell and the mean value of the mRNA enrichment per cell.

2.1.10. Statistical analysis. All statistical tests were performed using MATLAB. The two-sample *t test* test was performed using the ttest2 function. Significance levels were indicated as *$p < 0.05$, **$p < 0.01$, ***$p < 0.001$, and not significant (n.s.).

2.2 *In vitro* methods

2.2.1. Protein production and purification. Three protein fragments (human Caprin-1 (1 aa - 709 aa), human G3BP1 (1 aa - 466 aa), and G3BP1-ΔIDR2 (described in plasmid production section)) were used for in vitro experiments, including electrophoretic mobility gel shift assay (EMSA) and Atomic Force Microscopy (AFM).

These protein fragments were overexpressed with a His6 Tag for purification. G3BP1-ΔIDR2-His6 was generated using the previously obtained RFP-G3BP1-ΔIDR2 plasmid. The protein fragments were overexpressed in E. coli BL21 (DE3) at 37 °C in 1 L of 2YT-ampicillin medium. After the optical density of the cultures reached 0.7, 1 mM IPTG was added, and the cultures were maintained under agitation for 3h at 37 °C. The cells were harvested and washed with 20 ml of cold 10 mM Tris-HCl buffer, pH 7.6, containing 100 mM KCl. The cell pellet was resuspended in 20 ml of Buffer solution A (Tris-HCl 25 mM, KCl 2M, DTT 1 mM, Complete EDTA-free Protease Inhibitors, PMSF 1 mM, Urea 8 M, pH 7.6) following the manufacturer's recommendations. Cells were disrupted

by sonication on ice (Bioblock Vibracell sonicator, model 72412). The resulting suspension was centrifuged at 4 °C for 30 min at 74,000xg in a TL100 Beckman centrifuge.

Full-length G3BP1 and Caprin1 proteins, as well as the G3BP1-ΔIDR2 construct, were purified using Ni^{2+} - NTA-agarose (Qiagen) following the manufacturer's recommendations. The supernatant was incubated for 2 h at 4°C with Ni^{2+} - NTA-agarose (Qiagen) (20 mg of proteins/ml of resin) pre-equilibrated in buffer A containing 10mM imidazole. The resin was then washed extensively with buffer A containing 10 mM imidazole, then with buffer solution A containing 15 mM imidazole. The next 3 washes were performed in Buffer solution B (Tris-HCl 25 mM, KCl 200 mM, DTT 1 mM, Complete EDTA-free Protease Inhibitors, PMSF 1 mM, Urea 8 M, pH 7.6) with a gradual increase of imidazole concentration from 20 mM to 50 mM. The elution of the proteins was performed in Buffer solution B by progressively increasing the imidazole concentrations (from 75 mM to 300 mM). After visualizing the purification steps by SDS-PAGE (Laemmli, 1970) using a 12% poly-acrylamide gel, pure protein fractions were pooled and buffer-exchanged against desalting buffer (HEPES 50 mM, KCl 25 mM, TCEP 1 mM Urea 8 M pH 7.6) by using a Superdex PD-10 column (GE Healthcare). The final preparations were snap-frozen and stored at -80°C.

2.2.2. Immunoprecipitation assay and western blot. HEK293 cells were grown on 6-well plates to 90% confluence and co-transfected with indicated plasmids using Lipofectamine 2000 according to manufacturer's instructions for 22-24 hours. RFP-G3BP1 FL, -G3BP1-ΔC, -G3BP1-ΔN and -G3BP1-ΔIDR2 plasmids were used at 3 µg/well, Caprin1-GFP plasmid was used at 2 µg/well and YBX-1-GFP plasmid was used at 1 µg/well. The cells were placed on ice and rinsed twice with PBS, then lysis buffer (50 mM Tris, 150 mM NaCl, 1% NP40, 100 mM of PMSF with RNAse A and protease inhibitors added) was added and

the samples were incubated on ice for 10 minutes. Afterwards, lysed cells were transferred to 1,5 ml tubes and centrifuged for 10 minutes at 10000g at 4°C. The supernatant was collected into fresh tubes and inputs prepared (10 µl of lysate and 5 µl of Laemmli buffer 5x).

For immunoprecipitation, 1 µl per sample of binding antibodies (Mouse Anti-GFP monoclonal antibody, Sigma) was added to 450 µl of supernatant, and incubated for 1 hour at 4°C on multivortex. Afterwards, 30 µl per sample of pre-washed (3 times wash with lysis buffer) protein G sepharose fastflow beads were added to IP samples and incubated for 1 hour at 4°C on multivortex. Next, supernatant was removed and the sample was washed 4 times with IP wash buffer (50 mM Tris, 150 mM NaCl, 0,1% NP40) and samples were prepared for SDS-PAGE by adding 30 µl of 5x Laemmli buffer per sample and heated up for 5 minutes.

For Western blot analysis, first, proteins were separated on 10 % SDS-PAGE and transferred onto Amersham Protran 0.45 NC nitrocellulose Western blotting membrane (Cytiva). Afterwards, the membrane was blocked with non-fat dry milk 5% for 1 hour at room temperature then washed with TBS-Tween buffer (20 mM Trizma Base, 143 mM NaCl, pH 7.6, 1% Tween 20) incubated overnight at 4°C with primary antibodies (rabbit TagRFP Polyclonal Antibody, Thermofisher, 1:5000, Mouse Anti-GFP monoclonal antibody, Sigma, 1:5000). After a wash step, the secondary antibodies (LI-COR IRDye, IRDye 800CW goat-anti-rabbit 1:5000, IRDye 680RD goat-anti-mouse 1:5000) were added to the membrane in TBS-Tween buffer for 1 hour at RT. The membrane was washed with TBS-Tween buffer, bound antibodies were detected with Amersham Typhoon Bioimager.

2.2.3. Electrophoretic mobility shift assay. Purified G3BP1, G3BP1-ΔIDR2 and Caprin1 proteins were serially diluted in HEPES 50 mM, KCl 25 mM,

TCEP 1 mM pH 7.6 buffer solution until final concentration of 300 mM/well of Urea was achieved. M13mp18 single-stranded DNA (New England Biolabs) was incubated on 95˚C for 5 minutes, cooled down on ice and diluted in HEPES 50 mM, KCl 25 mM, TCEP 1 mM pH 7.6 buffer solution to contain 100 ng/well. In case of mixtures of G3BP1 and Caprin1, proteins were pre-mixed and incubated with ssDNA for 10 minutes before loading. Samples were analyzed on 0.5% agarose gel (with BET 5% in TAE 0.5x) for 1.5 hours at 25V

2.2.4. Atomic Force Microscopy (AFM) imaging. Full-length G3BP1 and Caprin1 proteins were incubated at room temperature alone or mixed at the indicated concentration with 2luc mRNA (2 ng/mL) in a Tris buffer (10 mM Tris, 15 mM KCl, 2 mM $MgCl_2$, 1 mM DTT, 10 mM Putrescine, pH 6.8). A 10 µL droplet was deposited on a freshly cleaved mica surface, which was quickly immersed in a diluted uranyl acetate solution (0.02 % in water) to fix the sample. The samples were dried with filter paper before imaging. AFM scans were obtained using PeakForce tapping mode in air with Nanoscope V Multimode 8 software (Bruker, Santa Barbara, CA). This model enables continuous force-distance curves recording using Scanasyst-Air probes (Bruker). Images were captured at 1512x1512 pixels at a line rate of 1.5Hz. The “particle analysis” tool on the Nanoscope Analysis software (version 1.70) was used to determine the molecular dimensions of particles (protein aggregates and mRNA: protein complexes) from at least two independent samples. Basically, a threshold of 2 nm was applied to discard small particles or patterns (uranyl acetate background) and free mRNA from the analysis, and at least 6 scanned areas (total area = 100 μm^2) were analyzed.

CHAPTER 3

RESULTS AND DISCUSSION

3.1. G3BP1 binds Caprin1 *in vivo*, and the recruitment of Caprin1 to stress granules is affected by G3BP1

In order to form complex RNA-protein assemblies, RBPs form multi-node networks, in which key proteins with high valencies represent nodes and lower valency proteins represent bridges (Chapter 1.2.). G3BP1 is a central protein in such a network in the case of stress granules. Despite that, each protein is still selective in its binding to other proteins and RNA, which creates complex but organized systems. To begin our investigation, we asked whether G3BP1 can interact with a broad selection of RBPs directly or through RNA or whether its interactome is highly specific. To approach this, first, we tested the interaction of G3BP1 with cytoplasmic RBPs from different families hosting various RNA-binding domains. Among them, FXR1 is an mRNA-binding protein that hosts three KH domains, an RGG-box, and is involved in miRNA processing, localization, stability, and regulation of RNAs (120). YBX1 is a DNA/RNA-binding protein with one CSD domain (121). eIF4B is a translation initiation factor with a single RRM and large IDRs. eIF4B is a component of cap-dependent translation and enhances the activity of RNA helicase eIF4A (122), and PABPC1L is an important paralog of the PABPC1 protein, hosts 4 RRMs, and is involved in colorectal cancer (123). Like G3BP1, G3BP2 possesses a single RRM and RGG-box on the C-terminus (Chapter 1.2.2) and Caprin1, where RNA-binding capability comes only from the RGG-box low-complexity sequence (Chapter 1.3.1). KIF5C is a molecular kinesin, a protein that facilitates trafficking along microtubules (124), and is not an RBP that was used as a control.

In order to access the protein and RNA binding capabilities of G3BP1 and the subsequent role of G3BP1 in the recruitment of RNA to stress granules, we

used a microtubule-bench recruitment assay, which was developed in the SABNP laboratory (118). In short, in order to observe and quantify the interaction between two proteins *in vivo*, the bait protein, labeled with RFP-tag, is brought to microtubules via fusion to a microtubule-binding domain (MBD), and the prey protein is labeled with GFP-tag (see Figure 3.1, *a* for the experimental principle). Both plasmids are co-transfected simultaneously, so we can observe the appearance of microtubules in the GFP channel, indicating the presence of interaction. The recruitment score is measured by automatic detection of the microtubules (spots) in the fluorescence channel of the bait protein and then measuring the fluorescence increase in spots for the prey protein channel (Materials and methods and figure 2.1 for details). In the case of RNA-binding proteins, mRNA present in the cytoplasm can affect the interaction, as RBPs are known to form higher orders of assembly by forming complexes with mRNA. The MT bench assay allows us to anchor protein-RNA-protein complexes and compare recruitment scores across robust datasets. Here, we tested the recruitment of the selection of RBPs to G3BP1. The obtained results show that Caprin1, closely followed by YBX1, has the strongest recruitment scores, while the rest of the tested proteins show low levels of interaction compared with control samples, which were co-transfected with G3BP1-RFP-MBD and GFP-tag. Surprisingly, G3BP2, a known heterodimerization partner of G3BP1 (90), showed levels of interaction lower than expected, suggesting some conditionality in the interaction of G3BP1 and 2 (Figure 3.1, *b*). We speculate that relatively low recruitment of G3BP2 to G3BP1 may be linked to the experiment being conducted in non-stressed cells. Homo- or heterodimerization of G3BP is a key prerequisite for SG assembly, and in the absence of stress, the affinity between G3BP1 and 2 may be decreased to prevent spontaneous condensate formation. Additional experiments, such as the MT bench recruitment assay in arsenite stress conditions, for example, may be needed to investigate this observation.

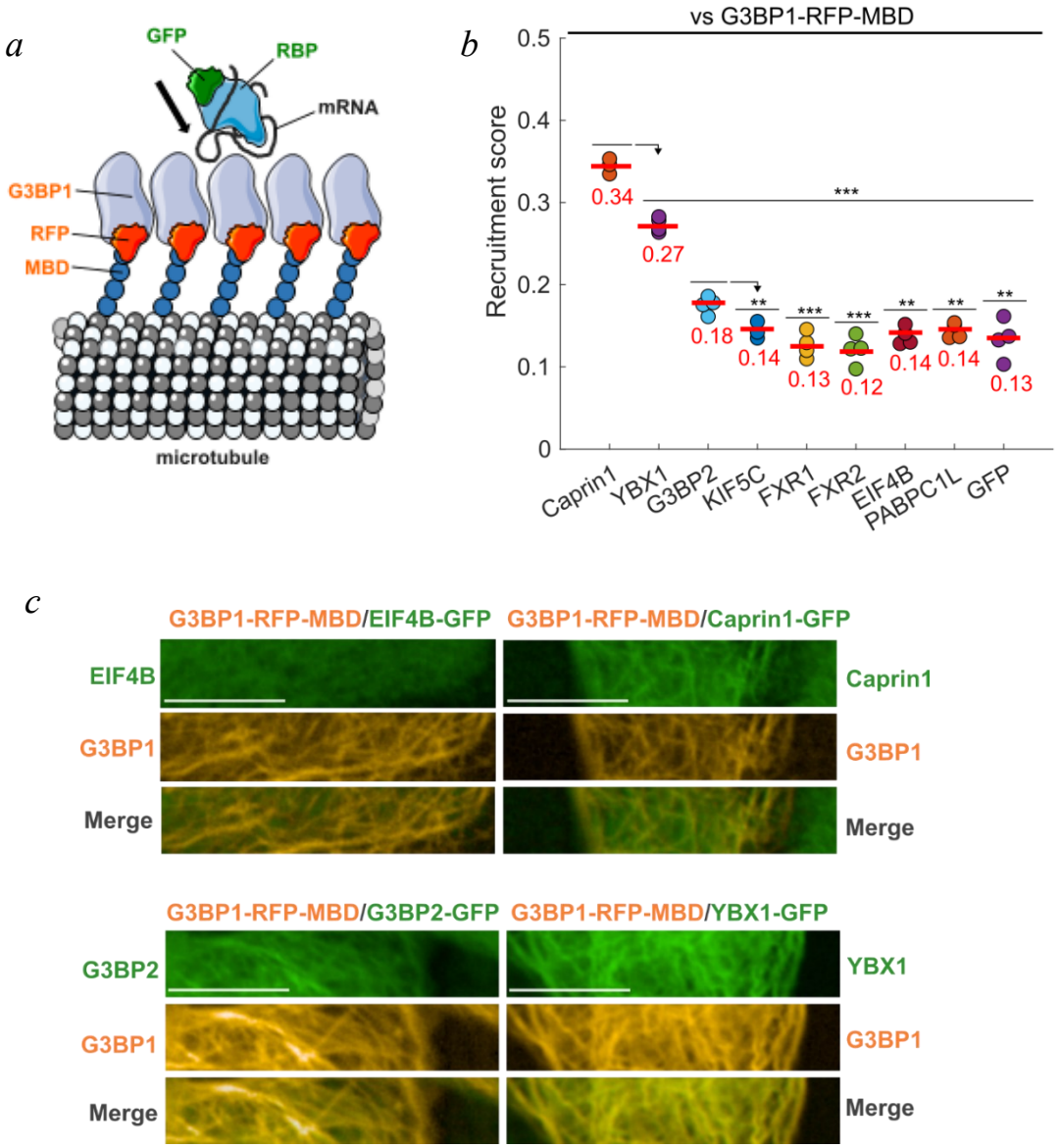

Figure 3.1. G3BP1 selectively recruits Caprin1 to microtubules. *a* - Principle of the microtubule bench recruitment assay used to measure the recruitment of prey protein brought to microtubule-fused prey protein in HeLa cells. MBD – microtubule binding domain. *b* - G3BP1 recruits Caprin1 to microtubules the strongest out of the selection of RBPs **$p < 0.01$, ***$p < 0.001$, paired t-test. Each dot represents the mean value of single cell analysis in a single well (see Materials and methods for details). c - Representative images of MT bench recruitment of EIF4B, Caprin1, G3BP2 and YBX1 to G3BP1-RFP-MBD. Scale bar: 10 μm

Thus, we confirm that G3BP1 selectively binds cytoplasmic RBPs *in vivo* even in the presence of mRNA, and interacts with Caprin1 the strongest out of the selection.

The combination of structured and low complexity domains of RNA-binding proteins in conjunction with RNA is the driving force behind liquid-liquid phase separation. While the ability of proteins to undergo LLPS requires direct protein-protein interaction, additional factors, such as self-adhesion of LC sequences and RNAs acting as scaffolds, contribute to the promotion of LLPS. We inquired about G3BP1's ability to form compartments in which it is mixed with other RBPs. For this, we conducted a mixing MT bench assay (119), in which we confined RFP- or GFP-tagged proteins to microtubules via fusion to MBD and observed the formation of separate phases formed by two proteins or a mostly homogenous distribution of proteins along microtubules (see Materials and Methods and Figure 2.2). Our results obtained when G3BP1 and several RBPs are brought on microtubules show that G3BP1 mixing with itself is highest, closely followed by mixing with Caprin1 (Figure 3.2 *b*). Despite the results of the MT bench recruitment assay, in which YBX1 is recruited strongly to G3BP1 bound on microtubules (Figure 3.2, *b*), in the mixing assay, YBX1 demixes with G3BP1, indicating that despite RNA-mediated interaction between those 2 proteins, they tend to form separate compartments in vivo. In the case of PABPC1L, G3BP1 strongly demixes with it and no significant recruitment is detected in the MT bench recruitment assay (Figure 3.2 *b*). The mixing score evaluation reveals that the multimerization of G3BP1 with itself drives the formation of homogeneous compartments in which other RBPs are not easily accepted, regardless of their RNA affinity. The integration of RBPs like Caprin1 in the G3BP1-rich phase requires specific interaction in addition to their potential RNA binding

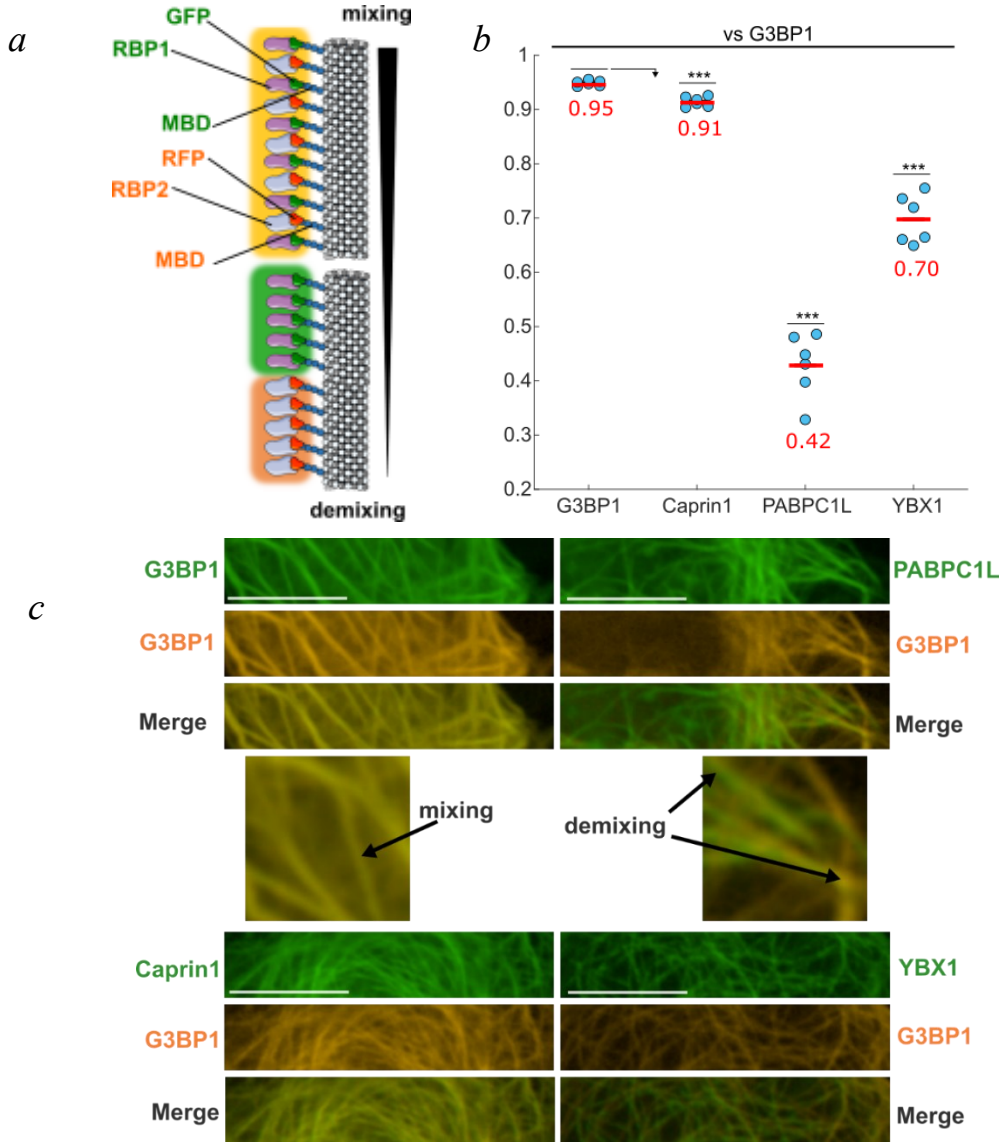

Figure 3.1. G3BP1 mixes well with itself and Caprin1. *a* - Principle of the microtubule bench mixing assay used to measure the mixing score of two GFP- or RFP labeled proteins in HeLa cells. MBD – microtubule binding domain. Pairs of tested RBPs fused with MBD were co-expressed to automatically measure their mixing along microtubules. The mixing score was measured for different pairs of proteins with HCS imager and automated pipeline. *b* - G3BP1 mixes well with Caprin1 and itself, but not PABPC1L or YBX-1. ***$p < 0.001$, paired t-test. Each dot represents the mean value of single cell analysis in a single well (see Materials and Methods). *c* - Representative images of mixing between G3BP1, Caprin1, PABPC1L and G3BP1. Arrows indicate examples of mixing and demixing. Scale bar: 10 µm

As mentioned earlier, G3BP1 possesses a notable ability to undergo LLPS due to the self-adhesion of its unstructured intrinsically disordered regions and RNA-binding ability. A combination of these features allows G3BP1 to form cytoplasmic condensates – stress granules in cooperation with multiple other cytoplasmic RBPs. Consequently, there is a strong link between the protein and RNA binding abilities of G3BP1 and its ability to form condensates and perform one of its key roles – stress granule assembly. Stress granules present a perfect model environment for looking at G3BP1 condensation abilities in vivo since cellular stress can be controllably triggered using such stress factors as sodium arsenite, which results in the formation of said SGs. Moreover, all stress-induced condensates that appear in response to oxidative stress contain wild-type G3BP1, as without G3BP1 or its paralog protein G3BP2 stress granules assembly in response to oxidative stress cannot be triggered (3). Given G3BP1 centrality in the SG network, it is interesting to observe the relationship between the enrichment of G3BP1 in SGs and the recruitment of other stress granule RBPs to this cytoplasmic condensate.

As such, we conducted an overexpression experiment in which, G3BP1 was silenced using si-RNA targeting endogenous G3BP1, and several proteins out of the selection namely YBX1, Caprin1, G3BP2, and KIF5C were overexpressed (Figures 21, 22, 23). KIF5C is not associated with SG assembly and function, thus serving as a control (Figure 23A). Cells were subjected to 300 μM sodium arsenite to induce oxidative stress, giving us model conditions for observation of mRNA and protein recruitment behavior to SGs. We performed mRNA *in situ* hybridization (Materials and Methods for details) to detect mRNA in the cytoplasm and stress granules and measure respective levels of mRNA enrichment in G3BP1-silenced and non-silenced cells. We measured the enrichment level of G3BP1 and the selection of proteins in stress granules, as well as mRNA enrichment, and compared the data for normal conditions and si-G3BP1 conditions. In cells treated with non-targeting siRNA (si-NEG), all three tested

proteins are enriched in SGs, while KIF5C is not accumulated in SGs (Figure 3.3). The enrichment of YBX1 is 14.8% higher than that of Caprin1, and the enrichment of G3BP1 is 19.7%. Both of these proteins are important nodes in SGs and are heavily recruited to them (Figure 3.3).

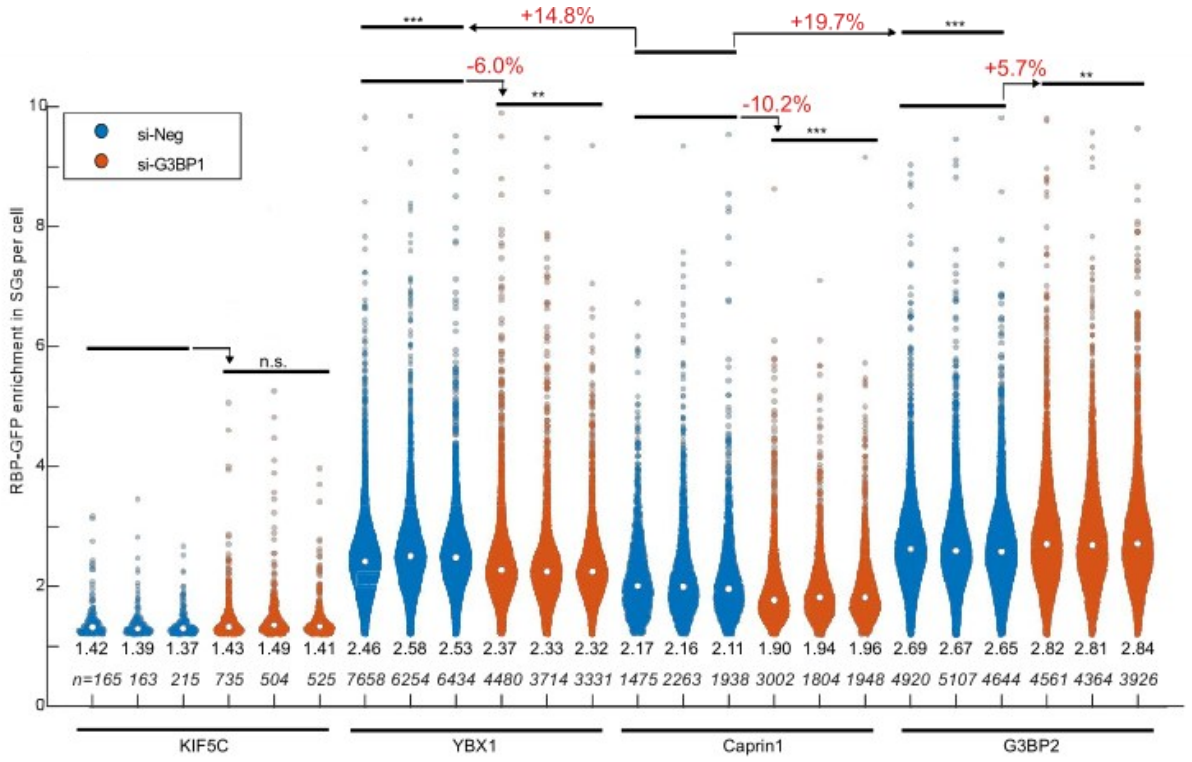

Figure 3.3. The level of G3BP1 enrichment in SGs influences stress granule RBPs recruitment to SGs. Violin plots represent the mean per cell relative enrichment level of different GFP-labeled RBPs in stress granules in HeLa cells subjected to oxidative stress conditions. Each violin represents data for all cells in the well, and each condition is shown in triplicate (see Materials and methods for details). n: number of cells analyzed. **p < 0.01, ***p < 0.001, paired t-test, n.s., non-significant

In cells treated by siRNA targeting endogenous G3BP1, for all 3 tested proteins, the recruitment into SGs was affected by G3BP1 silencing, while the control protein was not affected. In the conditions of a 29% decrease in G3BP1 expression level in the cytoplasm following silencing with si-G3BP1 (Figure 3.5, *b*), the relative enrichment level of YBX1 in SGs was decreased by 6%, the level

of Caprin1 decreased by 10%, and the level of G3BP2 increased by 5,7% (Figure 3.3), thus making Caprin1 the most negatively affected protein out of selection. For G3BP2, an increase in the enrichment level of this protein in SGs after G3BP1 silencing shows substitution that was demonstrated previously (78).

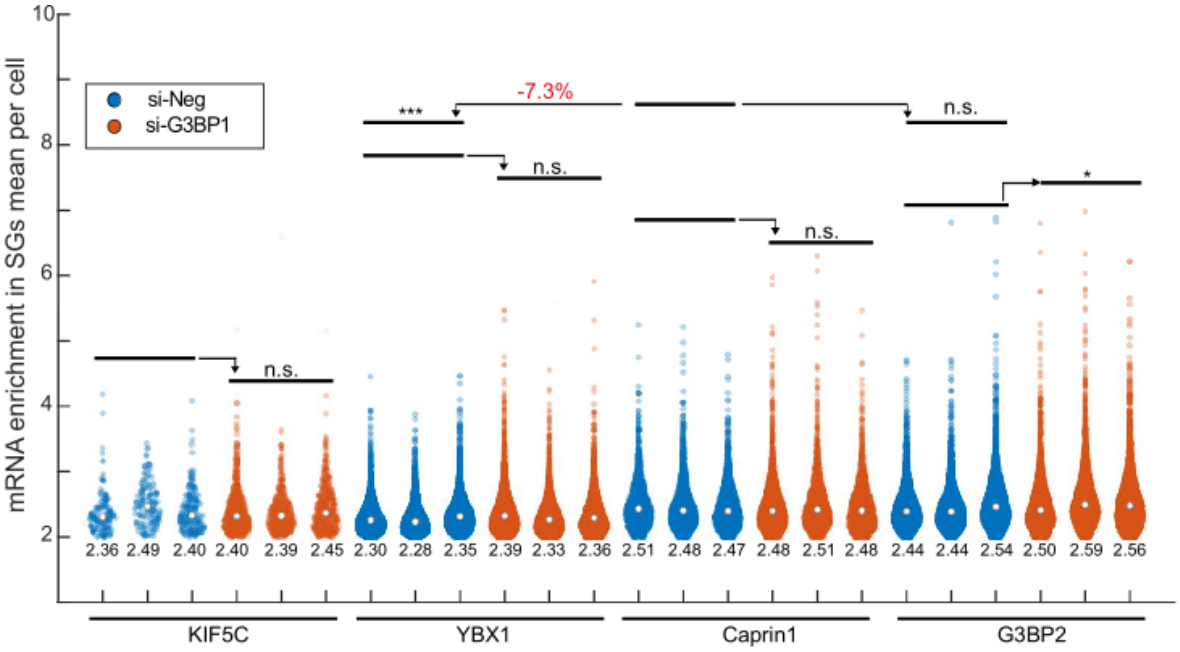

Figure 3.4. The level of G3BP1 enrichment in SGs influences and mRNA recruitment to SGs. Violin plots represent mean per cell relative enrichment level of different GFP-labeled RBPs in stress granules in Hela cells subjected to oxidative stress conditions. Each violin represents data for all cells in the well and each condition is shown in triplicate (see Materials and methods for details) *p < 0.05, **p < 0.01, ***p < 0.001, paired t-test, n.s., non-significant

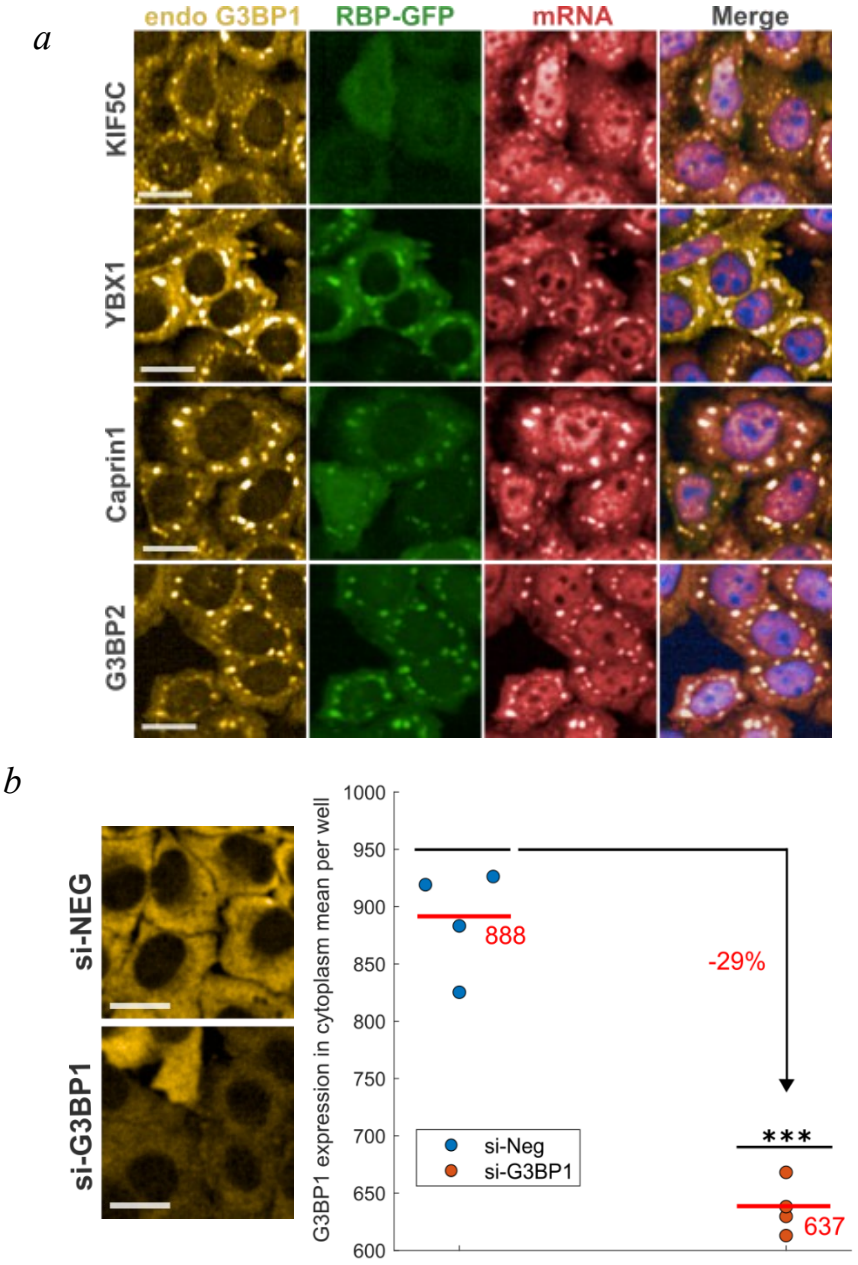

Figure 3.5. Overexpression of stress granule RBPs in HeLa cells with endogenous G3BP1 depleted. *a* - Representative images of HeLa cells subjected to oxidative stress via 300mM sodium arsenite expressing GFP-labeled RBPs, with endogenous G3BP1 tracked via specific antibodies, and mRNA tracked via oligo-dT-(Cy5) fluorescent probe. Scale bar: 20 µm. *b* - Right side: representative images of HeLa cells treated with negative control siRNA and siRNA targeting G3BP1; endogenous G3BP1 expression level was tracked using anti-G3BP1 antibodies. Scale bar: 20 µm. Left side: The decrease in G3BP1 expression was calculated for four independent samples and amounted to 29%

Concomitant to the measurement of the RBP enrichment in stress granules, it is possible to follow the mRNA recruitment in these condensates (Figure 3.4). Firstly, the decrease in G3BP1 expression does not clearly affect mRNA enrichment in SGs, regardless of whether the RBP is overexpressed. Conversely, Caprin1 and G3BP2 overexpression lead to an equal increase in mRNA levels in SGs compared to YBX1. In addition, while G3BP2 enrichment in SGs is significantly higher compared to Caprin1 (+ 19.7%, see figure 3.2), the levels of mRNA enrichment are equal, which suggests a particular role of Caprin1 in mRNA recruitment in SGs.

3.2. G3BP1-Caprin1 complex RNA-binding properties

Caprin1 is one of the best-studied interactors of G3BP1, and results from Chapter 1 suggest that there is a link between Caprin1 binding with G3BP1 and mRNA recruitment to stress granules under arsenite stress conditions. RNA binding of G3BP1 is facilitated by the RRM domain and RGG-boxes at the C-terminus (Chapter 1.2.1), and Caprin1 binds RNA only with RGG-boxes at the C-terminus (Chapter 1.3.1). We decided to delve into the RNA binding of both proteins further and search for a link between G3BP1's own RNA binding capabilities and the potential to bind RNA of the G3BP1-Caprin1 complex. Simultaneously with tracking the prey protein that binds to the bait fused to MBD, in the MT bench recruitment experiment, we can observe the level of mRNA recruitment to the bait protein. Performing *in situ* hybridization with an oligo-dT-(Cy5) fluorescent probe allows us to measure the increase of Cy5 fluorescence on microtubules occupied by bait protein (see Materials and Methods and Figure 3.6, *b* for experiment principle). We performed such MT bench recruitment to compare the RNA binding of G3BP1 with both endogenous and overexpressed

Caprin1-GFP and observe if overexpression of Caprin1 will influence the RNA binding of G3BP1 bound to microtubules.

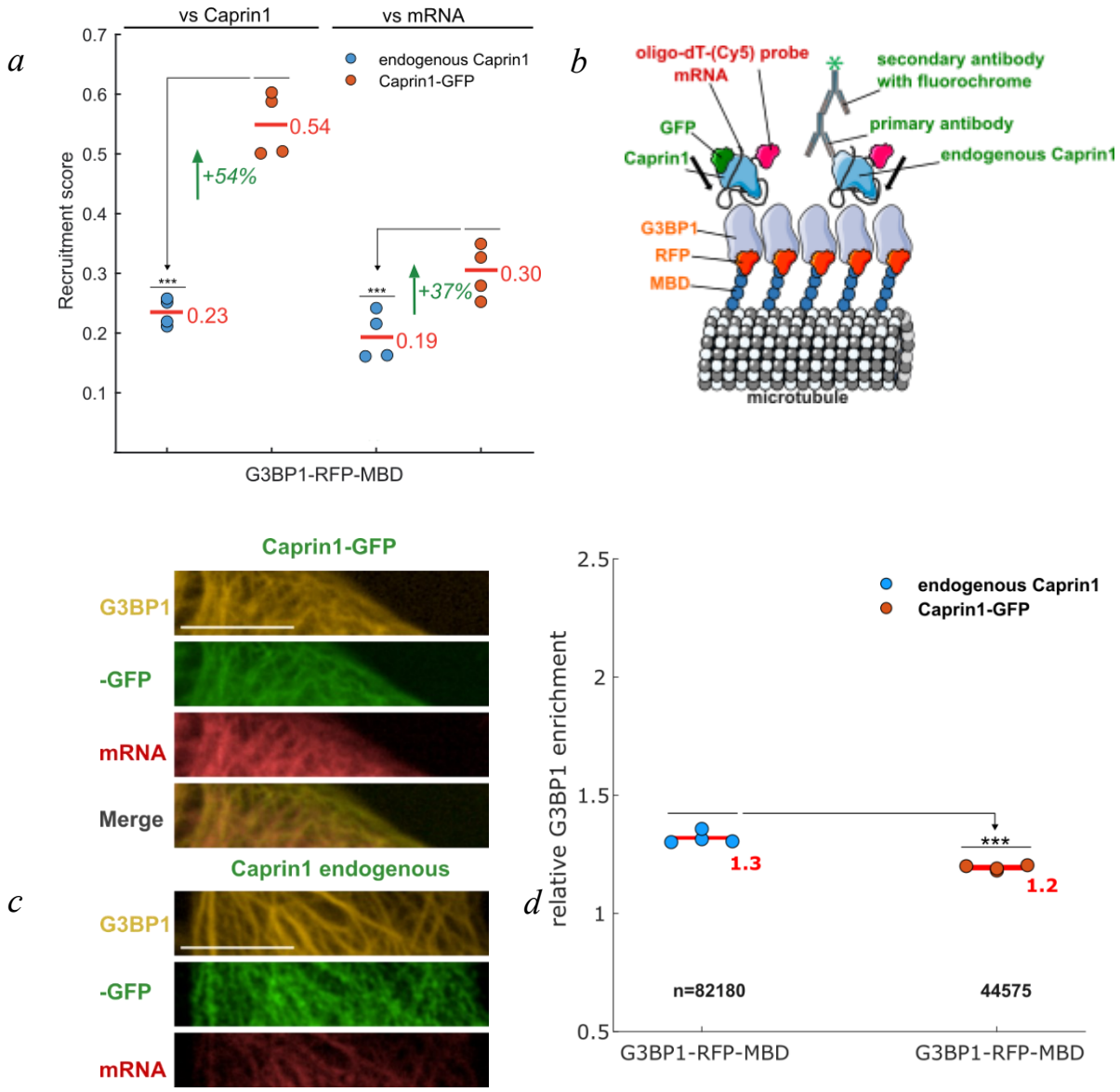

Figure 3.6. Caprin1 overexpression enhances mRNA recruitment to G3BP1 bound to microtubules. *a* - mRNA enrichment on G3BP1-decorated microtubules in the presence or absence of Caprin1-GFP overexpression. ***p < 0.001, paired t-test. *b* - Principle of the MT-bench recruitment assay. *c* - Representative images of G3BP1-RFP-MBD, Caprin1-GFP or endogenous Caprin1, and mRNA recruitment in HeLa cells. Scale bar: 10 µm. *d* - Relative enrichment of G3BP1 on microtubules with or without Caprin1-GFP co-expression. n indicates the number of analyzed spots. ***p < 0.001, paired t-test

For endogenous Caprin1 detection, we immunostained cells with a-Caprin1 antibodies and selected secondary antibodies with a fluorochrome that emits in the (500-550 nm) spectrum. With close to equal enrichment of G3BP1 on microtubules (Figure 3.6, *d*), we observed 54% increase in recruitment score for Caprin1 on microtubules in samples with overexpressed Caprin1 as compared to samples with only endogenous Caprin1. Consequently, the level of RNA recruitment to G3BP1-enriched microtubules was 37% higher in samples with overexpressed Caprin1 as opposed to endogenous. We concluded that the abundance of Caprin1 recruited to G3BP1 in the case of overexpression leads to the recruitment of additional mRNA to the complex of G3BP1-Caprin1 (Figure 3.6, *a*).

In order to access the nucleic acid binding of G3BP1 or Caprin1 without interference from other proteins, we obtained a nucleic acid binding profile for both proteins *in vitro* via a series of electrophoretic mobility shift assay (EMSA) experiments with long single-stranded DNA m13mp18 as a model for nucleic acid binding of these 2 proteins. Both proteins are able to decrease the electrophoretic mobility of m13mp18 ssDNA individually, with Caprin1 doing so at a lower nucleotide-to-protein ratio than G3BP1. We observed a minimal amount of G3BP1 that shifted 100 ng of ssDNA to 16 pmol, and for Caprin1, the shift started at 6 pmol. Large complexes that are unable to enter the gel formed at 64 pmol for G3BP1 and 12 pmol for Caprin1. This indicates that Caprin1 *in vitro* can bind large single-stranded nucleic acids at approximately 3 times the rate of G3BP1(Figure 3.7).

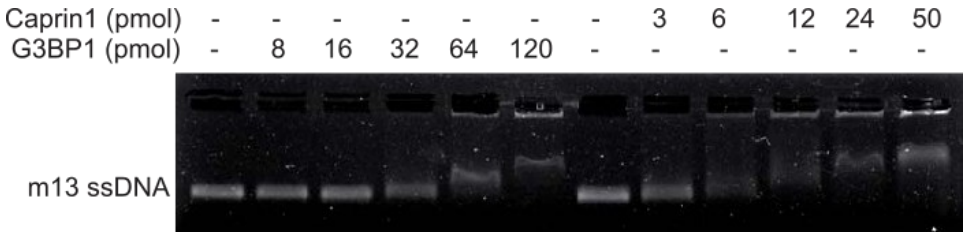

Figure 3.7. G3BP1 and Caprin1 bind nucleic acids *in vitro*. Electrophoretic mobility shift assay demonstrating the direct interaction between G3BP1 with ssDNA(wells 2-6) and Caprin1 with ssDNA (wells 7-12). One hundred nanograms of m13mp18 ssDNA were incubated with increasing concentrations of G3BP1 or Caprin1

Next, we tried to dissect the nucleic acid-binding ability of the G3BP1-Caprin1 complex further by performing EMSA. We started with the least amount of both proteins that are able to shift 100 ng ssDNA and incrementally increased Caprin1 quantity in the sample, and compared it to the nucleic acid binding profile of equimolar quantities of both Caprin1 and G3BP1 individually (Figure 3.8). We noticed that the mix of G3BP1 and Caprin1 was able to decrease the mobility of ssDNA at a lower protein-to-nucleotide ratio than G3BP1 alone. Moreover, an incremental increase of Caprin1 load led to the formation of large complexes that are unable to penetrate the gel earlier than in the case of pure G3BP1. In contrast, 28 pmol of G3BP1 alone was able to partially shift the sample, as we observed the formation of 2 bands, and while G3BP1-Caprin1-nucleic acid complex was completely in the well at 38 pmol combined, 38 pmol of G3BP1 only partially shifted 100 ng on m13mp18 ssDNA. Consequently, it appears that Caprin1 and G3BP1 act synergistically in nucleic acid binding and Caprin1 has a prominent role in the formation of large G3BP1-Caprin1-nucleic acid complexes (Figure 3.9).

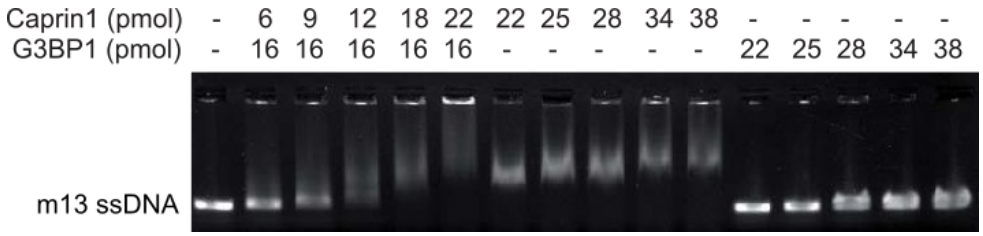

Figure 3.8. Caprin1 enhances G3BP1 binding to nucleic acids. Proteins were mixed with a constant amount of G3BP1 and an increasing amount of Caprin1 (wells 2-6) and compared to equimolar amounts of Caprin1 (wells 7-11) and G3BP1(wells 12-16)

To reinforce the idea of Caprin1's prominence in RNA binding by the G3BP1-Caprin1 complex, we performed EMSA in which we used the constant value of one component while gradually increasing the amount of the other one. We observed that a 3 pmol increase in Caprin1 quantity resulted in a visible shift and formation of large complexes in wells, while a 4 pmol incremental increase in G3BP1 was much less efficient in shifting model nucleic acid (Figure 3.9).

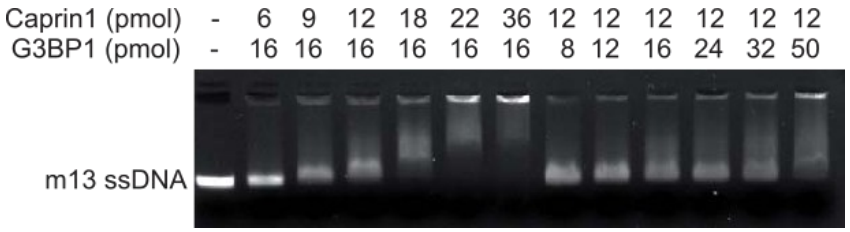

Figure 3.9. G3BP1-Caprin1 complex forms large aggregates with nucleic acids. Proteins were mixed with a constant amount of G3BP1 and an increasing amount of Caprin1 (wells 2-7) and a constant amount of Caprin1 and an increasing amount of G3BP1 (wells 8-13) to observe the formation of large complexes unable to enter the gel in case of an increase in Caprin1 concentration

Atomic Force Microscopy (AFM) enables the observation and analysis of multimolecular assemblies on a nanometric scale. Both G3BP1 and Caprin1 are able to form isolated complexes with mRNA within a few minutes of incubation

time at the indicated concentrations (Figure 3.10, *a*). G3BP1 alone forms larger complexes with mRNA than Caprin1 alone. When 2 proteins were incubated together with mRNA at a comparable nucleic acid/protein ratio, we observed the appearance of larger condensates alongside isolated complexes. The presence of protein in these condensates is revealed by the higher height of the condensate (white color) than the isolated mRNA (left image, brown color). The presence of multiple mRNA/protein complexes in these condensates is confirmed by the measurement of the average area of the complexes and their comparison when isolated proteins are incubated with mRNA or the G3BP1-Caprin1 mixture (Figure 3.10, *b*). The formation of these large mRNA/protein complexes could explain the presence of bands remaining in the well in previous EMSA experiments (Figures 3.7, 3.8, and 3.9). Thus, G3BP1 alone at a moderate protein/nucleotide ratio is only able to form isolated complexes in which the mRNA appeared stretched. The formation of condensates due to G3BP1 multimerization requires a high protein/nucleotide ratio. The presence of Caprin1 triggers the formation of condensates at a very low protein/nucleotide ratio: Caprin1 is not only a bridge between G3BP1/mRNA complexes but actively participates in the recruitment of mRNA.

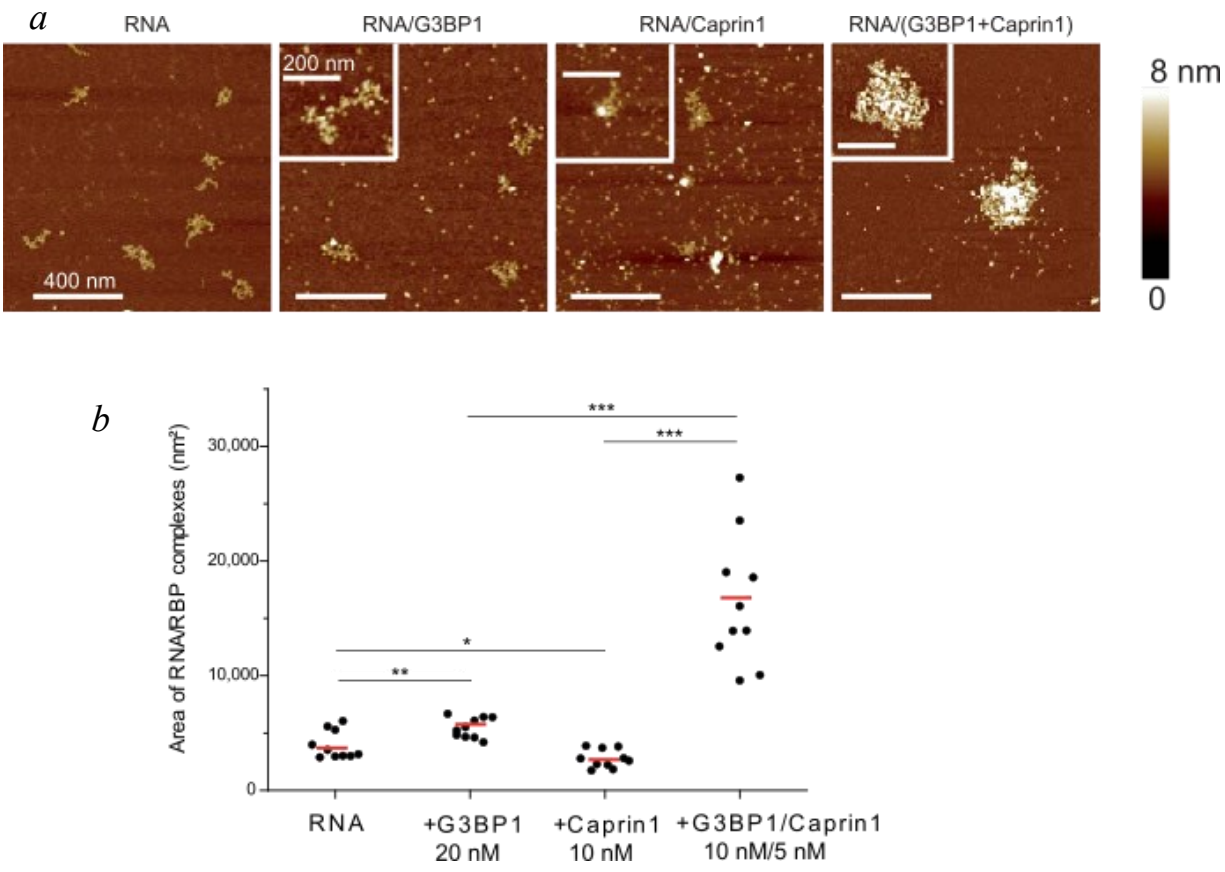

Figure 3.10. G3BP1-Caprin1 mix forms larger assemblies with 2Luc mRNA than RBP/RNA assemblies of individual proteins. *a* - atomic force microscopy images and zooms in on specific assemblies of G3BP1/mRNA, Caprin1/mRNA, and a 1:2 mixture of the two RBPs with 2Luc mRNA. Proteins (20 nM for G3BP1, 10 nM for Caprin1) were incubated with 2Luc mRNA (protein/nucleotide ratio of 1/100) for 15 min before sample deposition and fixation. Z scale 8 nm. The scale bar represents 400 nm. *b* -, scatter plot representing the area of RBP/mRNA assemblies observed on AFM images in (*a*) and comparison with free mRNA. Except for the mRNA alone condition, only areas of RBP/mRNA complexes with a height higher than 2 nm are plotted, and free mRNA molecules were discarded from this analysis. The plot gathers the data from two independent experiments. Lines show mean values. Significances between areas of RBP/mRNA assemblies were obtained using t-test; *$p < 0.05$, **$p < 0.01$, ***$p < 0.005$

3.3. Caprin1 improves RNA binding of G3BP1 *in vivo* if G3BP1 possesses RNA-binding domains and the ability to bind Caprin1

Having confirmed that the G3BP1-Caprin1 complex has increased mRNA binding capabilities compared to individual proteins and establishing that overexpressed Caprin1 enhances mRNA binding of G3BP1, we set out to further investigate which components of G3BP1 are at play in the complex's RNA binding. Moreover, while it is known that Caprin1 can bind mRNA *in vitro*, which we confirmed by EMSA and AFM experiments, Caprin1's contribution to the recruitment of mRNA to condensates *in vivo* remains unclear.

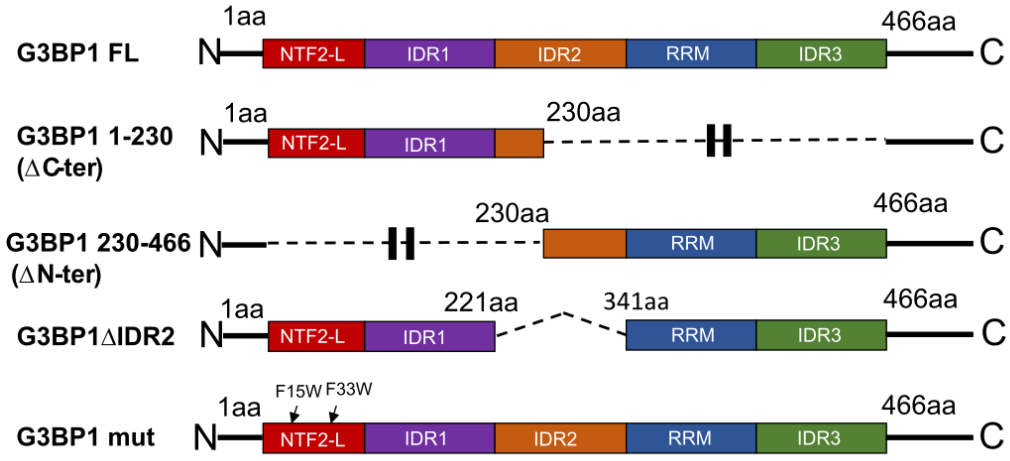

Figure 3.11. Deletion constructs and point mutations of G3BP1. NTF2-L: nuclear transfer factor 2-like domain, IDR1: intrinsically disordered region 1(acidic-rich region), IDR2: intrinsically disordered region 2 (proline-rich region), IDR3: intrinsically disordered region 3(RGG-rich region), F15W and F33W – point mutations described in Sheehan et al. (125) which decrease the affinity of G3BP1 with Caprin1

To separate G3BP1 into functional parts, we prepared several deletion constructs, with the G3BP1-ΔC (1-230 aa) construct lacking RRM and RGG-box (IDR3) on the C-terminus, the G3BP1-ΔN (230-466 aa) construct with the N-terminal NTF2-L domain responsible for interaction with Caprin1 and acidic-rich

IDR1 absent. We also prepared a G3BP1-ΔIDR2 construct. According to (3), IDR2 is enriched in proline amino acid residues and performs the role of the regulatory sequence of G3BP1 conformation, which, in turn, controls RNA binding of G3BP1. We also prepared several point mutation constructs for G3BP1, namely -F15W and -F33W, which are detrimental to G3BP1-Caprin1 binding (125) (Figure 3.11).

To begin, we confirmed our constructs with immunoprecipitation (IP) in RNA-free conditions. Previous research shows that G3BP1 binds Caprin1 in the NTF2-L domain on the N-terminus, and it is the only required domain of G3BP1 for this protein-protein interaction (3.2 Literature review). The results of IP confirmed that constructs with the NTF2-L domain present, such as G3BP1 FL, G3BP1-ΔC, and G3BP1-ΔIDR2, are able to bind Caprin1, while G3BP1-ΔN loses the interaction with Caprin1. Additionally, we showed that YBX1 binding to G3BP1 is RNA-dependent since the absence of RNA abolished this interaction in IP (Figure 3.12).

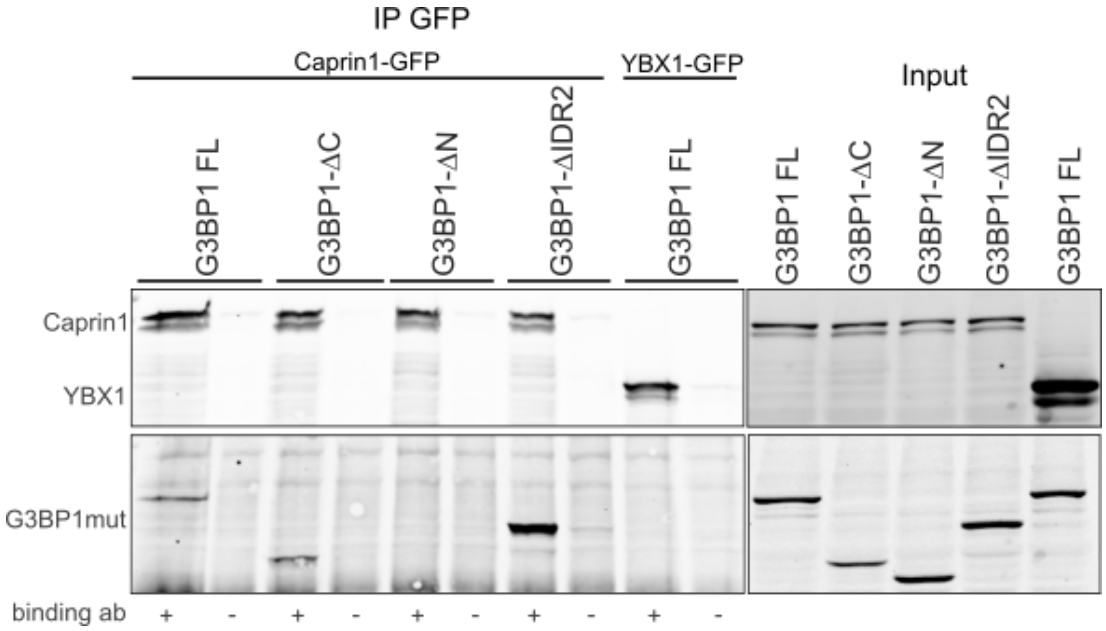

Figure 3.12. Caprin1 interacts with G3BP1 FL, -ΔC and -ΔIDR2 deletion constructs but not -ΔN in RNA-free conditions *in vitro* shown via Western blot analysis of immunoprecipitation assay. Right panel: HEK293 cells were co-transfected with Caprin1-GFP or YBX1-GFP and RFP-G3BP1 FL, RFP-G3BP1-ΔC, RFP-G3BP1-ΔN or RFP-G3BP1-ΔIDR2. G3BP1 FL - YBX1 co-transfection was used as a control. Cells were lysated with buffer containing RNAse A and immunoprecipitation was performed using a-GFP antibodies. Western blot analysis shows that Caprin1 is able to bind G3BP1 FL, -ΔC and -ΔIDR2 but not G3BP1-ΔN in RNA-free conditions. Left panel: Cell lysates

With the general picture of G3BP1 binding to Caprin1 confirmed and consistent with previous research (Chapter 1.3.2), we set out to explore which G3BP1 domains are crucial for enhancing mRNA recruitment by G3BP1 in the presence of Caprin1 (Figure 3.13). We performed an MT-bench recruitment assay with G3BP1 deletion constructs and point mutation constructs fused to RFP-MBD serving as bait, and endogenous Caprin1 serving as prey, and measured mRNA labeled with cyanine5 oligo-(dT)-probe, endogenous Caprin1, and G3BP1mut-RFP-MBD fluorescence levels on microtubules (Figure 3.13, *a*). The results show

that the correlation between fluorescence intensity of bait protein (G3BP1 constructs) and prey (endogenous Caprin1) sharply decreased for G3BP1-ΔN, -ΔIDR2, F15W, and F33W constructs, while no significant decrease was observed for -ΔC construct (Figure 3.13, *b*).

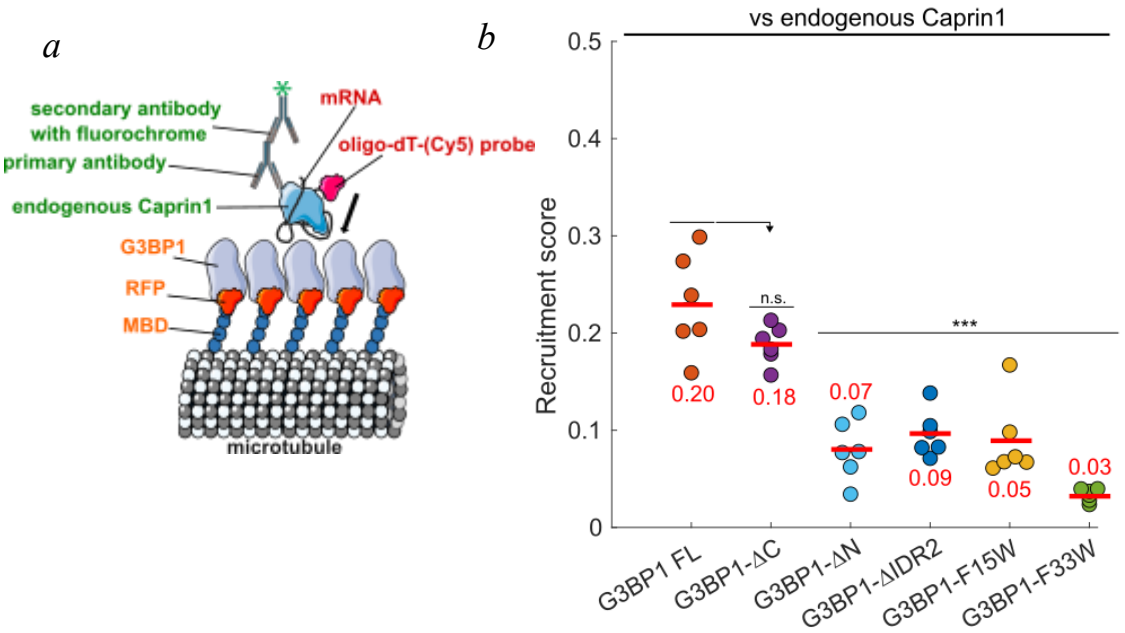

Figure 3.13. Recruitment of Caprin1 to G3BP1 depends on its N-terminal domain. *a* -Principle of the microtubule bench recruitment assay. *b* - G3BP1 FL and G3BP1-ΔC recruits Caprin1 to microtubules, while the recruitment is impaired for G3BP1-ΔN and -ΔIDR2 constructs as well as both F15W and F33W mutants. ***p < 0.001, paired t-test). Each dot represents the mean value of single cell analysis in a single well (see Materials and Methods for details)

As for mRNA recruitment (Figure 3.14, *a*), while G3BP1-ΔN construct and G3BP1-F15W and -F33W mutated constructs the recruitment score was comparable to full-length G3BP1, for G3BP1-ΔC construct it was abolished, due to the lack of RRM and RGG-box of G3BP1 in this construct. Interestingly, the mRNA recruitment for the ΔIDR2 construct was completely absent, even though

G3BP1-ΔIDR2 still has both RRM and RGG-box and can bind Caprin1 as per immunoprecipitation results (Figure 3.12).

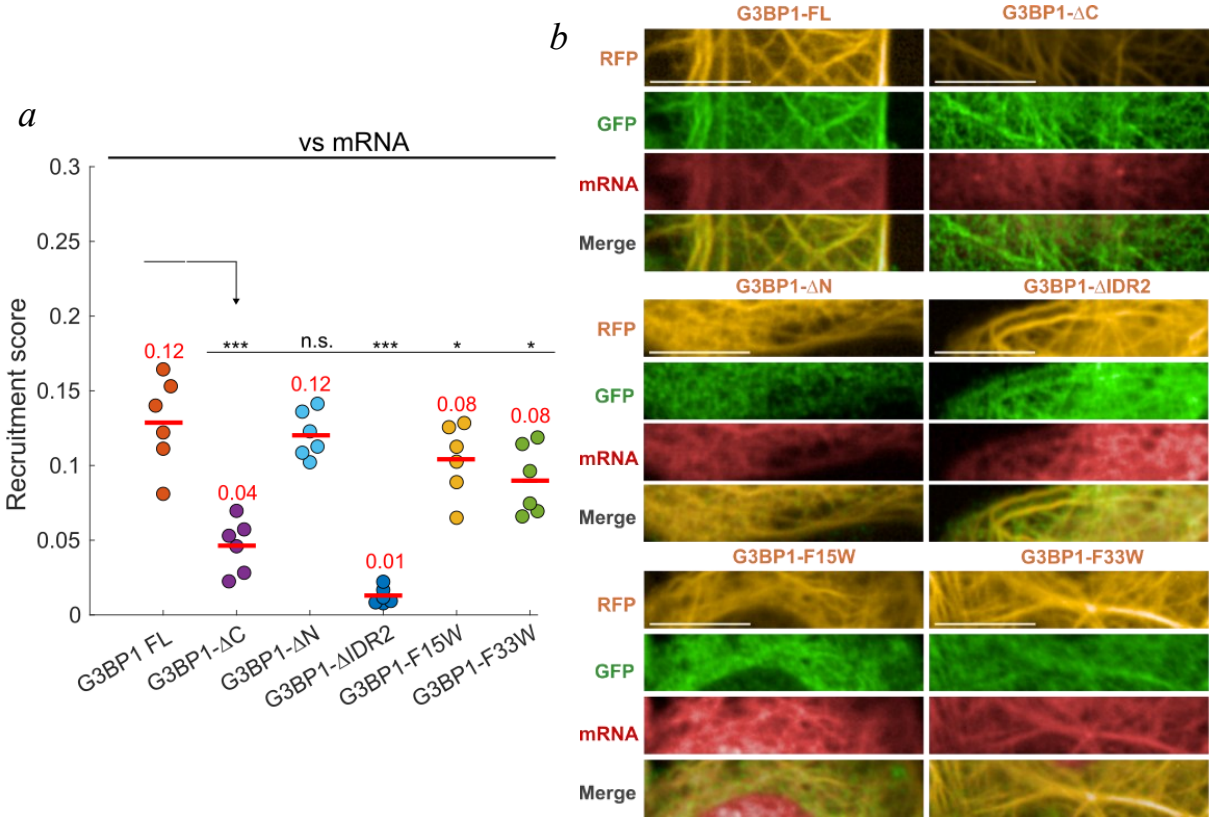

Figure 3.14. Recruitment of mRNA to G3BP1 depends on its C-terminal domains. *a* - mRNA recruitment to G3BP1-ΔN, -F15W and -F33W mutants is comparable to G3BP1 FL, while it is severely decreased for G3BP1-ΔC and G3BP1-ΔIDR2 constructs. *p < 0.05, ***p < 0.001, paired t-test. n.s., non-significant. Each dot represents the mean value of single-cell analysis in a single well (see Materials and methods for details). *a* - Representative images of immunostained endogenous Caprin1, as well as oligo-dT-(Cy5)-labeled mRNA recruitment to RFP-labeled G3BP1 deletion and point mutation constructs fused to MBD. MBD: microtubule-binding domain. Scale bar: 10 μm

While Caprin1 is a major partner of G3BP1, it is by no means the only one; hence, we examined the mRNA recruitment behavior of G3BP1-ΔIDR2 in the presence of several other protein partners of G3BP1 that are overexpressed in the cell. To that end, we performed an MT bench recruitment experiment where we overexpressed several GFP-labeled proteins, such as G3BP2 and YBX1 – both known partners of G3BP1 and observed the mRNA recruitment to G3BP1-ΔIDR2 on microtubules compared to the same interaction of full-length G3BP1, while using Caprin1 as a positive control (Figure 3.15). Similarly to G3BP1-ΔIDR2-Caprin1 behavior, it appears that regardless of which G3BP1 partner protein we overexpress, the G3BP1-ΔIDR2 construct still exhibits almost complete absence of mRNA recruitment, thus demonstrating that the RNA-binding deficiency of this construct does not depend on partner proteins and is not compensated by their overexpression.

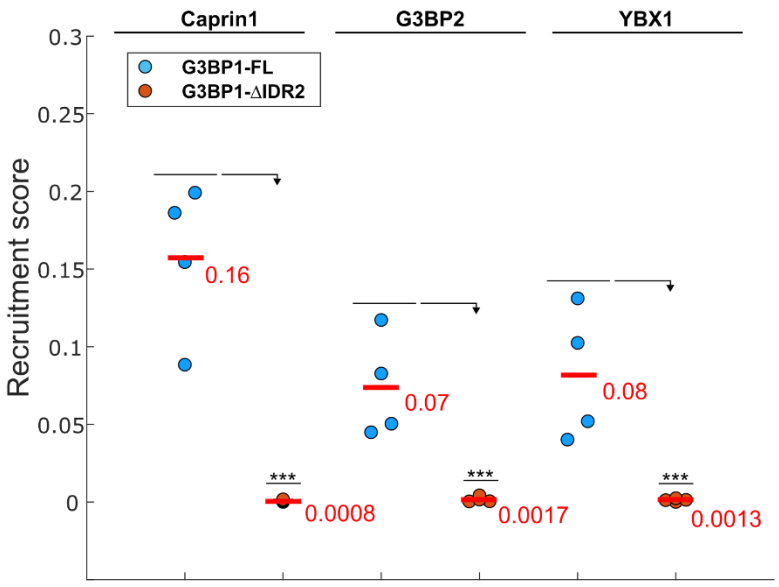

Figure 3.15. MT-bench assay mRNA recruitment to G3BP1 or G3BP1-ΔIDR2 in the presence of G3BP1 partner proteins. MT-bench assay in HeLa cells co-expressing MBD-fused G3BP1 or G3BP1-ΔIDR2 together with GFP-tagged Caprin1, G3BP2 or YBX1. The scatter plot shows colocalization between G3BP1/G3BP1-ΔIDR2 and mRNA based on RFP and Cy5 fluorescence intensities. Data are from four independent experiments; red lines indicate mean values. Statistical significance was determined by t-test; ***$p < 0.005$

Next, we conducted an EMSA experiment to verify differences in RNA binding between G3BP1 FL and G3BP1-ΔIDR2 *in vitro*. G3BP1-ΔIDR2 construct was unable to decrease the electrophoretic mobility of nucleic acid at the same protein-to-nucleotide ratio as full-length G3BP1, and the earliest point of the mobility decrease happened at 400 pmol concentration of G3BP1-ΔIDR2, thus confirming that this construct has decreased nucleic binding ability (Figure 3.16).

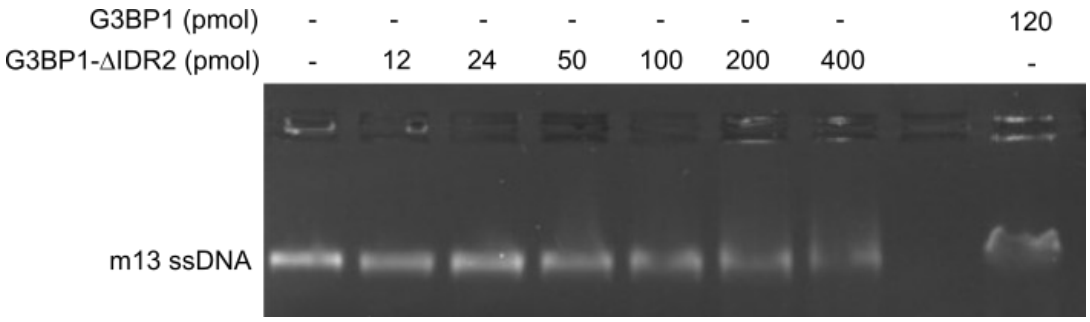

Figure 3.16. G3BP1-ΔIDR2 has decreased nucleic acid binding ability compared to full-length G3BP1. Electrophoretic mobility shift assay demonstrating the difference in ssDNA binding between G3BP1 (well 9) and G3BP1-ΔIDR2 (wells 2-7). One hundred nanograms of m13mp1 m13mp18 ssDNA were incubated with gradually increased concentrations of G3BP1-ΔIDR2 and compared to ssDNA gel-mobility reduction ability of 120 pmol of G3BP1

We then analyzed the interplay between G3BP1-ΔIDR2 and Caprin1 for nucleic acid binding. Whenever the interaction between nucleic acid, G3BP1-ΔIDR2, and Caprin1 is forced in an EMSA experiment, we observe that the EM shift profile of the resulting complex is similar to that of Caprin1 alone, suggesting that G3BP1-ΔIDR2 does not form well-defined nucleoprotein complexes in EMSA. At higher concentrations of G3BP1-ΔIDR2 (Fig. 3.17, wells 13 and 14), the DNA signal becomes diffuse, consistent with the formation of heterogeneous protein-DNA complexes or aggregates with variable electrophoretic mobility. This diffuse character of the bands suggests the formation of heterogeneous nucleoprotein assemblies rather than discrete, stable complexes.

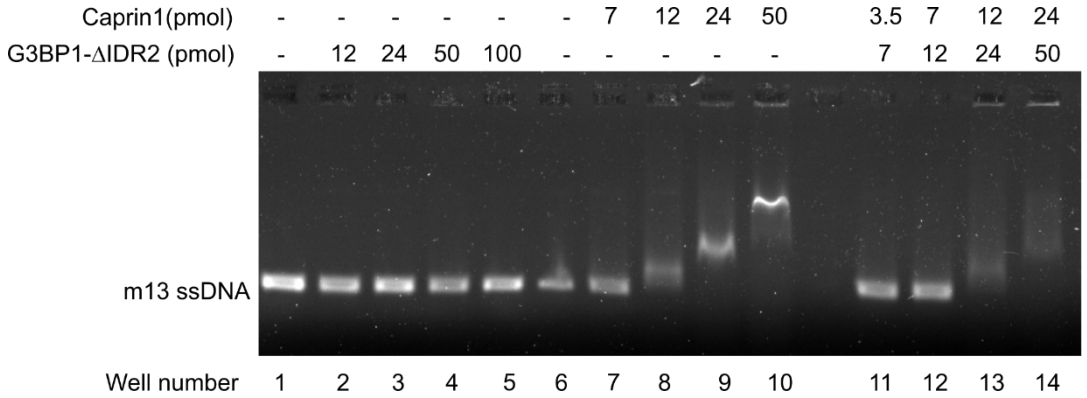

Figure 3.17. Caprin1 does not enhance G3BP1-ΔIDR2 binding to nucleic acids. Proteins were mixed with a constant amount of m13mp18 ssDNA and an increasing amount of Caprin1 and G3BP1-ΔIDR2 (wells 2—6) and compared to equimolar amounts of Caprin1 (wells 7—10) and G3BP1-ΔIDR2 (wells 11—14)

Consequently, we conducted an MT bench recruitment experiment in which G3BP1 constructs are brought on microtubules, and Caprin1 is overexpressed, to see if the trend of the G3BP1 RNA-binding pattern observed in Figure 3.14, A, will continue for different constructs of G3BP1. Here, the highest Caprin1 recruitment coefficient was observed for the interaction with G3BP1 FL, followed by the -ΔC construct. Both G3BP1 point mutation constructs show a 50% decrease in Caprin1 recruitment, with the lowest score observed for the construct lacking the NTF2-L domain. G3BP1-ΔIDR2 and -ΔC constructs maintain a relatively high and similar Caprin1 recruitment level compared to G3BP1 FL. (Figure 3.18, *a*). The trend for mRNA recruitment remained similar, with G3BP1 FL-Caprin1 interaction bringing more mRNA to microtubules than all of the deletion constructs, while point mutation constructs retained around 50% of the mRNA binding of full-length G3BP1 (Figure 3.18, *b*). Once again, we detected nearly complete abolishment of mRNA binding for the -ΔIDR2 construct even with Caprin1 overexpressed, possibly indicating that G3BP1-ΔIDR2 adopts such a conformation that closes the mRNA binding surfaces of both proteins involved. Consequently, while -ΔC and -ΔIDR2 constructs can recruit additional

Caprin1 to microtubules, this additional Caprin1 cannot bring more mRNA to the G3BP1-Caprin1 complex if G3BP1 itself lacks either the RNA-interacting domains or Caprin1 binding motif in NTF2-L domain.

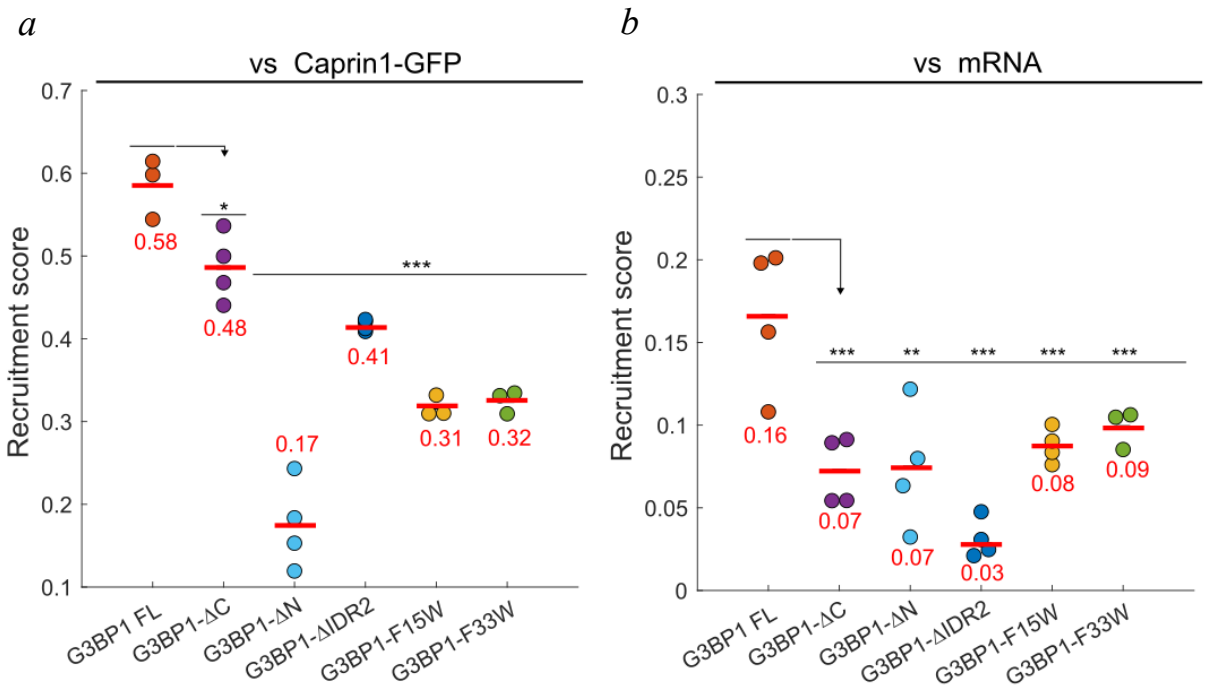

Figure 3.18. Overexpressed Caprin1 improves mRNA binding of only full-length G3BP1. *a* - G3BP1 FL, G3BP1-ΔC, and -ΔIDR2 recruit overexpressed Caprin1 to microtubules in much greater capacity than G3BP1-ΔN, -F15W and -F33W mutants. *p < 0.05, ***p < 0.001, paired t-test. *b* - Overexpressed Caprin1 improves mRNA binding of G3BP1 FL but not the rest of the deletion and point mutation constructs. **p < 0.01, ***p < 0.001, paired t-test. n.s., non-significant. (*a*, *b*) Each dot represents the mean value of single-cell analysis in a single well (see Materials and Methods for details)

If Caprin1 is brought on microtubules via co-transfection of Caprin1-GFP-MBD and RFP-labeled mutant constructs of G3BP1, which are overexpressed at the same time (Figure 3.19, *a*), G3BP1 FL and G3BP1-ΔIDR2 are recruited to

microtubules, while -ΔC and -ΔN constructs recruitment is comparable to the negative control (Figure 3.19, *b*).

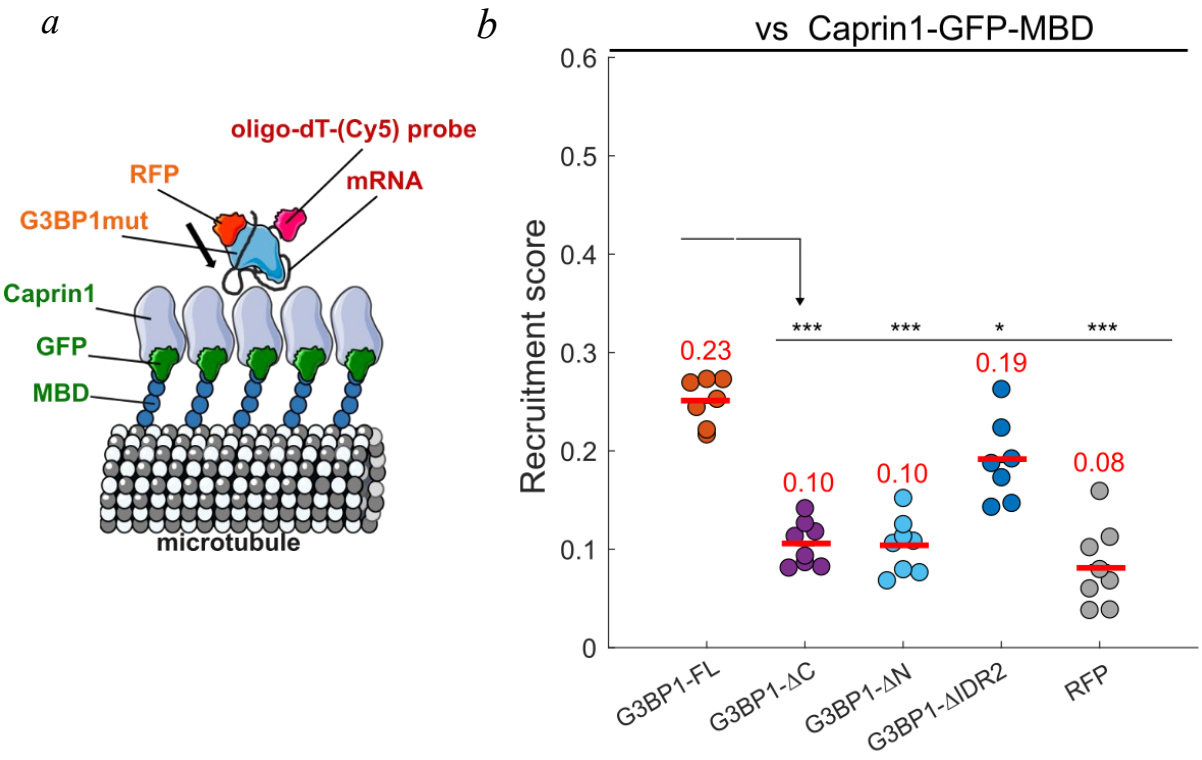

Figure 3.19. G3BP1 FL and G3BP1-ΔIDR2 are brought to microtubules enriched with Caprin1. *a* - Principle of the microtubule bench recruitment assay used to measure the recruitment of prey protein brought to microtubule-fused prey protein in HeLa cells as well as measure the enrichment of mRNA on microtubules via oligo-dT-(Cy5) fluorescent probe. The recruitment score for pairs of proteins and mRNA was measured with an HCS imager and automated pipeline. *b* - Caprin1 recruits G3BP1 FL and G3BP1-ΔIDR2 to microtubules, while the recruitment is impaired for G3BP1-ΔC and -ΔN constructs. *p < 0.05, ***p < 0.001, paired t-test). Each dot represents the mean value of single cell analysis in a single well (see Materials and Methods for details)

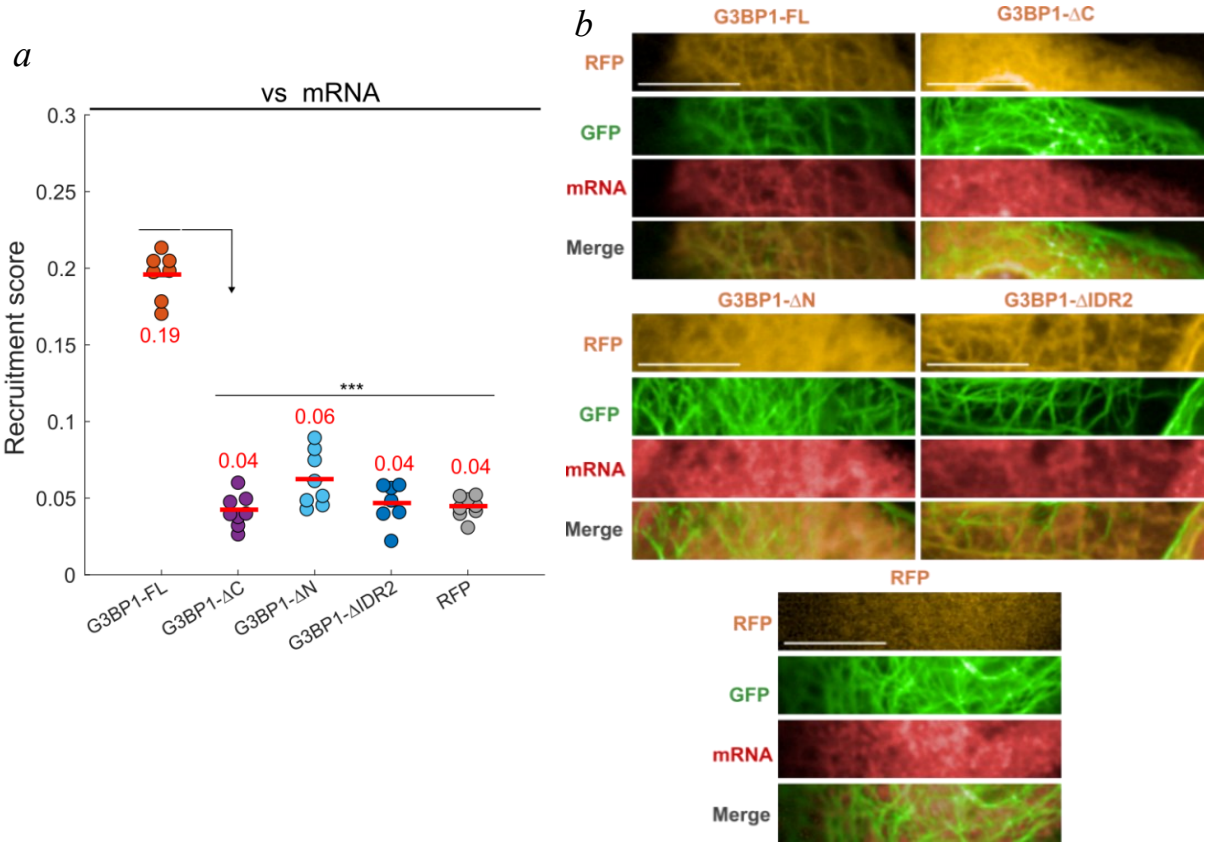

Figure 3.20. Caprin1 mRNA binding is improved only by full-length G3BP1. *a* - mRNA recruitment to Caprin1 greatly improves in cells transfected with full-length G3BP1. ***$p < 0.001$, paired t-test. Each dot represents the mean value of single cell analysis in a single well (see Materials and Methods for details). *b* -. Representative images of RFP-labeled G3BP1 deletion constructs as well as oligo-dT-(Cy5)-labeled mRNA recruitment to GFP-labeled Caprin1 fused to MBD. MBD: microtubule-binding domain. Scale bar: 10 µm

Curiously, Caprin1 mRNA binding appears to be minimal when co-expressed with the RFP tag. G3BP1-ΔC, -ΔN, and -ΔIDR2 constructs fail to bring additional mRNA to Caprin1. When Caprin1 is co-expressed with full-length G3BP1, on the other hand, the recruitment score improves dramatically. Thus, in this experiment, Caprin1 can recruit G3BP1 only when both the NTF2-L domain and RNA-binding domains of G3BP1 are present. The mRNA binding capabilities

of Caprin1 *in vivo* seem to be reliant on full-length G3BP1, as all other constructs failed to improve the mRNA binding score (Figure 3.20, *a*).

In view of observed changes in protein-protein binding between G3BP1 and Caprin1, as well as associated mRNA recruitment changes, we inquired how the introduction of deletions and disrupting point mutations would affect the ability of G3BP1 and Caprin1 to form compartments on microtubules. As such, we tested the ability of G3BP1 deletion mutants to mix with G3BP1 FL and Caprin1. We performed an MT bench mixing experiment, in which G3BP1 mutants fused to RFP-MBD were co-expressed with G3BP1 FL fused to GFP-MBD or Caprin1-GFP-MBD, respectively (see Figure 3.21, *a* for the experiment principle).

When G3BP1 deletion mutants are co-expressed with G3BP1 full length on microtubules, the highest mixing score is obtained for G3BP1 FL – G3BP1 FL interaction, while -ΔC, -ΔN, and -ΔIDR2 mixing scores are reduced (Figure 3.21, *b*). G3BP1-ΔC construct cannot bind RNA, and as such may prefer homotypic interactions through the NTF2-L domain and not enter the RNA-rich phase of full-length G3BP1. On the opposite, the G3BP1-ΔN construct lacks dimerization sequence in the NTF2-L domain, and as such prefers to form separate compartments with RNA and not full-length G3BP1. The G3BP1-ΔIDR2 construct mixing pattern is interesting since we know that while both the NTF2-L domain and RNA binding domains are present in this construct, it lacks RNA binding ability but still has a dimerization sequence in NTF2-L. We propose that G3BP1-ΔIDR2 is unable to undergo conformational change, since the absence of the spacer IDR2 may impede the formation of the closed conformation. This leads to G3BP1 lacking IDR2 being unable to interact with mRNA to any significant degree and partially disrupts dimerization. Consequently, we can observe G3BP1-ΔIDR2 demixing with the RNA-rich G3BP1 compartment.

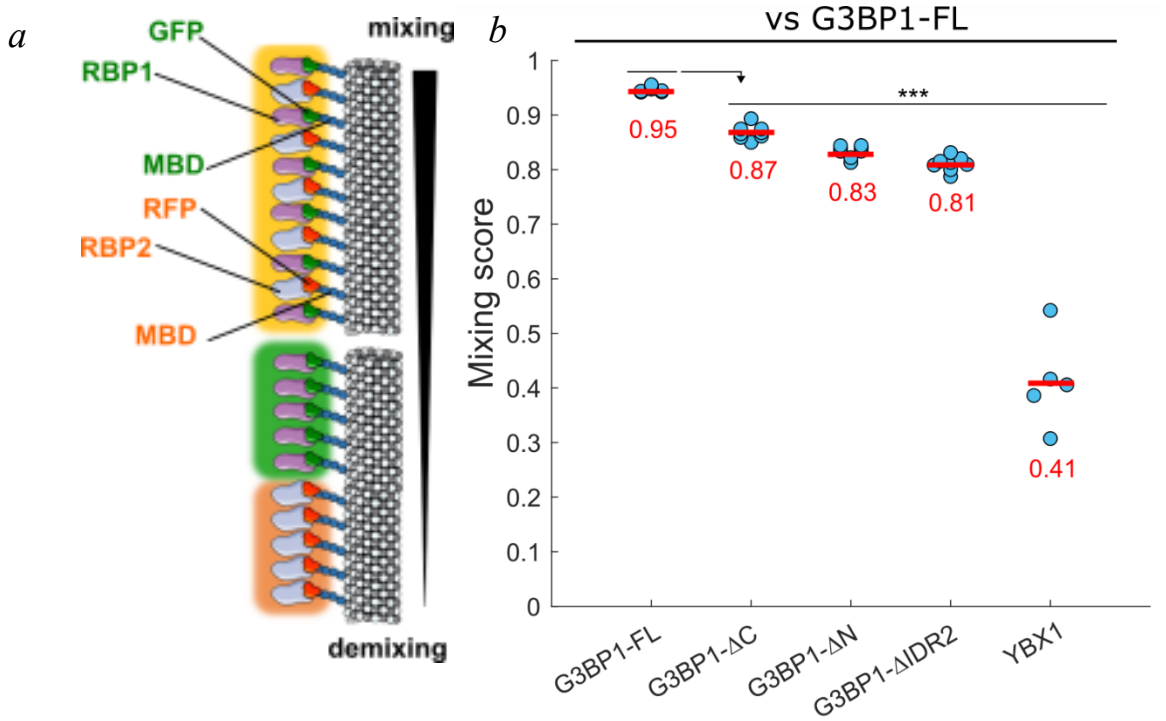

Figure 3.21. Homotypic mixing of G3BP1 on microtubules is decreased when paired with G3BP1-ΔC, G3BP1-ΔN, and G3BP1-ΔIDR2 deletion constructs. *a* - Principle of the microtubule bench mixing assay used to measure the mixing score of two GFP- or RFP labeled proteins in HeLa cells. Pairs of tested RBPs fused with MBD were co-expressed to automatically measure their mixing along microtubules. The mixing score was measured for different pairs of proteins with an HCS imager and automated pipeline. MBD: microtubule-binding domain. *b* - The homotypic mixing of G3BP1 is disrupted whenever paired with G3BP1-ΔC, G3BP1-ΔN, and G3BP1-ΔIDR2 deletion constructs, the bar indicates mean values. ***$p < 0.001$, paired t-test. Each dot represents the mean value of single cell analysis in a single well (see Materials and Methods and Figure 2.2 for details)

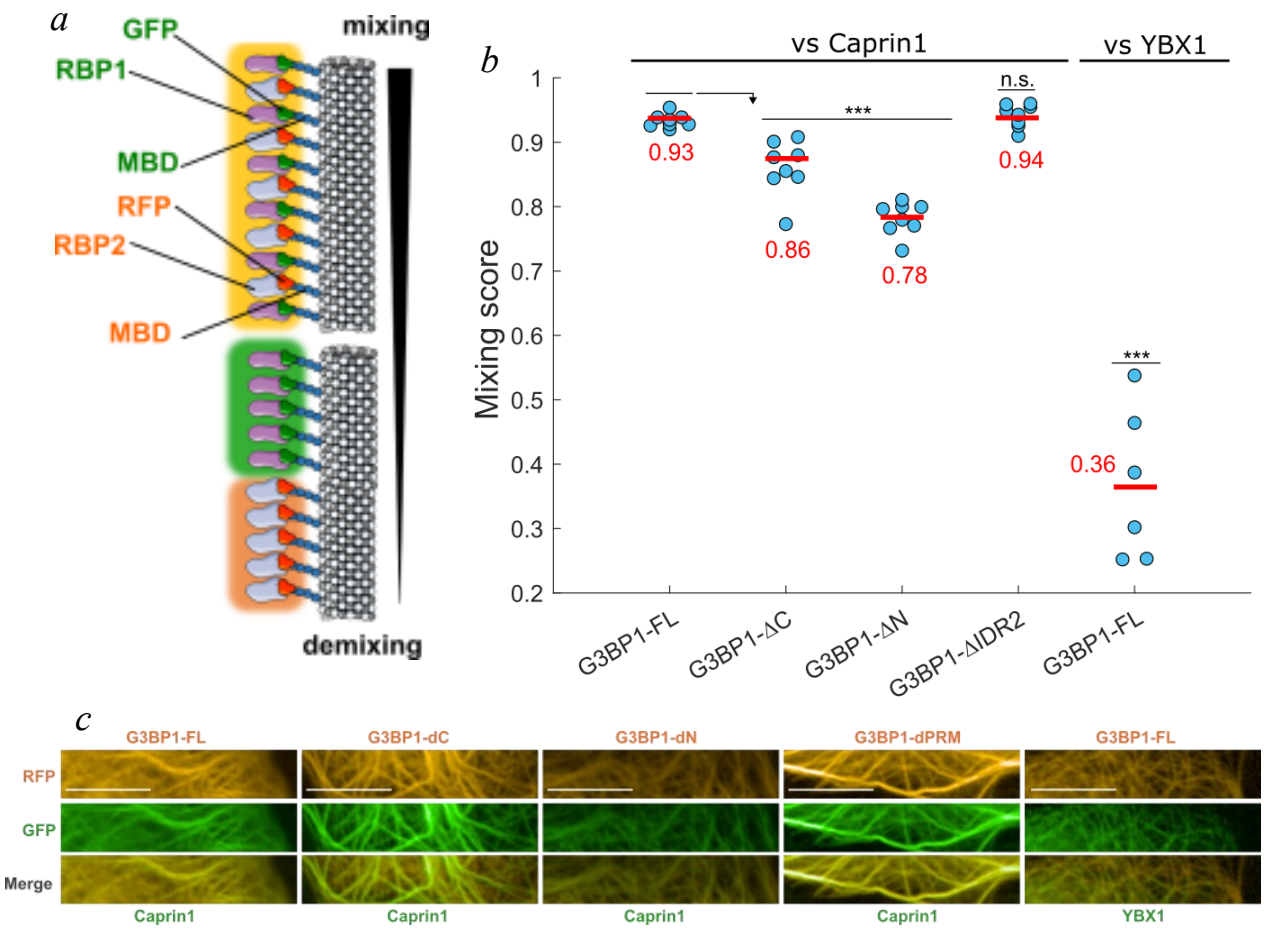

Figure 3.22. Heterotypic mixing of G3BP1 with Caprin1 on microtubules is decreased with G3BP1-ΔC, G3BP1-ΔN deletion constructs but not affected for mixing with G3BP1-ΔIDR2. *a* -Principle of the MT-bench mixing assay used to quantify the co-localization of GFP- and RFP-tagged proteins along microtubules in HeLa cells. MBD, microtubule-binding domain. *b* - Mixing of Caprin1 with G3BP1 was reduced for G3BP1-ΔC and G3BP1-ΔN, but not for G3BP1-ΔIDR2. Bars indicate mean values; each dot represents the mean single-cell value from one well. ***p < 0.001, paired t-test; n.s., non-significant. *c* - Representative images of Caprin1 mixing with full-length G3BP1 and G3BP1 deletion constructs. Scale bar: 10 µm

When G3BP1 deletion mutants are co-expressed on microtubules with Caprin1, the highest mixing scores are observed for G3BP1 FL and G3BP1-ΔIDR2. The loss of G3BP1 N-terminus seems to be more detrimental to G3BP1 and Caprin1 forming a compartment than the loss of C-terminus, since the mixing score for G3BP1-ΔC-Caprin1 is higher than that of -ΔN (Figure 3.22, *b*). G3BP1-ΔIDR2, on the other hand, retains a mixing score equal to full-length G3BP1 mixing with Caprin1. Comparing results from Figures 3.21, *b* and 3.22, *b*, we can conclude, that the low mixing between G3BP1 FL and -ΔIDR2 occurs due to an impaired mRNA binding by -ΔIDR2 detected during the MT bench experiment (Figure 3.18, *b*). Alternatively, the recruitment of Caprin1 by the G3BP1-ΔIDR2 construct on MT observed in Figure 3.18, *a*, could be the consequence of a good mixing between these 2 constructs independently of the mRNA recruitment. G3BP1 lacking IDR2 has a strong affinity for homotypic interactions with Caprin1 and a lower affinity for homotypic interactions with G3BP1. Since G3BP1-G3BP1 dimerization (79) and Caprin1-G3BP1 interaction both occur in SGs, we can assume that these two interactions are not antagonistic or exclusive, which reinforces the idea that G3BP1 lacking IDR2 preferably forms heterotypic interactions with Caprin1 over homotypic interactions with G3BP1 FL.

Additionally, we tested the mixing between different point mutation constructs of G3BP1 and Caprin1 (Figure 3.23). For that, in addition to G3BP1-F15W and -F33W mutants of G3BP1, we generated -Y40A mutant for G3BP1 and -L378P mutant for Caprin1. L378P mutation targets one of the amino acid residues in the Caprin1 G3BP1 interacting motif (GIM) and disrupts G3BP1-Caprin1 binding (6). Y40A mutation of G3BP1 disrupts the dimerization of G3BP1 (77). We observed no significant changes in mixing between point-mutation constructs, indicating that the compartmentalization of the G3BP1-Caprin1 complex relies more on the structural features of both proteins than on

the ability of both proteins to interact with each other or their individual ability to bind to mRNA.

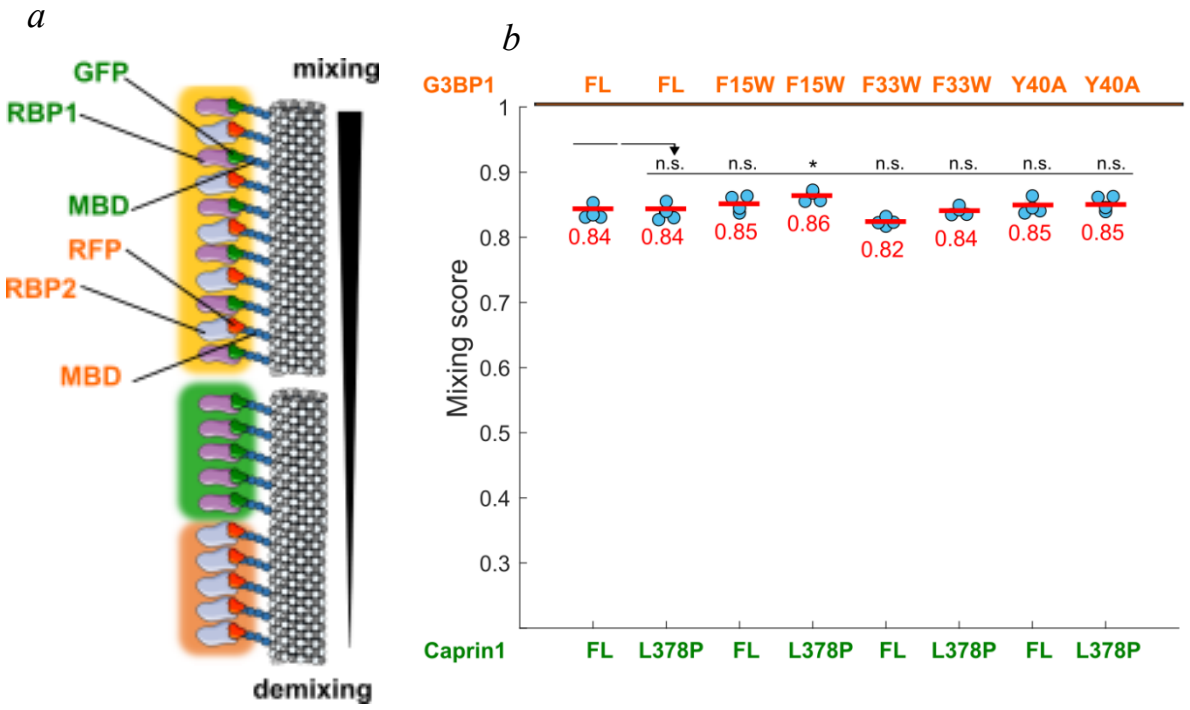

Figure 3.23. Heterotypic mixing of G3BP1 with Caprin1 on microtubules is not affected by the introduction of point mutations in interacting regions of both proteins. *a* - Principle of the microtubule bench mixing assay used to measure the mixing score of two GFP- or RFP labeled proteins in HeLa cells. Pairs of tested RBPs fused with MBD were co-expressed to automatically measure their mixing along microtubules. The mixing score was measured for different pairs of proteins with an HCS imager and automated pipeline. MBD: microtubule-binding domain. *b* - The heterotypic mixing of G3BP1 with Caprin1 is not disrupted whenever point mutations F15W, F33W, or Y40A in the G3BP1 NTF2-L domain or point mutation L378P in Caprin1 GIM are introduced. *p < 0.05, paired t-test. n.s., non-significant. Each dot represents the mean value of single cell analysis in a single well (see Materials and Methods and Figure 2.2 for details)

3.3 Roles of G3BP1 domains in SG assembly and mRNA recruitment to SG

G3BP1 mRNA binding *in vivo* is improved by Caprin1, but only when G3BP1 itself can bind mRNA. In search of a link between the G3BP1-Caprin1 complex's ability to bind mRNA and generate condensates, we conducted several stress granule assays to dissect this process. G3BP1 is an SG-nucleator protein, and as such, it is able to induce SG assembly when overexpressed even if cells are not subjected to stress factors (89). We tested the ability of different functional domains of G3BP1 to undergo LLPS and form condensates in both unstressed conditions and in cells subjected to sodium arsenite. Firstly, we overexpressed different constructs of G3BP1 without inducing oxidative stress in cells to observe the condensation ability of G3BP1 constructs. It is important to mention how we designate stress granules. Since this RNP is comprised of mRNA stalled in translation, visualizing mRNA using an oligo-dT-(Cy5) fluorescent probe allows us to distinguish these mRNA-rich condensates. We measured several parameters, including the total area of stress granules generated and G3BP1 constructs enrichment in these condensates. Full-length G3BP1 was able to induce the assembly of additional SGs and accumulate in them, with total SG area per cell reaching 20,5 μm^2 and the average fluorescence level of overexpressed G3BP1 FL in SGs reaching 2,5 times more than the fluorescence level in cytoplasm. Liposome-based DNA carriers such as Lipofectamine 2000, which are commonly used for transient transfection, are known to induce cellular stress (126). Given that, even in cells not subjected to sodium arsenite or any other stressor, we can observe a small number of stress granules (Figure 3.24, *c*). G3BP1-ΔC and -ΔN constructs were unable to accumulate in stress granules, and the total area of SGs for these constructs reached 11.2 μm^2 and 12.2 μm^2 on average, respectively (Figure 3.24, *a*, *b*). In the case of G3BP1-ΔC, this construct lacks RNA-binding domains and thus is unable to participate in SG assembly, while in the case of the G3BP1-ΔN construct, it appears that G3BP1 RNA-binding domains alone cannot

trigger SG formation, and the NTF2-L domain is required to do so. As for G3BP1-ΔIDR2, while this construct was able to partially accumulate in SGs with an enrichment coefficient reaching 1.9, no significant increase in total area of SGs (12.8 μm^2) was observed. As discussed before, IDR2 is an important regulatory sequence that allows G3BP1 to undergo conformational change. G3BP1-ΔIDR2 construct can enter stress granules due to its ability to form heterotypic interactions with Caprin1 and homotypic interaction with G3BP1 FL, but has reduced ability to generate new SGs due to its low mRNA-binding capacity.

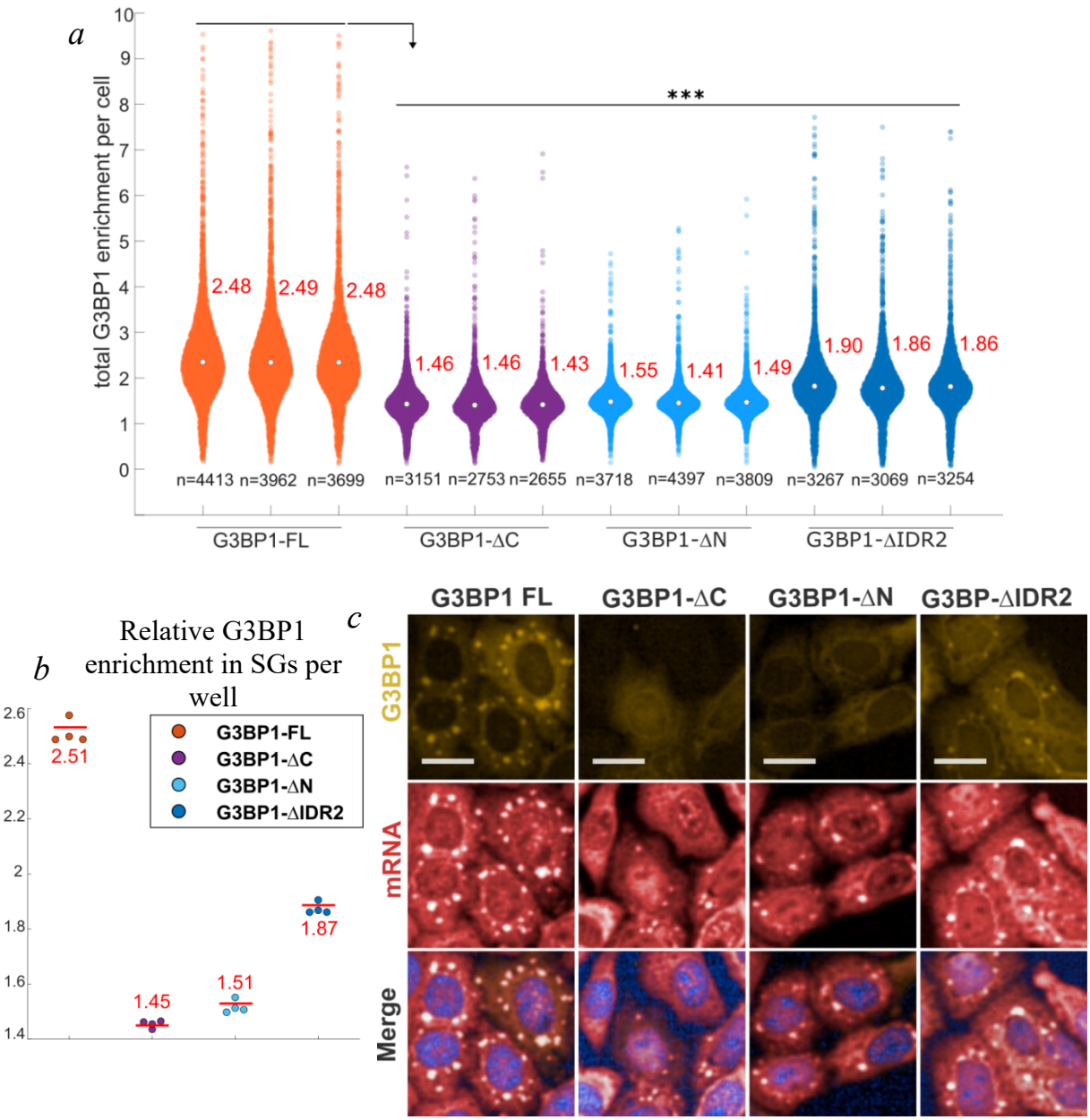

Figure 3.24. Deletion of either the N-terminus or C-terminus impairs G3BP1 accumulation in stress granules. *a,b* - B. Relative enrichment of full-length G3BP1 and G3BP1 deletion constructs in SGs, quantified per cell (*a*) and per well (*b*) in HeLa cells. Full-length G3BP1 and, to a lesser extent, G3BP1-ΔIDR2 accumulated in SGs, whereas G3BP1-ΔC and G3BP1-ΔN did not. n indicates the number of analyzed cells. **p < 0.01, ***p < 0.001, paired t-test; n.s., non-significant. *c* - Representative images of HeLa cells expressing RFP-tagged G3BP1 deletion constructs, with mRNA detected using an oligo-dT-(Cy5) probe. Scale bar: 20 μm

We evaluated the impact of Caprin1 in the recruitment of different G3BP1 constructs to SGs. For that, we set up an add-back experiment, in which, firstly, we designed a small interfering RNA that corresponds to the 3`UTR sequence of G3BP1 mRNA and silenced endogenous G3BP1. Next, we overexpressed G3BP1 constructs and either Caprin1-GFP or GFP-tag in G3BP1-silenced cells, induced oxidative stress using sodium arsenite (Figure 3.25). We compared such parameters as enrichment of G3BP1 constructs, enrichment of Caprin1, and average mRNA accumulation in all SGs per cell for G3BP1-silenced cells versus cells treated with negative control si-RNA.

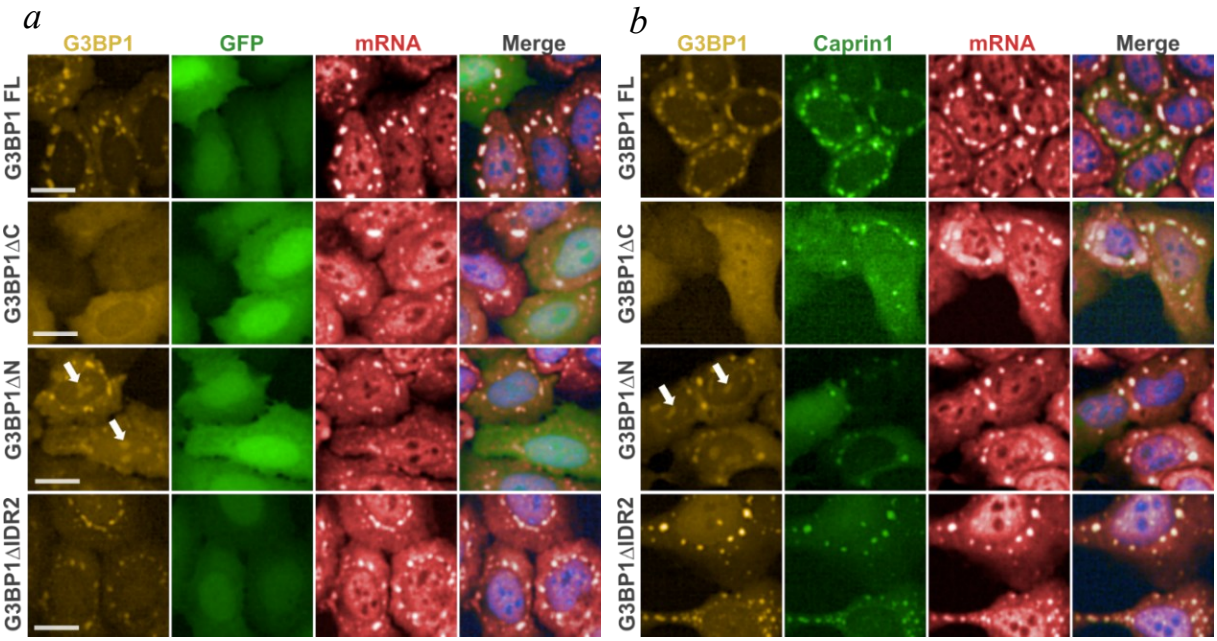

Figure 3.25. Addback of G3BP1 deletion constructs to HeLa cells with endogenous G3BP1 depleted and Caprin1 overexpressed. *a* - Representative images of Hela cells with endogenous G3BP1 silenced with siRNA and co-expressing GFP-tag or GFP-labeled Caprin1 (*b*) and RFP-labeled G3BP1 deletion constructs, subjected to oxidative stress via 300mM sodium arsenite, with mRNA tracked via oligo-dT-(Cy5) fluorescent probe. White arrows indicate depositions of G3BP1-ΔN in the nucleus. Scale bar: 20 µm

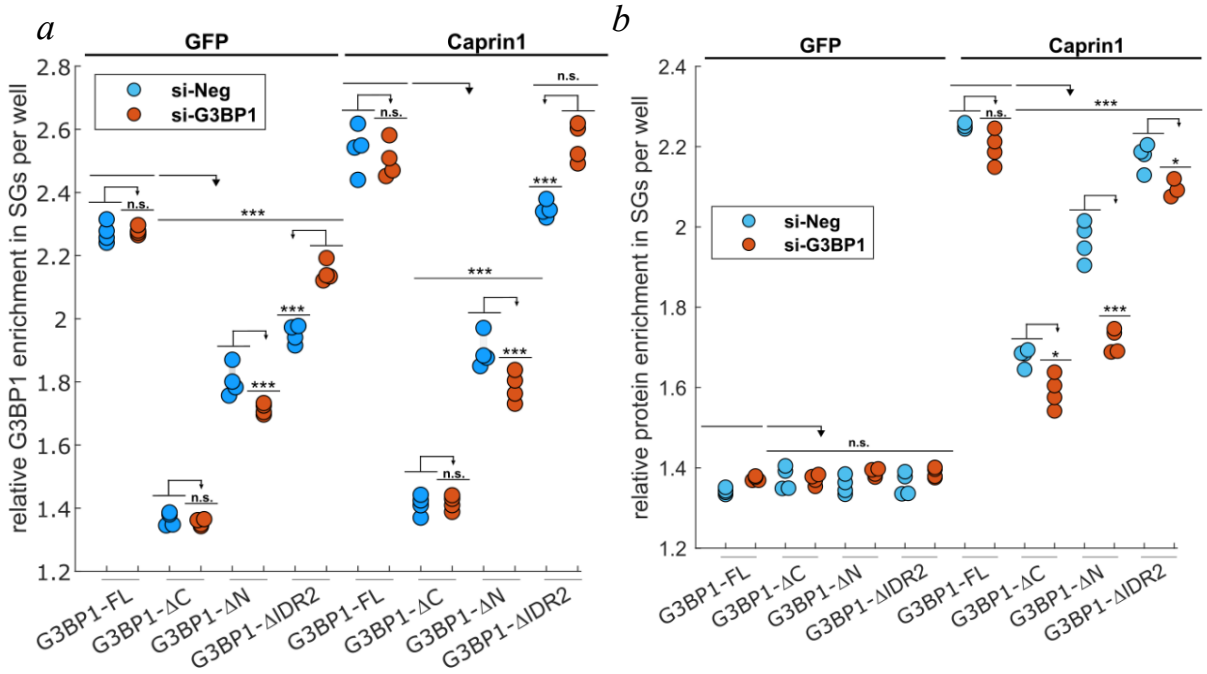

Figure 3.26. Depletion of endogenous G3BP1 negatively influences Caprin1 recruitment to SGs in stress conditions. G3BP1 FL and G3BP1-ΔIDR2 rescue Caprin1 recruitment to SGs, while G3BP1-ΔC and -ΔN are unable to do so. *a* - Overexpressed Caprin1 is accumulated the most in cells co-transfected with G3BP1 FL. Silencing of G3BP1 leads to a decrease in Caprin1 enrichment in SGs, but is rescued by G3BP1 FL and partially by G3BP1-ΔIDR2. Each dot represents data for the mean enrichment value for all cells in the well (see Materials and Methods for details) *p < 0.05, ***p < 0.001, paired t-test, n.s., non-significant. *b* - Overexpressed Caprin1 improves G3BP1 FL and -ΔIDR2 recruitment to SGs but does not affect -ΔC or -ΔN recruitment to SGs. Each dot represents data for mean enrichment value for all cells in the well (see Materials and methods for details), ***p < 0.001, paired t-test, n.s., non-significant

If we look at G3BP1 constructs` pattern of enrichment in SGs (Figure 3.25, *a*), we observe that in arsenite-stressed cells, G3BP1 constructs accumulate in SGs in a fashion mostly similar to non-stressed conditions observed in Figure 3.24.

G3BP1 FL was the highest recruited protein, with no significant difference in recruitment between si-NEG and si-G3BP1 conditions. G3BP1-ΔC was unable to accumulate in SGs due to its inability to bind RNA and G3BP1-ΔN recruitment in SGs is also strongly affected, with a slight decrease for cells treated with si-G3BP1. G3BP1-ΔIDR2 accumulation in SGs is similar to full-length G3BP1, especially in the siG3BP1 context. Interestingly, regardless of Caprin1 or GFP-tag co-expression, in si-G3BP1 conditions, G3BP1-ΔIDR2 enrichment in SGs was higher in si-G3BP1 conditions than in si-NEG conditions. This indicates that if endogenous G3BP1 is depleted (Figure 2.2), G3BP1-ΔIDR2 is abundant in SGs, but if endogenous G3BP1 expression level is not modified, it takes priority on SG entry over G3BP1-ΔIDR2, likely due to the latter having low mixing ability with G3BP1 FL (Figure 3.23, *b*). Looking at the pattern of Caprin1 recruitment to SGs (Figure 3.26, *b*), the highest enrichment was achieved in cells that co-expressed Caprin1 and G3BP1 FL, with no difference between si-NEG and si-G3BP1 conditions. Since G3BP1-ΔC was unable to enter SGs, this construct had no influence on Caprin1 enrichment in SGs. Consequently, we observe a decrease in Caprin1 enrichment in si-G3BP1 conditions. In the case of Caprin1 co-expression with G3BP1-ΔN, we observe a sharp drop in Caprin1 enrichment in si-G3BP1 conditions. While G3BP1-ΔN can enter SGs, it fails to rescue Caprin1 recruitment to SGs due to a lack of the NTF2-L domain. As for co-expression with G3BP1-ΔIDR2, Caprin1 recruitment is comparable to that of co-expression with full-length G3BP1, and the similar mixing ability between Caprin1 and G3BP1 FL or -ΔIDR2 may explain that. Additionally, if Caprin1 is co-expressed with either G3BP1 FL or G3BP1-ΔIDR2, the enrichment of all three proteins in SGs is overall improved, which coincides with our previous observations (Figure 3.9, Figure 3.10, *a*) that G3BP1 and Caprin1 form large condensates whenever they can interact with each other and mRNA.

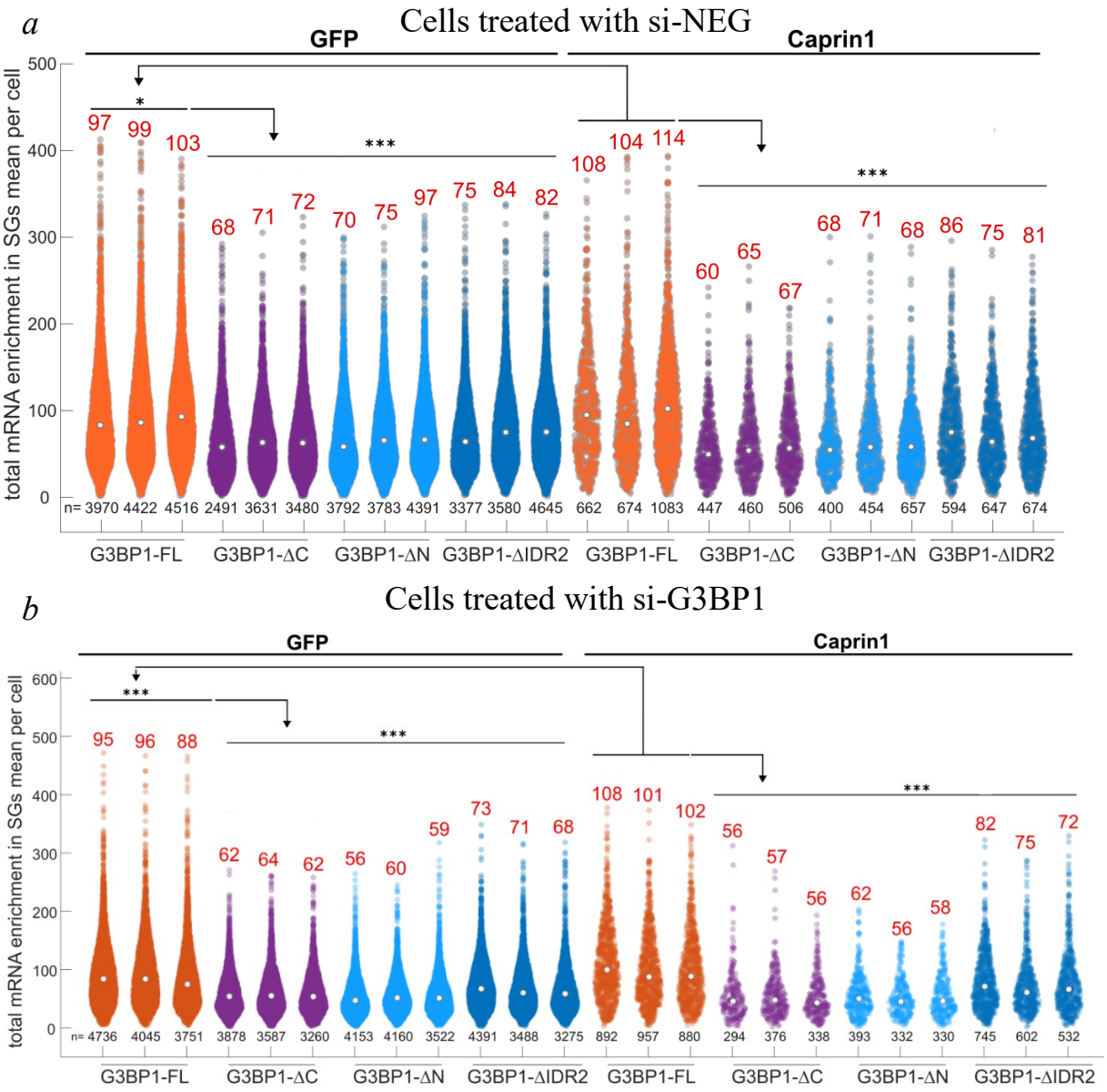

Figure 3.27. Overexpression of Caprin1 improves total mRNA enrichment in SGs under conditions of oxidative stress for full-length G3BP1. *a,b* - Violin plots showing mean per-cell total mRNA enrichment in SGs in HeLa cells co-expressing GFP or Caprin1-GFP with RFP-tagged G3BP1 deletion constructs under control siRNA (*a*) or G3BP1 3′UTR siRNA (*b*) conditions. Caprin1 increased mRNA enrichment in SGs formed by full-length G3BP1, whereas G3BP1-ΔIDR2 showed only partial rescue, and G3BP1-ΔC/ΔN failed to restore mRNA enrichment. Each violin represents cells from one well; each condition was analyzed in triplicate. n indicates the number of analyzed cells. *p < 0.05, ***p < 0.001, paired t-test; n.s., non-significant

Concurrently with the measurement of protein enrichment in SGs, we analyzed total mRNA enrichment in SGs (Figure 3.27). This parameter is obtained by multiplying the mean value of the total area of all SGs per cell by the enrichment (the fluorescence in SGs divided by the fluorescence in cytoplasm) of the oligo-dT-(Cy5) fluorescent probe we used to detect mRNA. Such an approach allows us to measure the overall amount of mRNA in SGs in stress conditions and determine the impact of Caprin1 overexpression on mRNA recruitment to stress granules. Compared to cells treated with si-NEG (Figure 3.27, *a*), stress granules in cells treated with si-G3BP1 (Figure 3.27, *b*) accumulate less mRNA overall, which displays G3BP1's importance for mRNA recruitment to SGs. Addback of G3BP1 FL facilitated the highest recruitment of mRNA to SGs. This aligns with results obtained in Figures 3.4 and 3.6, *a*, where Caprin1 improves mRNA recruitment of full-length G3BP1 both on microtubules and in SGs. G3BP1-ΔC and -ΔN constructs failed both to improve mRNA recruitment to SGs in cells treated with si-NEG and rescue mRNA recruitment to SGs in cells treated with si-G3BP1. Co-expression of Caprin1 with these 2 constructs did not affect recruitment to SGs for both G3BP1-ΔC and -ΔN as well as mRNA.

Cells with overexpressed G3BP1-ΔIDR2 construct accumulated the second largest amount of mRNA, with silencing of G3BP1 having minimal effect on SG assembly. While G3BP1-ΔIDR2 can’t bind mRNA (Figures 3.14, 3.20, *b*), its recruitment to SGs is rescued by Caprin1 overexpression, since the recruitment of G3BP1-ΔIDR2 improved in cells with co-expressed Caprin1 compared to cells with co-expressed GFP tag (Figure 3.26, *b*).

CHAPTER 4

ANALYSIS AND SUMMARY OF THE OBTAINED RESULTS

G3BP1 is a central protein in the formation of stress granules – cytoplasmic RNP granules that emerge as a response to cellular stress. While not the only protein activating SG assembly, the G3BP family of proteins is considered irreplaceable for this process, as double G3BP1/G3BP2 knockout cells failed to assemble SGs under stress conditions (3). LLPS is the main driving force behind the SG assembly process, in which weak transient interactions between RBPs and RNAs facilitate condensation in a concentration-dependent manner. As a result, SGs are a complicated network with hundreds of RNA and protein components orchestrating the fate of mRNA in adverse conditions. G3BP1 possesses several characteristics, which makes it a versatile player in the maintenance of RNA in the cytoplasm, be that in stress conditions or outside them (Chapter 1.2.3). Namely, apart from structured domains like NTF2-L and RRM, G3BP1 possesses intrinsically disordered regions, which have a propensity for self-adhesion or weak interactions with RNA or proteins due to positively or negatively charged AA stretches, respectively (Chapter 1.2.2). The flexibility conferred by IDRs lies at the core of the G3BP1 SG-assembling role. In non-stressed conditions, negatively charged IDR1 and positively charged IDR3 interact with each other, granting G3BP1 a closed conformation, with IDR2 acting as a spacer. Due to the release of mRNA from polysomes during stress, the influx of negatively charged mRNA outcompetes IDR1, and, in combination with post-translational modifications in IDR2, G3BP1 adopts an open conformation, in which the C-terminus of G3BP1 binds mRNA, and the formation of SGs occurs (3). Detailed analysis of the RNA binding of G3BP1 shows that it is conducted mostly through RRM, and a wide variety of RNAs are targeted without the strict consensus sequences required for binding. The particular affinity for long single-stranded

RNAs is essential for G3BP1, as in conditions of cellular stress, the cytoplasm is overflown with mRNAs stalled in translation, and the G3BP1 SG assembly role requires RNA binding in order to facilitate conformational change, as highlighted in (Chapter 2.3.2). In the conditions of global translational arrest and release of mRNAs from polysomes, enhanced mRNA binding capacity is needed to outcompete numerous cytoplasmic RBPs. Such additional mRNA binding capability can come from protein-protein interactions that create suitable RNA binding interfaces to handle the influx of mRNA following their release from polysomes. The importance of RNA binding for G3BP1-mediated stress granule assembly is further supported by overexpression experiments, in which full-length G3BP1 was able to induce SG assembly in the absence of a stressor, while G3BP1-ΔC or -ΔN constructs failed to do so (Figure 3.25). At the same time, in cells subjected to sodium arsenite stress, the G3BP1-ΔN construct was able to enter pre-existing SGs. Since this construct retains RNA-binding capability, it may be recruited to pre-existing stress granules together with endogenous G3BP1-associated mRNA targets (Figure 3.25).

Caprin1 represents a major interaction partner of G3BP1 in SGs, in particular through the G3BP1-Caprin1-USP10 mechanism described in (Chapter 3.2). Caprin1 is an RBP itself, although hosting only an RGG box at the C-terminus but not structured RNA-binding domains, but also an intrinsically disordered protein with a large portion of amino acids on the C-terminus being aromatic amino acids – prominent drivers of LLPS (127). While G3BP1-Caprin1 interaction in SGs has been known for a long time (78), using high-throughput screening, we show that G3BP1 has a particular affinity for Caprin1 as opposed to other cytoplasmic RBPs, and the impact of G3BP1 loss in SGs is reflected on Caprin1 the most (Figure 3.3). As for RNA binding, Caprin1 and G3BP1 show cooperativity in binding *c-myc* mRNA (23). Here, we show that overexpression of Caprin1 increases mRNA uptake in G3BP1-rich condensates (Figures 3.3, 3.27). On the interaction level, we confirmed that both proteins are able to bind

nucleic acids without. Furthermore, we observed the cooperative effect of the G3BP1-Caprin1 mix in nucleic acid binding compared to both proteins alone as well as large aggregates that are unable to enter the gel in EMSA experiments (Figures 3.7, 3.8, and 3.9). We showed the formation of G3BP1 and Caprin1 assemblies with mRNA targets on the nanomolecular scale and observed the formation of much bigger aggregates if the proteins are mixed together (Figure 3.10). Overexpression of Caprin1 leads to an increased amount of mRNA recruited to G3BP1 bound to microtubules in MT bench experiments (Figure 3.6). The RNA-binding ability of G3BP1 is extremely important to enable this effect, as the G3BP1 construct with the C-terminus removed was able to bind Caprin1 but failed to achieve any significant level of mRNA binding even when Caprin1 was overexpressed (Figures 3.14, 3.18, B). With the N-terminus absent, the interaction of G3BP1 with Caprin1 was abolished, but the RNA-binding ability of the C-terminus of G3BP1 persisted. Caprin1 appears to have limited mRNA-binding ability in vivo: when used as a bait to attract mRNA, the level of interaction is weak and improves only when full-length G3BP1 is overexpressed (Figure 3.18).

Analysis of G3BP1 domain organization demonstrated that, if G3BP1 is divided into functional parts, that being dimerization and protein interaction NTF2-L domain, central IDRs, and RNA-binding tandem of RRM and RGG-box, it appears that none of them are essential for SG formation. Remarkably, if any or all of these parts are substituted for domains with similar properties, SG assembly still occurs in G3BP1/2 KO cells, albeit with a likely very different composition of the condensates (3). These observations suggest that what matters for G3BP1-driven condensate formation is not only the properties of individual domains but also the organization and N-terminus to C-terminus position of each individual domain.

Analysis of protein compartmentalization using the MT bench approach can demonstrate the ability of proteins to form separate compartments. This is

achieved by binding proteins under scrutiny to microtubules via MBD and observing the potential for homotypic or heterotypic interactions (Figure 2.2). Since both G3BP1 and Caprin1 have the ability to undergo LLPS with specific biologically important intent, it is important to understand if there are any caveats in the compartmentalization of G3BP1 and Caprin1. We show that loss of the C-terminus or N-terminus of G3BP1 is detrimental to both homotypic interaction of G3BP1 (Figure 3.21) and heterotypic interactions with Caprin1 (Figure 3.22). Moreover, the structural integrity of G3BP1 appears to be more important than the integrity of binding sites, as the introduction of point mutations in the NTF2-L domain of G3BP1 and GIM of Caprin1, respectively, failed to disrupt the compartmentalization in the same way as the introduced deletions were able to do (Figure 3.23).

The G3BP1-ΔIDR2 construct case is a prime example of structural integrity being a key factor for G3BP1 functionality in SGs. As mentioned before, the regulation of G3BP1 conformation relies on the interplay between 3 IDRs. G3BP1-ΔIDR2 maintains the capability to recruit Caprin1 as well as the ability to form heterotypic interactions when confined to microtubules, comparable to full-length G3BP1. However, despite both RRM and RGG-box RNA-binding domains being present, this construct fails to recruit mRNA in vivo (Figure 3.14A, 3.18) as well as *in vitro*, where the ability of G3BP1-ΔIDR2 to decrease the electrophoretic mobility of nucleic acids was strongly reduced (Figure 3.16). This defect appears to compromise the role of G3BP1 in stress granule assembly, as G3BP1-ΔIDR2, like -ΔC and -ΔN constructs of G3BP1, failed to induce SG assembly in the absence of stressor, but can still enter pre-existing SGs (Figure 3.24), which coincides with G3BP1-ΔIDR2's inability to assemble SGs in G3BP1/2 KO cells (3). Nevertheless, in the case of sodium arsenite-induced stress, G3BP1-ΔIDR2 was able to enter SGs, and Caprin1 overexpression only increased its recruitment to condensates, which, however, was not enough to

achieve the level of mRNA enrichment in SGs observed with both full-length G3BP1 and Caprin1 co-overexpressed (Figures 3.26, 3.27). The obtained results may indicate that deletion of IDR2 alters the conformational organization of G3BP1 and disrupts its ability to undergo conformational transitions required for efficient RNA binding. It may be assumed that the removal of flexible IDR2, forces negatively charged IDR1 and RRM into closer proximity, and as a result, RRM is no longer able to bind RNA targets, while G3BP1 retains some affinity for RNA binding through positively charged IDR3.

In summary, the obtained results expand current understanding of the functional relationship between G3BP1 and Caprin1 during stress granule assembly. The data demonstrate that efficient mRNA recruitment to stress granules depends on cooperative interactions between G3BP1 and Caprin1, while direct RNA binding by G3BP1 remains indispensable for this process. Furthermore, the results indicate that preservation of G3BP1 structural integrity is essential for proper RNA recruitment and stress granule formation (Figure 4.1).

G3BP1-ΔIDR2 retains the ability to bind Caprin1 and enter stress granules, which results in Caprin1 recruitment to SGs being rescued by overexpression of G3BP1-ΔIDR2. At the same time, this construct loses nearly all RNA-binding potential both *in vivo* and *in vitro,* regardless of Caprin1 overexpression. Based on the obtained results, a model may be proposed in which G3BP1 lacking IDR2 is misfolded, cannot undergo conformational change, and adopts a closed conformation. Consequently, despite both RRM and IDR3 hosting RGG-box still present, only IDR3 RNA binding is available for interaction, and as such, the ability to bind Caprin1 is largely unaffected.

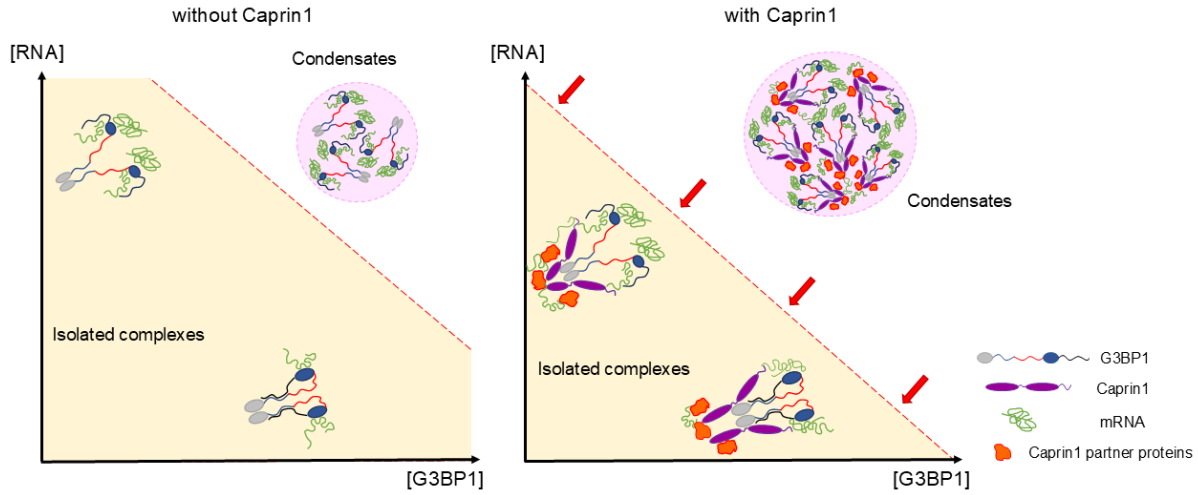

Figure 4.1. Caprin1 enhances the mRNA recruitment of G3BP1 and promotes the formation of larger G3BP1-mRNA-enriched aggregates. Red arrows indicate the decrease in the LLPS threshold of G3BP1 in the case of Caprin1 presence in the system

CONCLUSIONS

In the present work, we investigated the interplay between G3BP1 and Caprin1 proteins both *in vivo* and *in vitro*, and characterized their roles in mRNA binding and recruitment to stress granules. It was established that Caprin1 functions as a regulatory interaction partner of G3BP1 and enhances the ability of G3BP1 to recruit mRNA in both cellular and in vitro conditions. It was demonstrated that efficient mRNA binding and accumulation within stress granules depend on the integrity of G3BP1 functional domains and on the ability of G3BP1 to simultaneously interact with both Caprin1 and mRNA. Furthermore, the G3BP1-Caprin1 complex was shown to promote the formation of functionally active ribonucleoprotein condensates and to influence the composition and RNA enrichment of stress granules, thereby expanding current understanding of the molecular mechanisms regulating stress granule assembly and the cooperative interactions of RNA-binding proteins during liquid–liquid phase separation.

1. The interaction between G3BP1 and Caprin1 in the cellular environment was characterized and compared with interactions between G3BP1 and stress granule-associated RNA-binding proteins containing diverse RNA-binding domains. It was demonstrated that G3BP1 forms a particularly strong and functionally prominent interaction with Caprin1 compared to other tested cytoplasmic RNA-binding proteins, confirming the specific role of the G3BP1–Caprin1 complex in stress granule-associated processes.

2. The dependency between the level of G3BP1 in stress granules and the recruitment of partner proteins and mRNA was analyzed. It was established that depletion of G3BP1 significantly impairs recruitment of Caprin1 to stress granules and reduces mRNA accumulation within stress granules. At the same time, recruitment of additional stress granule-associated proteins, including

YBX1 and G3BP2, was dependent on the presence of functional G3BP1, demonstrating the central role of G3BP1 in organizing stress granule composition.

3. The RNA-binding properties of the G3BP1-Caprin1 complex were characterized both in vivo and in vitro. It was shown that co-expression of Caprin1 enhances mRNA recruitment to G3BP1-containing condensates in cells. In vitro experiments using electrophoretic mobility shift assay and atomic force microscopy demonstrated the formation of larger protein–RNA assemblies in the presence of both G3BP1 and Caprin1 compared to individual proteins, indicating cooperative RNA-binding activity of the complex.

4. The roles of individual G3BP1 functional domains in mRNA binding and interaction with Caprin1 were determined. It was established that both N-terminal and C-terminal regions of G3BP1 are required for efficient interaction with Caprin1 and for mRNA recruitment. Deletion of these regions impaired both stress granule assembly and RNA recruitment. In addition, the IDR2 region was shown to be important for maintaining the RNA-binding functionality of G3BP1, since the G3BP1-ΔIDR2 construct displayed strongly impaired mRNA-binding capacity despite retaining partial interaction with Caprin1 and localization to stress granules.

5. The role of the G3BP1-Caprin1 complex in mRNA recruitment to stress granules was evaluated. It was demonstrated that Caprin1 alone is insufficient to mediate efficient mRNA recruitment in the absence of functional G3BP1. Enhanced recruitment of mRNA to stress granules occurred only in the presence of full-length G3BP1 capable of both RNA binding and interaction with Caprin1. These findings indicate that Caprin1 functions as a regulatory co-factor that enhances G3BP1-mediated mRNA recruitment and contributes to the formation of functionally active stress granule ribonucleoprotein condensates.

6. The obtained results expand current understanding of molecular mechanisms regulating stress granule assembly and RNA recruitment. The study demonstrated that cooperative interaction between G3BP1 and Caprin1

contributes to the formation of RNA-enriched condensates and supports the model in which RNA binding and multivalent protein interactions collectively regulate stress granule assembly through liquid-liquid phase separation.

7. The results obtained in this work may serve as a basis for further studies of stress granule dysfunction in neurodegenerative diseases and other pathological conditions associated with aberrant aggregation of RNA-binding proteins, since both G3BP1 and Caprin1 participate in neuronal ribonucleoprotein granules and stress granule-associated pathological processes.

BIBLIOGRAPHY

1. Mitrea, D. M., & Kriwacki, R. W. (2016). Phase separation in biology: functional organization of a higher order. Cell Communication and Signaling : CCS, 14, 1. https://doi.org/10.1186/s12964-015-0125-7

2. Kang, W., Wang, Y., Yang, W., Zhang, J., Zheng, H., & Li, D. (2021). Research Progress on the Structure and Function of G3BP. Frontiers in Immunology, 12, 718548. https://doi.org/10.3389/fimmu.2021.718548

3. Yang, P., Mathieu, C., Kolaitis, R.-M., Zhang, P., Messing, J., Yurtsever, U., Yang, Z., Wu, J., Li, Y., Pan, Q., Yu, J., Martin, E. W., Mittag, T., Kim, H. J., & Taylor, J. P. (2020). G3BP1 Is a Tunable Switch that Triggers Phase Separation to Assemble Stress Granules. Cell, 181(2), 325-345.e28. https://doi.org/10.1016/j.cell.2020.03.046

4. Somasekharan, S. P., Zhang, F., Saxena, N., Huang, J. N., Kuo, I.-C., Low, C., Bell, R., Adomat, H., Stoynov, N., Foster, L., Gleave, M., & Sorensen, P. H. (2020). G3BP1-linked mRNA partitioning supports selective protein synthesis in response to oxidative stress. Nucleic Acids Research, 48(12), 6855–6873. https://doi.org/10.1093/nar/gkaa376

5. Sidibé, H., Dubinski, A., & Vande Velde, C. (2021). The multi-functional RNA-binding protein G3BP1 and its potential implication in neurodegenerative disease. Journal of Neurochemistry, 157(4), 944–962. https://doi.org/10.1111/jnc.15280

6. Schulte, T., Panas, M. D., Williams, L., Kedersha, N., Fleck, J. S., Tan, T. J. C., Olsson, A., Morro, A. M., Hanke, L., Nilvebrant, J., Giang, K. A., Nygren, P.-Å., Anderson, P., Achour, A., & McInerney, G. M. (2021). Caprin-1 binding to the critical stress granule protein G3BP1 is regulated by pH. https://doi.org/10.1101/2021.02.05.429362

7. Song, X., Chen, B., Liang, Y., Li, Y., Zhang, H., Han, D., Wang, Y., Ye, F., Wang, L., Zhao, W., & Yang, Q. (2022). CircEIF3H-IGF2BP2-HuR scaffold complex promotes TNBC progression via stabilizing HSPD1/RBM8A/G3BP1 mRNA. Cell Death Discovery, 8, 261. https://doi.org/10.1038/s41420-022-01055-9

8. Sahoo, P. K., Kar, A. N., Samra, N., Terenzio, M., Patel, P., Lee, S. J., Miller, S., Thames, E., Jones, B., Kawaguchi, R., Coppola, G., Fainzilber, M., & Twiss, J. L. (2020). A Ca2+-Dependent Switch Activates Axonal Casein Kinase 2α Translation and Drives G3BP1 Granule Disassembly for Axon Regeneration. Current Biology : CB, 30(24), 4882-4895.e6. https://doi.org/10.1016/j.cub.2020.09.043

9. Nakayama, K., Ohashi, R., Shinoda, Y., Yamazaki, M., Abe, M., Fujikawa, A., Shigenobu, S., Futatsugi, A., Noda, M., Mikoshiba, K., Furuichi, T., Sakimura, K., & Shiina, N. (2017). RNG105/caprin1, an RNA granule protein for dendritic mRNA localization, is essential for long-term memory formation. eLife, 6, e29677. https://doi.org/10.7554/eLife.29677

10. Lo, L. H.-Y., Dong, R., Lyu, Q., & Lai, K.-O. (2020). The Protein Arginine Methyltransferase PRMT8 and Substrate G3BP1 Control Rac1-PAK1 Signaling and Actin Cytoskeleton for Dendritic Spine Maturation. Cell Reports, 31(10), 107744. https://doi.org/10.1016/j.celrep.2020.107744

11. Wolozin, B. (2019). The Evolution of Phase-Separated TDP-43 in Stress. Neuron, 102(2), 265–267. https://doi.org/10.1016/j.neuron.2019.03.041

12. Ash, P. E. A., Vanderweyde, T. E., Youmans, K. L., Apicco, D. J., & Wolozin, B. (2014). Pathological stress granules in Alzheimer's disease. Brain Research, 1584, 52–58. https://doi.org/10.1016/j.brainres.2014.05.052

13. Vanderweyde, T., Yu, H., Varnum, M., Liu-Yesucevitz, L., Citro, A., Ikezu, T., Duff, K., & Wolozin, B. (2012). Contrasting Pathology of the Stress Granule Proteins TIA-1 and G3BP in Tauopathies. Journal of Neuroscience, 32(24), 8270–8283. https://doi.org/10.1523/JNEUROSCI.1592-12.2012

14. Vedove, A. D., Natarajan, J., Zanni, G., Eckenweiler, M., Muiños-Bühl, A., Storbeck, M., Boixet, J. G., Barresi, S., Pizzi, S., Hölker, I., Körber, F., Franzmann, T. M., Bertini, E. S., Kirschner, J., Alberti, S., Tartaglia, M., & Wirth, B. (2022). CAPRIN1P512L causes aberrant protein aggregation and associates with early-onset ataxia. Cellular and Molecular Life Sciences, 79(10), 526. https://doi.org/10.1007/s00018-022-04544-3

15. Maharana, S., Wang, J., Papadopoulos, D. K., Richter, D., Pozniakovsky, A., Poser, I., Bickle, M., Rizk, S., Guillén-Boixet, J., Franzmann, T. M., Jahnel, M., Marrone, L., Chang, Y.-T., Sterneckert, J., Tomancak, P., Hyman, A. A., & Alberti, S. (2018). RNA buffers the phase separation behavior of prion-like RNA binding proteins. Science, 360(6391), 918–921. https://doi.org/10.1126/science.aar7366

16. Baradaran-Heravi, Y., Van Broeckhoven, C., & van der Zee, J. (2020). Stress granule mediated protein aggregation and underlying gene defects in the FTD-ALS spectrum. Neurobiology of Disease, 134, 104639. https://doi.org/10.1016/j.nbd.2019.104639

17. Kelaini, S., Chan, C., Cornelius, V. A., & Margariti, A. (2021). RNA-Binding Proteins Hold Key Roles in Function, Dysfunction, and Disease. Biology, 10(5), 366. https://doi.org/10.3390/biology10050366

18. Nietfeld, W., Mentzel, H., & Pieler, T. (1990). The Xenopus laevis poly(A) binding protein is composed of multiple functionally independent RNA-binding domains. The EMBO Journal, 9(11), 3699–3705.

19. Lunde, B. M., Moore, C., & Varani, G. (2007). RNA-binding proteins: Modular design for efficient function. Nature Reviews. Molecular Cell Biology, 8(6), 479–490. https://doi.org/10.1038/nrm2178

20. Mittal, A., Holehouse, A. S., Cohan, M. C., & Pappu, R. V. (2018). Sequence-to-Conformation Relationships of Disordered Regions Tethered to Folded Domains of Proteins. Journal of Molecular Biology, 430(16), 2403–2421. https://doi.org/10.1016/j.jmb.2018.05.012

21. Castello, A., Fischer, B., Eichelbaum, K., Horos, R., Beckmann, B. M., Strein, C., Davey, N. E., Humphreys, D. T., Preiss, T., Steinmetz, L. M., Krijgsveld, J., & Hentze, M. W. (2012). Insights into RNA Biology from an Atlas of Mammalian mRNA-Binding Proteins. Cell, 149(6), 1393–1406. https://doi.org/10.1016/j.cell.2012.04.031

22. Phan, A. T., Kuryavyi, V., Darnell, J. C., Serganov, A., Majumdar, A., Ilin, S., Raslin, T., Polonskaia, A., Chen, C., Clain, D., Darnell, R. B., & Patel, D. J. (2011). Structure-function studies of FMRP RGG peptide recognition of an RNA duplex-quadruplex junction. Nature Structural & Molecular Biology, 18(7), 796–804. https://doi.org/10.1038/nsmb.2064

23. Solomon, S., Xu, Y., Wang, B., David, M. D., Schubert, P., Kennedy, D., & Schrader, J. W. (2007). Distinct Structural Features of Caprin-1 Mediate Its Interaction with G3BP-1 and Its Induction of Phosphorylation of Eukaryotic Translation InitiationFactor 2 α , Entry to Cytoplasmic Stress Granules, and Selective Interaction with a Subset of mRNAs. Molecular and Cellular Biology, 27(6), 2324–2342. https://doi.org/10.1128/MCB.02300-06

24. Kuechler, E. R., Budzyńska, P. M., Bernardini, J. P., Gsponer, J., & Mayor, T. (2020). Distinct Features of Stress Granule Proteins Predict Localization in Membraneless Organelles. Journal of Molecular Biology, 432(7), 2349–2368. https://doi.org/10.1016/j.jmb.2020.02.020

25. Millar, S. R., Huang, J. Q., Schreiber, K. J., Tsai, Y.-C., Won, J., Zhang, J., Moses, A. M., & Youn, J.-Y. (2023). A New Phase of Networking: The Molecular Composition and Regulatory Dynamics of Mammalian Stress Granules. Chemical Reviews, 123(14), 9036–9064. https://doi.org/10.1021/acs.chemrev.2c00608

26. King, O. D., Gitler, A. D., & Shorter, J. (2012). The tip of the iceberg: RNA-binding proteins with prion-like domains in neurodegenerative disease. Brain Research, 1462, 61–80. https://doi.org/10.1016/j.brainres.2012.01.016

27. Pabis, M., Popowicz, G. M., Stehle, R., Fernández-Ramos, D., Asami, S., Warner, L., García-Mauriño, S. M., Schlundt, A., Martínez-Chantar, M. L., Díaz-Moreno, I., & Sattler, M. (2019). HuR biological function involves RRM3-mediated dimerization and RNA binding by all three RRMs. Nucleic Acids Research, 47(2), 1011–1029. https://doi.org/10.1093/nar/gky1138

28. Feracci, M., Foot, J. N., Grellscheid, S. N., Danilenko, M., Stehle, R., Gonchar, O., Kang, H.-S., Dalgliesh, C., Meyer, N. H., Liu, Y., Lahat, A., Sattler, M., Eperon, I. C., Elliott, D. J., & Dominguez, C. (2016). Structural basis of RNA recognition and dimerization by the STAR proteins T-STAR and Sam68. Nature Communications, 7(1), 10355. https://doi.org/10.1038/ncomms10355

29. Nag, S., Goswami, B., Das Mandal, S., & Ray, P. S. (2022). Cooperation and competition by RNA-binding proteins in cancer. Seminars in Cancer Biology, 86, 286–297. https://doi.org/10.1016/j.semcancer.2022.02.023

30. Banani, S. F., Lee, H. O., Hyman, A. A., & Rosen, M. K. (2017). Biomolecular condensates: Organizers of cellular biochemistry. Nature Reviews. Molecular Cell Biology, 18(5), 285–298. https://doi.org/10.1038/nrm.2017.7

31. An, H., de Meritens, C. R., & Shelkovnikova, T. A. (2021). Connecting the “dots”: RNP granule network in health and disease. Biochimica et Biophysica Acta (BBA) - Molecular Cell Research, 1868(8), 119058. https://doi.org/10.1016/j.bbamcr.2021.119058

32. Fuxreiter, M. (2020). Fuzzy protein theory for disordered proteins. Biochemical Society Transactions, 48(6), 2557–2564. https://doi.org/10.1042/BST20200239

33. Harmon, T. S., Holehouse, A. S., Rosen, M. K., & Pappu, R. V. (2017). Intrinsically disordered linkers determine the interplay between phase separation and gelation in multivalent proteins. eLife, 6, e30294. https://doi.org/10.7554/eLife.30294

34. Gupte, R., Liu, Z., & Kraus, W. L. (2017). PARPs and ADP-ribosylation: Recent advances linking molecular functions to biological outcomes. Genes & Development, 31(2), 101–126. https://doi.org/10.1101/gad.291518.116

35. Sanders, D. W., Kedersha, N., Lee, D. S. W., Strom, A. R., Drake, V., Riback, J. A., Bracha, D., Eeftens, J. M., Iwanicki, A., Wang, A., Wei, M.-T., Whitney, G., Lyons, S. M., Anderson, P., Jacobs, W. M., Ivanov, P., & Brangwynne, C. P. (2020). Competing Protein-RNA Interaction Networks Control Multiphase Intracellular Organization. Cell, 181(2), 306-324.e28. https://doi.org/10.1016/j.cell.2020.03.050

36. Jain, S., Wheeler, J. R., Walters, R. W., Agrawal, A., Barsic, A., & Parker, R. (2016). ATPase modulated stress granules contain a diverse proteome and substructure. Cell, 164(3), 487–498. https://doi.org/10.1016/j.cell.2015.12.038

37. Youn, J.-Y., Dunham, W. H., Hong, S. J., Knight, J. D. R., Bashkurov, M., Chen, G. I., Bagci, H., Rathod, B., MacLeod, G., Eng, S. W. M., Angers, S., Morris, Q., Fabian, M., Côté, J.-F., & Gingras, A.-C. (2018). High-Density Proximity Mapping Reveals the Subcellular Organization of mRNA-Associated Granules and Bodies. Molecular Cell, 69(3), 517-532.e11. https://doi.org/10.1016/j.molcel.2017.12.020

38. Protter, D. S. W., & Parker, R. (2016). Principles and Properties of Stress granules. Trends in Cell Biology, 26(9), 668. https://doi.org/10.1016/j.tcb.2016.05.004

39. Riggs, C. L., Kedersha, N., Ivanov, P., & Anderson, P. (2020). Mammalian stress granules and P bodies at a glance. Journal of Cell Science, 133(16), jcs242487. https://doi.org/10.1242/jcs.242487

40. Markmiller, S., Soltanieh, S., Server, K. L., Mak, R., Jin, W., Fang, M. Y., Luo, E.-C., Krach, F., Yang, D., Sen, A., Fulzele, A., Wozniak, J. M., Gonzalez, D. J., Kankel, M. W., Gao, F.-B., Bennett, E. J., Lécuyer, E., & Yeo, G. W. (2018). Context-Dependent and Disease-Specific Diversity in Protein Interactions within

Stress Granules. Cell, 172(3), 590-604.e13. https://doi.org/10.1016/j.cell.2017.12.032

41. Panas, M. D., Ivanov, P., & Anderson, P. (2016). Mechanistic insights into mammalian stress granule dynamics. The Journal of Cell Biology, 215(3), 313–323. https://doi.org/10.1083/jcb.201609081

42. Goswami, B., Nag, S., & Ray, P. S. (2024). Fates and functions of RNA-binding proteins under stress. WIREs RNA, 15(1), e1825. https://doi.org/10.1002/wrna.1825

43. Gingras, A.-C., Gygi, S. P., Raught, B., Polakiewicz, R. D., Abraham, R. T., Hoekstra, M. F., Aebersold, R., & Sonenberg, N. (1999). Regulation of 4E-BP1 phosphorylation: A novel two-step mechanism. Genes & Development, 13(11), 1422–1437.

44. de la Parra, C., Ernlund, A., Alard, A., Ruggles, K., Ueberheide, B., & Schneider, R. J. (2018). A widespread alternate form of cap-dependent mRNA translation initiation. Nature Communications, 9(1), 3068. https://doi.org/10.1038/s41467-018-05539-0

45. Tauber, D., Tauber, G., Khong, A., Van Treeck, B., Pelletier, J., & Parker, R. (2020). Modulation of RNA Condensation by the DEAD-Box Protein eIF4A. Cell, 180(3), 411-426.e16. https://doi.org/10.1016/j.cell.2019.12.031

46. Hofmann, S., Kedersha, N., Anderson, P., & Ivanov, P. (2021). Molecular mechanisms of stress granule assembly and disassembly. Biochimica et Biophysica Acta (BBA) - Molecular Cell Research, 1868(1), 118876. https://doi.org/10.1016/j.bbamcr.2020.118876

47. Kedersha, N., Cho, M. R., Li, W., Yacono, P. W., Chen, S., Gilks, N., Golan, D. E., & Anderson, P. (2000). Dynamic Shuttling of Tia-1 Accompanies the Recruitment of mRNA to Mammalian Stress Granules. The Journal of Cell Biology, 151(6), 1257–1268.

48. Wheeler, J. R., Matheny, T., Jain, S., Abrisch, R., & Parker, R. (2016). Distinct stages in stress granule assembly and disassembly. eLife, 5, e18413. https://doi.org/10.7554/eLife.18413

49. Gilks, N., Kedersha, N., Ayodele, M., Shen, L., Stoecklin, G., Dember, L. M., & Anderson, P. (2004). Stress granule assembly is mediated by prion-like aggregation of TIA-1. Molecular Biology of the Cell, 15(12), 5383–5398. https://doi.org/10.1091/mbc.e04-08-0715

50. Mazroui, R., Huot, M.-E., Tremblay, S., Filion, C., Labelle, Y., & Khandjian, E. W. (2002). Trapping of messenger RNA by Fragile X Mental Retardation protein into cytoplasmic granules induces translation repression. Human Molecular Genetics, 11(24), 3007–3017. https://doi.org/10.1093/hmg/11.24.3007

51. Kedersha, N., Chen, S., Gilks, N., Li, W., Miller, I. J., Stahl, J., & Anderson, P. (2002). Evidence That Ternary Complex (eIF2-GTP-tRNAi Met)–Deficient Preinitiation Complexes Are Core Constituents of Mammalian Stress Granules. Molecular Biology of the Cell, 13(1), 195–210. https://doi.org/10.1091/mbc.01-05-0221

52. Stöhr, N., Lederer, M., Reinke, C., Meyer, S., Hatzfeld, M., Singer, R. H., & Hüttelmaier, S. (2006). ZBP1 regulates mRNA stability during cellular stress. The Journal of Cell Biology, 175(4), 527–534. https://doi.org/10.1083/jcb.200608071

53. Anderson, P., & Kedersha, N. (2002). Stressful initiations. Journal of Cell Science, 115(Pt 16), 3227–3234. https://doi.org/10.1242/jcs.115.16.3227

54. Takahara, T., & Maeda, T. (2012). Transient Sequestration of TORC1 into Stress Granules during Heat Stress. Molecular Cell, 47(2), 242–252. https://doi.org/10.1016/j.molcel.2012.05.019

55. Kim, W. J., Back, S. H., Kim, V., Ryu, I., & Jang, S. K. (2005). Sequestration of TRAF2 into Stress Granules Interrupts Tumor Necrosis Factor

Signaling under Stress Conditions. Molecular and Cellular Biology, 25(6), 2450–2462. https://doi.org/10.1128/MCB.25.6.2450-2462.2005

56. Reineke, L. C., & Lloyd, R. E. (2015). The stress granule protein G3BP1 recruits protein kinase R to promote multiple innate immune antiviral responses. Journal of Virology, 89(5), 2575–2589. https://doi.org/10.1128/JVI.02791-14

57. White, J. P., Cardenas, A. M., Marissen, W. E., & Lloyd, R. E. (2007). Inhibition of cytoplasmic mRNA stress granule formation by a viral proteinase. Cell Host & Microbe, 2(5), 295–305. https://doi.org/10.1016/j.chom.2007.08.006

58. Visser, L. J., Medina, G. N., Rabouw, H. H., de Groot, R. J., Langereis, M. A., de Los Santos, T., & van Kuppeveld, F. J. M. (2019). Foot-and-Mouth Disease Virus Leader Protease Cleaves G3BP1 and G3BP2 and Inhibits Stress Granule Formation. Journal of Virology, 93(2), e00922-18. https://doi.org/10.1128/JVI.00922-18

59. Bonenfant, G., Williams, N., Netzband, R., Schwarz, M. C., Evans, M. J., & Pager, C. T. (2019). Zika Virus Subverts Stress Granules To Promote and Restrict Viral Gene Expression. Journal of Virology, 93(12), e00520-19. https://doi.org/10.1128/JVI.00520-19

60. Kim, S. S.-Y., Sze, L., Liu, C., & Lam, K.-P. (2019). The stress granule protein G3BP1 binds viral dsRNA and RIG-I to enhance interferon-β response. The Journal of Biological Chemistry, 294(16), 6430–6438. https://doi.org/10.1074/jbc.RA118.005868

61. Somasekharan, S. P., El-Naggar, A., Leprivier, G., Cheng, H., Hajee, S., Grunewald, T. G. P., Zhang, F., Ng, T., Delattre, O., Evdokimova, V., Wang, Y., Gleave, M., & Sorensen, P. H. (2015). YB-1 regulates stress granule formation and tumor progression by translationally activating G3BP1. Journal of Cell Biology, 208(7), 913–929. https://doi.org/10.1083/jcb.201411047

62. Bassell, G. J., & Warren, S. T. (2008). Fragile X syndrome: Loss of local mRNA regulation alters synaptic development and function. Neuron, 60(2), 201–214. https://doi.org/10.1016/j.neuron.2008.10.004

63. Taylor, J. P., Robert H Brown, J., & Cleveland, D. W. (2016). Decoding ALS: From Genes to Mechanism. Nature, 539(7628), 197. https://doi.org/10.1038/nature20413

64. Seddighi, S., Qi, Y. A., Brown, A.-L., Wilkins, O. G., Bereda, C., Belair, C., Zhang, Y.-J., Prudencio, M., Keuss, M. J., Khandeshi, A., Pickles, S., Kargbo-Hill, S. E., Hawrot, J., Ramos, D. M., Yuan, H., Roberts, J., Sacramento, E. K., Shah, S. I., Nalls, M. A., … Ward, M. E. (2024). Mis-spliced transcripts generate de novo proteins in TDP-43–related ALS/FTD. Science Translational Medicine, 16(734), eadg7162. https://doi.org/10.1126/scitranslmed.adg7162

65. Dormann, D., & Haass, C. (2011). TDP-43 and FUS: A nuclear affair. Trends in Neurosciences, 34(7), 339–348. https://doi.org/10.1016/j.tins.2011.05.002

66. Mann, J. R., Gleixner, A. M., Mauna, J. C., Gomes, E., DeChellis-Marks, M. R., Needham, P. G., Copley, K. E., Hurtle, B., Portz, B., Pyles, N. J., Guo, L., Calder, C. B., Wills, Z. P., Pandey, U. B., Kofler, J. K., Brodsky, J. L., Thathiah, A., Shorter, J., & Donnelly, C. J. (2019). RNA Binding Antagonizes Neurotoxic Phase Transitions of TDP-43. Neuron, 102(2), 321-338.e8. https://doi.org/10.1016/j.neuron.2019.01.048

67. Dubinski, A., Gagné, M., Peyrard, S., Gordon, D., Talbot, K., & Velde, C. V. (2022). Stress granule assembly in vivo is deficient in the CNS of mutant TDP-43 ALS mice. Human Molecular Genetics, 32(2), 319. https://doi.org/10.1093/hmg/ddac206

68. Parker, F., Maurier, F., Delumeau, I., Duchesne, M., Faucher, D., Debussche, L., Dugue, A., Schweighoffer, F., & Tocque, B. (1996). A Ras-GTPase-activating protein SH3-domain-binding protein. Molecular and Cellular Biology, 16(6), 2561–2569.

69. Annibaldi, A., Dousse, A., Martin, S., Tazi, J., & Widmann, C. (2011). Revisiting G3BP1 as a RasGAP Binding Protein: Sensitization of Tumor Cells to

Chemotherapy by the RasGAP 317–326 Sequence Does Not Involve G3BP1. PLoS ONE, 6(12), e29024. https://doi.org/10.1371/journal.pone.0029024

70. Kennedy, D., French, J., Guitard, E., Ru, K., Tocque, B., & Mattick, J. (2002). Characterization of G3BPs: Tissue specific expression, chromosomal localisation and rasGAP120 binding studies. Journal of Cellular Biochemistry, 84(1), 173–187. https://doi.org/10.1002/jcb.1277

71. Jean-Philippe, J., Paz, S., & Caputi, M. (2013). hnRNP A1: The Swiss Army Knife of Gene Expression. International Journal of Molecular Sciences, 14(9), 18999–19024. https://doi.org/10.3390/ijms140918999

72. Van Impe, K., Hubert, T., De Corte, V., Vanloo, B., Boucherie, C., Vandekerckhove, J., & Gettemans, J. (2008). A New Role for Nuclear Transport Factor 2 and Ran: Nuclear Import of CapG. Traffic, 9(5), 695–707. https://doi.org/10.1111/j.1600-0854.2008.00720.x

73. Schulte, T., Liu, L., Panas, M. D., Thaa, B., Dickson, N., Götte, B., Achour, A., & McInerney, G. M. (2016). Combined structural, biochemical and cellular evidence demonstrates that both FGDF motifs in alphavirus nsP3 are required for efficient replication. Open Biology, 6(7), 160078. https://doi.org/10.1098/rsob.160078

74. Vognsen, T., Møller, I. R., & Kristensen, O. (2013). Crystal Structures of the Human G3BP1 NTF2-Like Domain Visualize FxFG Nup Repeat Specificity. PLoS ONE, 8(12), e80947. https://doi.org/10.1371/journal.pone.0080947

75. Tourrière, H., Gallouzi, I., Chebli, K., Capony, J. P., Mouaikel, J., van der Geer, P., & Tazi, J. (2001). RasGAP-Associated Endoribonuclease G3BP: Selective RNA Degradation and Phosphorylation-Dependent Localization. Molecular and Cellular Biology, 21(22), 7747–7760. https://doi.org/10.1128/MCB.21.22.7747-7760.2001

76. Panas, M. D., Kedersha, N., Schulte, T., Branca, R. M., Ivanov, P., & Anderson, P. (2019). Phosphorylation of G3BP1-S149 does not influence stress

granule assembly. The Journal of Cell Biology, 218(7), 2425–2432. https://doi.org/10.1083/jcb.201801214

77. Kim, S. S.-Y., Sim, D. C. N., Carissimo, G., Lim, H.-H., & Lam, K.-P. (2022). Bruton's tyrosine kinase phosphorylates scaffolding and RNA-binding protein G3BP1 to induce stress granule aggregation during host sensing of foreign ribonucleic acids. Journal of Biological Chemistry, 298(8), 102231. https://doi.org/10.1016/j.jbc.2022.102231

78. Kedersha, N., Panas, M. D., Achorn, C. A., Lyons, S., Tisdale, S., Hickman, T., Thomas, M., Lieberman, J., McInerney, G. M., Ivanov, P., & Anderson, P. (2016). G3BP–Caprin1–USP10 complexes mediate stress granule condensation and associate with 40S subunits. The Journal of Cell Biology, 212(7), 845–860. https://doi.org/10.1083/jcb.201508028

79. Zhang, P., Fan, B., Yang, P., Temirov, J., Messing, J., Kim, H. J., & Taylor, J. P. (2019). Chronic optogenetic induction of stress granules is cytotoxic and reveals the evolution of ALS-FTD pathology. eLife, 8, e39578. https://doi.org/10.7554/eLife.39578

80. Cléry, A., Blatter, M., & Allain, F. H.-T. (2008). RNA recognition motifs: Boring? Not quite. Current Opinion in Structural Biology, 18(3), 290–298. https://doi.org/10.1016/j.sbi.2008.04.002

81. McDonald, K. K., Aulas, A., Destroismaisons, L., Pickles, S., Beleac, E., Camu, W., Rouleau, G. A., & Vande Velde, C. (2011). TAR DNA-binding protein 43 (TDP-43) regulates stress granule dynamics via differential regulation of G3BP and TIA-1. Human Molecular Genetics, 20(7), 1400–1410. https://doi.org/10.1093/hmg/ddr021

82. Reineke, L. C., Tsai, W.-C., Jain, A., Kaelber, J. T., Jung, S. Y., & Lloyd, R. E. (2017). Casein kinase 2 is linked to stress granule dynamics through phosphorylation of the stress granule nucleating protein G3BP1. Molecular and Cellular Biology, 37(4), e00596-16. https://doi.org/10.1128/MCB.00596-16

83. Tsai, W.-C., Reineke, L. C., Jain, A., Jung, S. Y., & Lloyd, R. E. (2017). Histone arginine demethylase JMJD6 is linked to stress granule assembly through demethylation of the stress granule-nucleating protein G3BP1. The Journal of Biological Chemistry, 292(46), 18886–18896. https://doi.org/10.1074/jbc.M117.800706

84. Gal, J., Chen, J., Na, D.-Y., Tichacek, L., Barnett, K. R., & Zhu, H. (2019). The Acetylation of Lysine-376 of G3BP1 Regulates RNA Binding and Stress Granule Dynamics. Molecular and Cellular Biology, 39(22), e00052-19. https://doi.org/10.1128/MCB.00052-19

85. Jayabalan, A. K., Bhambhani, K., & Leung, A. K. L. (2023). PARP10 is Critical for Stress Granule Initiation. bioRxiv, 2023.10.13.562236. https://doi.org/10.1101/2023.10.13.562236

86. Gwon, Y., Maxwell, B. A., Kolaitis, R.-M., Zhang, P., Kim, H. J., & Taylor, J. P. (2021). Ubiquitination of G3BP1 mediates stress granule disassembly in a context-specific manner. Science, 372(6549), eabf6548. https://doi.org/10.1126/science.abf6548

87. Yang, Y., Luo, Y., Yang, C., Hu, R., Qin, X., & Li, C. (2023). TRIM25-mediated ubiquitination of G3BP1 regulates the proliferation and migration of human neuroblastoma cells. Biochimica Et Biophysica Acta. Gene Regulatory Mechanisms, 1866(3), 194954. https://doi.org/10.1016/j.bbagrm.2023.194954

88. Gallouzi, I., Parker, F., Chebli, K., Maurier, F., Labourier, E., Barlat, I., Capony, J.-P., Tocque, B., & Tazi, J. (1998). A Novel Phosphorylation-Dependent RNase Activity of GAP-SH3 Binding Protein: A Potential Link between Signal Transduction and RNA Stability. Molecular and Cellular Biology, 18(7), 3956–3965. https://doi.org/10.1128/MCB.18.7.3956

89. Tourrière, H., Chebli, K., Zekri, L., Courselaud, B., Blanchard, J. M., Bertrand, E., & Tazi, J. (2023). The RasGAP-associated endoribonuclease G3BP mediates stress granule assembly. The Journal of Cell Biology, 222(11), e200212128072023new. https://doi.org/10.1083/jcb.200212128072023new

90. Matsuki, H., Takahashi, M., Higuchi, M., Makokha, G. N., Oie, M., & Fujii, M. (2013). Both G3BP1 and G3BP2 contribute to stress granule formation. Genes to Cells: Devoted to Molecular & Cellular Mechanisms, 18(2), 135–146. https://doi.org/10.1111/gtc.12023

91. Aulas, A., Caron, G., Gkogkas, C. G., Mohamed, N.-V., Destroismaisons, L., Sonenberg, N., Leclerc, N., Parker, J. A., & Vande Velde, C. (2015). G3BP1 promotes stress-induced RNA granule interactions to preserve polyadenylated mRNA. The Journal of Cell Biology, 209(1), 73–84. https://doi.org/10.1083/jcb.201408092

92. Meyer, C., Garzia, A., Morozov, P., Molina, H., & Tuschl, T. (2020). The G3BP1-Family-USP10 Deubiquitinase Complex Rescues Ubiquitinated 40S Subunits of Ribosomes Stalled in Translation from Lysosomal Degradation. Molecular Cell, 77(6), 1193-1205.e5. https://doi.org/10.1016/j.molcel.2019.12.024

93. Fischer, J. W., Busa, V. F., Shao, Y., & Leung, A. K. L. (2020). Structure-Mediated RNA Decay by UPF1 and G3BP1. Molecular Cell, 78(1), 70-84.e6. https://doi.org/10.1016/j.molcel.2020.01.021

94. Sahoo, P. K., Lee, S. J., Jaiswal, P. B., Alber, S., Kar, A. N., Miller-Randolph, S., Taylor, E. E., Smith, T., Singh, B., Ho, T. S.-Y., Urisman, A., Chand, S., Pena, E. A., Burlingame, A. L., Woolf, C. J., Fainzilber, M., English, A. W., & Twiss, J. L. (2018). Axonal G3BP1 stress granule protein limits axonal mRNA translation and nerve regeneration. Nature Communications, 9(1), 3358. https://doi.org/10.1038/s41467-018-05647-x

95. Ge, Y., Jin, J., Li, J., Ye, M., & Jin, X. (2022). The roles of G3BP1 in human diseases (review). Gene, 821, 146294. https://doi.org/10.1016/j.gene.2022.146294

96. Hu, X., Xia, K., Xiong, H., & Su, T. (2021). G3BP1 may serve as a potential biomarker of proliferation, apoptosis, and prognosis in oral squamous cell

carcinoma. Journal of Oral Pathology & Medicine, 50(10), 995–1004. https://doi.org/10.1111/jop.13199

97. Xiong, R., Gao, J., & Yin, T. (2019). G3BP1 activates the TGF-β/Smad signaling pathway to promote gastric cancer. OncoTargets and Therapy, 12, 7149–7156. https://doi.org/10.2147/OTT.S213728

98. Min, L., Ruan, Y., Shen, Z., Jia, D., Wang, X., Zhao, J., Sun, Y., & Gu, J. (2015). Overexpression of Ras-GTPase-activating protein SH3 domain-binding protein 1 correlates with poor prognosis in gastric cancer patients. Histopathology, 67(5), 677–688. https://doi.org/10.1111/his.12695

99. Zhang, C., Liu, H., Zhao, W., Zhao, W., Zhou, H., & Shao, R. (2021). G3BP1 promotes human breast cancer cell proliferation through coordinating with GSK-3β and stabilizing β-catenin. Acta Pharmacologica Sinica, 42(11), 1900–1912. https://doi.org/10.1038/s41401-020-00598-w

100. Bikkavilli, R. K., & Malbon, C. C. (2011). Arginine methylation of G3BP1 in response to Wnt3a regulates β-catenin mRNA. Journal of Cell Science, 124(13), 2310–2320. https://doi.org/10.1242/jcs.084046

101. Prentzell, M. T., Rehbein, U., Cadena Sandoval, M., De Meulemeester, A.-S., Baumeister, R., Brohée, L., Berdel, B., Bockwoldt, M., Carroll, B., Chowdhury, S. R., Von Deimling, A., Demetriades, C., Figlia, G., De Araujo, M. E. G., Heberle, A. M., Heiland, I., Holzwarth, B., Huber, L. A., Jaworski, J., … Thedieck, K. (2021). G3BPs tether the TSC complex to lysosomes and suppress mTORC1 signaling. Cell, 184(3), 655-674.e27. https://doi.org/10.1016/j.cell.2020.12.024

102. Wang, R., Cao, L., Thorne, R. F., Zhang, X. D., Li, J., Shao, F., Zhang, L., & Wu, M. (2021). LncRNA GIRGL drives CAPRIN1-mediated phase separation to suppress glutaminase-1 translation under glutamine deprivation. Science Advances, 7(13), eabe5708. https://doi.org/10.1126/sciadv.abe5708

103. Omer, A., Barrera, M. C., Moran, J. L., Lian, X. J., Di Marco, S., Beausejour, C., & Gallouzi, I.-E. (2020). G3BP1 controls the senescence-

associated secretome and its impact on cancer progression. Nature Communications, 11(1), 4979. https://doi.org/10.1038/s41467-020-18734-9

104. Fung, G., Ng, C. S., Zhang, J., Shi, J., Wong, J., Piesik, P., Han, L., Chu, F., Jagdeo, J., Jan, E., Fujita, T., & Luo, H. (2013). Production of a Dominant-Negative Fragment Due to G3BP1 Cleavage Contributes to the Disruption of Mitochondria-Associated Protective Stress Granules during CVB3 Infection. PLOS ONE, 8(11), e79546. https://doi.org/10.1371/journal.pone.0079546

105. Cheng, J., Gao, S., Zhu, C., Liu, S., Li, J., Kang, J., Wang, Z., & Wang, T. (2020). Typical Stress Granule Proteins Interact with the 3′ Untranslated Region of Enterovirus D68 To Inhibit Viral Replication. Journal of Virology, 94(7), 10.1128/jvi.02041-19. https://doi.org/10.1128/jvi.02041-19

106. Zhang, Y., Yao, L., Xu, X., Han, H., Li, P., Zou, D., Li, X., Zheng, L., Cheng, L., Shen, Y., Wang, X., Wu, X., Xu, J., Song, B., Xu, S., Zhang, H., & Cao, H. (2018). Enterovirus 71 inhibits cytoplasmic stress granule formation during the late stage of infection. Virus Research, 255, 55–67. https://doi.org/10.1016/j.virusres.2018.07.006

107. Galan, A., Lozano, G., Piñeiro, D., & Martinez-Salas, E. (2017). G3BP1 interacts directly with the FMDV IRES and negatively regulates translation. The FEBS Journal, 284(19), 3202–3217. https://doi.org/10.1111/febs.14184

108. Götte, B., Panas, M. D., Hellström, K., Liu, L., Samreen, B., Larsson, O., Ahola, T., & McInerney, G. M. (2019). Separate domains of G3BP promote efficient clustering of alphavirus replication complexes and recruitment of the translation initiation machinery. PLoS Pathogens, 15(6), e1007842. https://doi.org/10.1371/journal.ppat.1007842

109. Ellis, J. A., & Luzio, J. P. (1995). Identification and Characterization of a Novel Protein (p137) Which Transcytoses Bidirectionally in Caco-2 Cells. Journal of Biological Chemistry, 270(35), 20717–20723. https://doi.org/10.1074/jbc.270.35.20717

110. Shiina, N., Shinkura, K., & Tokunaga, M. (2005). A Novel RNA-Binding Protein in Neuronal RNA Granules: Regulatory Machinery for Local Translation. The Journal of Neuroscience, 25(17), 4420–4434. https://doi.org/10.1523/JNEUROSCI.0382-05.2005

111. Wu, Y., Zhu, J., Huang, X., & Du, Z. (2016). Crystal structure of a dimerization domain of human Caprin-1: Insights into the assembly of an evolutionarily conserved ribonucleoprotein complex consisting of Caprin-1, FMRP and G3BP1. Acta Crystallographica Section D Structural Biology, 72(6), 718–727. https://doi.org/10.1107/S2059798316004903

112. Shiina, N., Yamaguchi, K., & Tokunaga, M. (2010). RNG105 Deficiency Impairs the Dendritic Localization of mRNAs for Na + /K + ATPase Subunit Isoforms and Leads to the Degeneration of Neuronal Networks. The Journal of Neuroscience, 30(38), 12816–12830. https://doi.org/10.1523/JNEUROSCI.6386-09.2010

113. Portz, B., Lee, B. L., & Shorter, J. (2021). FUS and TDP-43 Phases in Health and Disease. Trends in Biochemical Sciences, 46(7), 550–563. https://doi.org/10.1016/j.tibs.2020.12.005

114. Horio, T., Ishikura, Y., Ohashi, R., & Shiina, N. (2023). Regulation of RNG105/caprin1 dynamics by pathogenic cytoplasmic FUS and TDP-43 in neuronal RNA granules modulates synaptic loss. Heliyon, 9(6), e17065. https://doi.org/10.1016/j.heliyon.2023.e17065

115. El Fatimy, R., Tremblay, S., Dury, A. Y., Solomon, S., De Koninck, P., Schrader, J. W., & Khandjian, E. W. (2012). Fragile Mental Retardation Protein Interacts with the RNA-Binding Protein Caprin1 in Neuronal RiboNucleoProtein Complexes. PLoS ONE, 7(6), e39338. https://doi.org/10.1371/journal.pone.0039338

116. Katoh, H., Okamoto, T., Fukuhara, T., Kambara, H., Morita, E., Mori, Y., Kamitani, W., & Matsuura, Y. (2013). Japanese Encephalitis Virus Core Protein Inhibits Stress Granule Formation through an Interaction with Caprin-1 and

Facilitates Viral Propagation. Journal of Virology, 87(1), 489–502. https://doi.org/10.1128/jvi.02186-12

117. Zhang, M., & Peng, S. (2023). The association and clinical relevance of phase-separating protein CAPRIN1 with noncoding RNA. Cell Stress and Chaperones, 28(2), 125–132. https://doi.org/10.1007/s12192-023-01320-5

118. Boca, M., Kretov, D. A., Desforges, B., Mephon-Gaspard, A., Curmi, P. A., & Pastré, D. (2015). Probing protein interactions in living mammalian cells on a microtubule bench. Scientific Reports, 5(1), 17304. https://doi.org/10.1038/srep17304

119. Maucuer, A., Desforges, B., Joshi, V., Boca, M., Kretov, D. A., Hamon, L., Bouhss, A., Curmi, P. A., & Pastré, D. (2018). Microtubules as platforms for probing liquid–liquid phase separation in cells – application to RNA-binding proteins. Journal of Cell Science, 131(11), jcs214692. https://doi.org/10.1242/jcs.214692

120. Khan, F. A., Fang, N., Zhang, W., & Ji, S. (2024). The multifaceted role of Fragile X-Related Protein 1 (FXR1) in cellular processes: An updated review on cancer and clinical applications. Cell Death & Disease, 15(1), 1–16. https://doi.org/10.1038/s41419-023-06413-8

121. Alkrekshi, A., Wang, W., Rana, P. S., Markovic, V., & Sossey-Alaoui, K. (2021). A comprehensive review of the functions of YB-1 in cancer stemness, metastasis and drug resistance. Cellular Signalling, 85, 110073. https://doi.org/10.1016/j.cellsig.2021.110073

122. Swain, B. C., Sarkis, P., Ung, V., Rousseau, S., Fernandez, L., Meltonyan, A., Aho, V. E., Mercadante, D., Mackereth, C. D., & Aznauryan, M. (2024). Disordered regions of human eIF4B orchestrate a dynamic self-association landscape. Nature Communications, 15(1), 8766. https://doi.org/10.1038/s41467-024-53136-1

123. Wu, Y.-Q., Ju, C.-L., Wang, B.-J., & Wang, R.-G. (2019). PABPC1L depletion inhibits proliferation and migration via blockage of AKT pathway in

human colorectal cancer cells. Oncology Letters, 17(3), 3439. https://doi.org/10.3892/ol.2019.9999

124. Kanai, Y., Okada, Y., Tanaka, Y., Harada, A., Terada, S., & Hirokawa, N. (2000). KIF5C, a novel neuronal kinesin enriched in motor neurons. Journal of Neuroscience, 20(17), 6374–6384. https://doi.org/10.1523/JNEUROSCI.20-17-06374.2000

125. Sheehan, C. T., Hampton, T. H., & Madden, D. R. (2022). Tryptophan mutations in G3BP1 tune the stability of a cellular signaling hub by weakening transient interactions with Caprin1 and USP10. Journal of Biological Chemistry, 298(12), 102552. https://doi.org/10.1016/j.jbc.2022.102552

126. Fiszer-Kierzkowska, A., Vydra, N., Wysocka-Wycisk, A., Kronekova, Z., Jarząb, M., Lisowska, K. M., & Krawczyk, Z. (2011). Liposome-based DNA carriers may induce cellular stress response and change gene expression pattern in transfected cells. BMC Molecular Biology, 12(1), 27. https://doi.org/10.1186/1471-2199-12-27

127. Lin, Y., Currie, S. L., & Rosen, M. K. (2017). Intrinsically disordered sequences enable modulation of protein phase separation through distributed tyrosine motifs. The Journal of Biological Chemistry, 292(46), 19110–19120. https://doi.org/10.1074/jbc.M117.800466

SUPPLEMENTARY A

AUTHOR'S PUBLICATIONS RELATED TO THE DISSERTATION TOPIC

1. Lavrynenko K., Rengifo-Gonzalez J. C., Joshi V., Pankivskyi S., Pastré D., Kropyvko S., Hamon L. mRNA recruitment by G3BP1 condensates is regulated by Caprin1 but requires G3BP1 binding to mRNA. Scientific Reports. 2025. 15:21066. doi: 10.1038/s41598-025-21066-7.
2. Lavrynenko K., Hamon L., Kropyvko S. Intrinsically disordered region 2 of G3BP1 is required for RNA recruitment by G3BP1–Caprin1 complex. Biopolymers and Cell. 2026. Vol. 42, No. 1. P. 44–53. doi: 10.7124/bc.000B34.
3. Lavrynenko K., Kropyvko S., Pastré D., Hamon L. Defining the interactions of G3BP1 with cytoplasmic RNA-binding proteins on cellular and biochemical levels. Biopolymers and Cell. 2023. Vol. 39, No. 1. P. 60–73. doi: 10.7124/bc.000A89.